Cognitive Radio-based Home Area Networks

Mohd Adib bin Sarijari

Cognitive Radio-based Home Area Networks

Proefschrift

ter verkrijging van de graad van doctor
aan de Technische Universiteit Delft,
op gezag van de Rector Magnificus Prof. ir. K.Ch.A.M. Luyben,
voorzitter van het College voor Promoties,
in het openbaar te verdedigen op
dinsdag, 19 april 2016 om 12.30 uur

door

Mohd Adib bin SARIJARI
Master of Science in Electrical Engineering
Universiti Teknologi Malaysia

geboren te Johor Bahru, Johor, Malaysia.

This dissertation has been approved by the
promotor: Prof.dr.ir. A.J. van der Veen
copromotor: Dr.ir. G.J.M. Janssen

Composition of the doctoral committee:

Rector Magnificus	voorzitter
Prof.dr.ir. A.J. van der Veen	Technische Universiteit Delft, promotor
Dr.ir. G.J.M. Janssen	Technische Universiteit Delft, copromotor

Independent members:

Prof.dr.ir G.J.T. Leus	Technische Universiteit Delft
Prof.dr. K.G. Langendoen	Technische Universiteit Delft
Prof.dr.ir. R.E. Kooij	TNO and Technische Universiteit Delft
Prof.dr.ir. S.M. Heemstra-de Groot	Technische Universiteit Eindhoven
Prof.dr.ir. G.J.M. Smit	Universiteit Twente

The research described in this thesis was supported by the government of Malaysia under the Ministry of Higher Education and Universiti Teknologi Malaysia.

ISBN 978-94-6186-626-4

To my beloved family

Summary

A future home area network (HAN) is envisaged to consist of a large number of devices that support various applications such as smart grid, security and safety systems, voice call, and video streaming. Most of these home devices are communicating based on various wireless networking technologies such as WiFi, ZigBee and Bluetooth, which typically operate in the already congested ISM licensed-free frequency bands. As these devices are located in a small physical space (i.e., limited by the size of the house), they might interfere with one another, which causes a severe limitation to the quality-of-service (QoS) such as throughput. These issues are further aggravated in dense cities where the HAN also receives interference from neighboring HANs. Cognitive radio (CR) is seen as one of the most promising technologies to solve these problems and at the same time fulfill the HANs communication needs. CR technology enables the HAN devices to intelligently exploit idle spectrum including licensed spectrum for their communications, avoiding from being interfered as well as causing interference to others (in particular the incumbent user). We study these problems and the appropriateness of CR as a candidate solution.

We start by designing a new communication system for HAN based on CR technology and clustered network topology, called TD-CRHAN. TD-CRHAN aims at sustainably and efficiently supports the ever-rising throughput demand as well as solving the interference issue in HAN. In TD-CRHAN, the achievable throughput is optimized to be just equal or slightly higher than the total network's throughput demand, instead of being maximized. We then mathematically model the proposed TD-CRHAN where in the model, general expressions of the cooperative spectrum sensing performance parameters are considered. This allows us to analyze the performance of TD-CRHAN for more realistic scenarios where the incumbent user

signal-to-noise-ratio (SNR) is not the same at different sensing devices. We provide the performance analysis on the proposed design numerically and through simulation.

As a cognitive radio based network also imposes additional overhead in energy consumption due to spectrum sensing, we then propose an energy efficient cooperative spectrum sensing (CSS) scheme. The scheme is designed based on the proposed TD-CRHAN. In this scheme we also ensure that the throughput demand is kept satisfied efficiently. From the difference in sensing devices' incumbent user SNR (that is previously considered), we select the optimal sensing devices for CSS with the corresponding sensing time and detection probability, which can be varied from one sensing device to another. We then evaluate the proposed CSS scheme and exhibit the gains obtained in energy- and throughput-efficiency.

Finally, we present a sensing device grouping and scheduling scheme for multi-channel CSS. In addition to the energy- and throughput-efficiency, this scheme addresses the fairness in spectrum sensing load distribution among the available sensing devices in a HAN. In this work, we consider the fairness objective as to maximize the lifetime of each sensing device to its expected lifetime. In the proposed scheme, we determine the optimal number of channels that should be used for the network and the selected channels. We also determine the optimal number of devices in each sensing group and which devices. Subsequently, we optimally schedule the formed sensing groups to sense the selected channels. We provide the results and the analysis on our proposed scheme to illustrate its performance.

Contents

Chapter 1

Introduction

1.1 Motivation

Spectrum Shortage

Today, wireless technology has become an important part of our life. At home, it brings ease and convenience to manage our surrounding including accessing the internet, connecting devices in the home entertainment system (e.g., TV, video player and audio system), opening and closing the garage, controlling electrical appliances, making a voice or video call, and many more.

Wireless technology functions by transmitting radio or electromagnetic waves at a certain frequency channel in the wireless spectrum. For home communication this usually occurs in a license-exempted frequency band such as the ISM 2.4-GHz band. As the number of devices requiring access to the spectrum in a house is becoming larger, using the license-exempted frequency band alone is not sufficient, particularly for a house that is situated in a dense city such as shown in Figure 1.1, because devices in neighboring residential units are also competing for spectrum. For instance, for the WiFi wireless network alone, besides our own house, often we can detect more than ten neighbors' access points in the surrounding which are also competing to access the 2.4-GHz ISM frequency band, nevertheless there are only three orthogonal channels available (e.g., WiFi channel 1, 6 and 11). Hence, it is very difficult (nearly impossible) to find a channel that is not overlapped for the home WiFi network to operate. The overlapped operating channel can cause interference or disturbance to the communication which results in a backoff or even a retransmission, which is costly in terms of delay and energy.

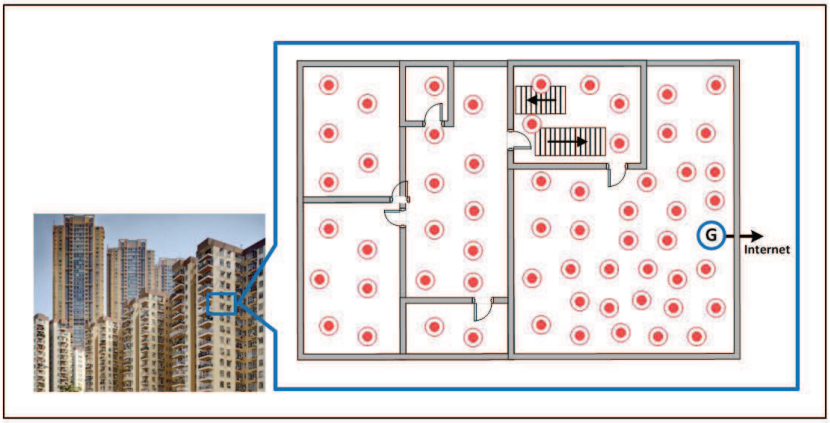

Figure 1.1: Scenario of a dense HAN in a dense city.

Moreover, in some areas in the house, the access point signal strength of some neighbors might be stronger than the one in our own house. In addition, the current fixed channel configuration practice for networks in the house can also cause a degradation in the devices' communication quality as time passes. Even though the network is initially configured to use a good channel (which is already quite difficult particularly for a non-technical end-user), the channel conditions might vary in time due to changing of the surrounding environment, for example due to a new wireless access point deployed by a neighbor. Furthermore, many new spectrum-hungry home wireless technologies and applications are being introduced. Worse, in the near future, it is envisioned that every device in the house will need to communicate in order to function (for example in the Smart Grid [1] and the Internet-of-Things [2] visions).

It is expected that if the rise of this communication demand is not dealt with properly, the home area networks (HAN) could fail at a certain point. The uncompressed video stream will be distorted, the voice call will be noisy, Internet browsing will have a long latency, and even worse, the home safety system such as the fire or smoke detector will fail to deliver an alert on an event of fire. Hence, a sustainable solution should be reached to prevent these problems.

Spectrum Sharing

As a partial solution, it is desired that the HAN can utilize any idle frequency channel in the spectrum, beyond the already overcrowded frequency channels in the license-exempted frequency bands [3]. Moreover, it has been well reported in the

literature that most of the allocated[1] licensed frequency channels in the spectrum are not utilized all the time, and moreover, in certain areas, particularly in the rural areas, some of the allocated spectrum is not even used [5, 6, 7, 8].

Therefore, it would be promising if every network in the house can autonomously select the best set of channels to operate. The networks should be able to change the currently used channels whenever needed (e.g., due to interference). Besides, as different areas in the house can be affected by different interference sources, it is desirable that home networks can operate in a distributed multi-channel manner, such that each area can operate using a different set of channels.

It has been recognized that one of the most promising technologies that can provide the aforementioned features is cognitive radio (CR). CR is defined as an intelligent wireless communication system that is aware of its surrounding environment e.g., spectrum utilization and conditions, and adapts its operation by making corresponding changes in certain communication parameters e.g., the operating frequency channel and transmission power, such that a reliable communication may be carried out [9]. CR enables devices in the house to opportunistically access and utilize an unused frequency channel (also known as a "spectrum hole" [6]) including the licensed bands. By exploiting CR's awareness ability, the frequency channel can also be dynamically vacated whenever the incumbent user of the channel is present or the channel quality has degraded to a certain level.

Other Solutions

Besides spectrum sharing, other possible solutions to the increasing communication demand in HAN include exploring a higher frequency band in the spectrum among the unlicensed bands such as the 60-GHz band, or utilizing multiple input multiple output (MIMO) technology.

Unlike the lower frequency spectrum of the unlicensed bands such as the 2.4-GHz and 5-GHz bands, the 60-GHz unlicensed band is relatively uncongested [10]. As recommended by the ITU-R, this band comprises of four orthogonal channels with a very wide bandwidth of 2.16 GHz. The upcoming WiFi based 802.11ad will be using this technology, which can achieve up to 7 Gbit/s. However, the usage of this band is targeted mainly for broadband applications such as uncompressed high definition (HD) video streaming, wireless display and multimedia backhaul.

[1] In the current practice, the spectrum is divided into bands, and each band is designated to a certain party for a certain application which is fixed. The main reason is to avoid collisions and interference, and prevent disasters such as the Titanic incident [4] from happening again.

Using this band requires a higher power compared to the lower bands. This is due to the fact that the signal attenuation is more severe mainly due to the increase of free space path loss (68 dB for propagation over 1 m) and shadowing (from a few dB to more than 30 dB) [10]. Because of the severe attenuation, it is suggested that this technology is mainly employed for a line-of-sight (LOS) communications [11, 12]. In addition, as highly directional antennas are needed at both transmitter and receiver to combat the propagation loss, this has increased the complexity particularly to the medium access control (MAC) layer protocol [11, 12].

In MIMO, the capacity of a channel is multiplied by using multiple antennas and exploiting diversity from the effect of multipath fading. It has been widely used in many commercial wireless technologies such as WiFi based IEEE 802.11n [13], WiMAX based IEEE 802.16-2004 [14], and 4G based 3rd generation partnership project (3GPP) long term evolution (LTE) [15]. At higher frequencies, the shorter wavelengths suggest that a very large number of antennas, in the order of hundreds or even thousands, can be supported. This is exploited in the recent technology called Massive MIMO [16]. In addition, MIMO technology has also emerged to support multiple users simultaneously. This new communication system is called Multi-user MIMO (MU-MIMO) which is basically an extension of space division multiple access (SDMA) [17]. However, MIMO imposes a high complexity in the hardware including the RF amplifier at the front end and the analog-to-digital converter. It also increases the complexity in signal processing at both transmitter and receiver ends as well as the power consumed.

1.2 Problem Statement

The main research question that we will address in this thesis is: how to make the HAN sustainable such that it is able to satisfy the growth of the throughput demand. We will propose a clustered topology and cognitive radio based communication solution called TD-CRHAN. However, CR-based communication brings new challenges, which need to be addressed to ensure its benefits. Challenges that will be explored in this thesis are as follows:

1. **How to optimally meet the throughput demand**. CR-based networks are currently considered as secondary networks. Such networks have to guarantee that in exploiting the spectrum holes, they do not cause any harmful interference to any legacy network such as the TV broadcasting, licensed wireless microphones, and first responder networks such as the terrestrial

trunked radio (TETRA) radio system. Hence, CR-based networks have to sense the spectrum before it can be utilized for data transmission. Typically, each CR frame or superframe will consist of two main parts: one part for spectrum sensing (usually is the first part), and another part for data transmission [18, 19, 20, 21, 22, 23, 24, 25, 26, 27, 28]. This spectrum sensing is a key component in CR that can degrades the communication throughput significantly compared to current networks. For example: in [22], more than 42% of the frame time is allocated to spectrum sensing; in [19] more than 48% of the frame time is required for spectrum sensing at -23 dB signal-to-noise-ratio (SNR). In addition, in a real-world implementation as reported in [29], 170 ms is required to sense a QPSK signal at a SNR of -1 dB, which is rather long and thus very costly in terms of throughput and energy. On the other hand, as the spectrum access in CR is not confined to any specific band and bandwidth size, it is important to ensure that the exploitation is not overdone. The spectrum exploited has to be optimized to the demand, and not cause any additional spectrum underutilization, in which increasing the spectrum utilization is supposed to be one of the important aims of CR [9]. Another challenge in meeting this throughput demand is the variation of environmental conditions at different areas within a house including interference sources, number of devices, type of obstacles, layout and size. In addressing this, a clustering network topology will be used. Consequently, each area can be treated differently, for example in terms of channel allocations.

2. **How to minimize the spectrum sensing energy overhead**. Besides throughput degradation, spectrum sensing also causes extra energy consumption to a network, as the transmission and the sensing power consumption are commonly (e.g. [22, 24, 30]) considered to be nearly the same. Specifically, this energy overhead is originated by the sensing time and the number of sensing devices required to achieve a certain sensing quality such that the requirements from the spectrum regulators or the standardization bodies are met, and at the same time the throughput demand is satisfied. Additionally, in practice, the incumbent user signal strength varies between different sensing devices in a house. This results in diverse sensing quality produced by each sensing device for a certain sensing time. Hence, it is important to determine the optimal number of sensing devices and which devices to use, together with the corresponding optimal spectrum sensing time and sensing qualities expected from each selected device, such that the sensing energy consump-

tion is minimized and at the same time satisfy the throughput demand.

3. **How to efficiently and fairly group and schedule sensing devices for spectrum sensing in a multi-channel network**. In a CR-based HAN that operates using multiple channels, multiple spectrum sensing groups should be formed. Each group then has to be optimally scheduled to sense a corresponding channel. In doing these, it is important that the energy consumption of the spectrum sensing is kept at a minimum and at the same time the throughput demand is maintained satisfied. In addition, as many sensing devices will be available in a dense HAN, it is very important to fairly distribute the spectrum sensing burden among these devices. Without a proper scheme, certain devices will always be loaded with a high sensing burden e.g., always be selected and given a relatively longer sensing time as compared to some other devices. This unbalanced spectrum sensing load distribution will cause the energy of the always-selected devices to be depleted quickly, while the others still have more remaining energy. Hence, a suitable fairness parameters should be identified and taken into consideration in formulating the sensing device grouping and scheduling scheme.

1.3 Related Work

Communication in HAN is becoming more challenging year after year. Currently, HAN operating based on many different wireless technologies particularly WiFi, ZigBee and Bluetooth. Many studies have shown that these technologies can be harmful to one another, particularly when many devices exist and need to communicate as envisioned in a future HAN. The performance of ZigBee technology under the coexistence of Bluetooth, WiFi and interference by microwave ovens has been studied in [31, 32]. The results from these experiments show a significant performance degradation of ZigBee coexisting with WiFi and microwave ovens. In addition, analytical results in [33] also give the same outcome.

A new communication system for HAN should be designed to sustainably support the communication demand in a house. Cognitive radio (CR), which was first introduced by Mitola [34], enables a new paradigm on how spectrum can be exploited. CR is seen as one of the most promising technologies to solve the aforementioned problems where it allows HAN devices to intelligently exploit idle spectrum, which is not limited to the unlicensed spectrum, for their communications.

Spectrum sensing is a crucial component of CR to reliably identify the idle spectrum [35]. Cooperative spectrum sensing is an approach where multiple sensing devices cooperate to assess the condition of the spectrum. This can considerably improve the sensing reliability by facilitating the sharing of sensing information between sensing devices, which can improve the sensing performance and reduce the effect of noise uncertainty, fading and shadowing [36]. By cooperation, the load from spectrum sensing also can be distributed among the available sensing devices in the network.

As a CR-based network has to sense the spectrum before utilizing it, this may result in a degradation to the achievable throughput as compared to a non-CR based network. Many publications address the effect of spectrum sensing on the achievable throughput. In [18], the spectrum sensing time is optimized to yield the maximum achievable throughput with a sufficient incumbent user protection constraint. [19] is the cooperative extension of this work that determines the optimal number of cooperating devices that should be used for achieving the same objective. A joint cooperative spectrum sensing and spectrum access framework is proposed in [20]. In this work, the spectrum sensing time, the number of cooperative sensing devices and the transmission probability are optimally defined such that the achievable throughput for a given channel set is maximized. Similarly, our previous work [21], and [22], aims at maximizing the achievable throughput by jointly considering the optimal spectrum sensing time, the number of cooperating sensing devices, and the fusion strategy. However, in practice, each network has a certain throughput demand. Targeting achievable throughput maximization without considering the actual demand may cause a significant unnecessary tight spectrum sensing requirement (e.g., spectrum sensing time, probability of detection and number of cooperating sensing devices). In this thesis, we will aim at tightly satisfying the throughput demand instead of maximizing it, and we will show that this will significantly reduce the above-mentioned spectrum sensing requirements.

Besides throughput, spectrum sensing also induces an extra energy overhead to the network [35]. Among the earliest works that addressed both throughput and energy efficiency together is by [23]. However, for the throughput, this work focuses on maximizing it instead of just tightly complying to the throughput demand. We will show that a significantly better energy efficiency can be achieved with the latter objective. One of the first works that takes the throughput demand into consideration in designing energy- and throughput-efficient cooperative spectrum sensing is published in [24]. The goal is to minimize the energy consumption from spectrum sensing while satisfying the throughput demand from the network. However, the

impact of different throughput demands to the spectrum sensing parameters and energy consumption are not analyzed. In addition, most of the current works assign the same value for the spectrum sensing time and optimization on the individual spectrum sensing performance parameters (i.e., detection and false alarm probabilities) are not considered. This turns out to be not optimal for a network that has different incumbent user signal strengths at different sensing devices, which is a more practical scenario in a HAN.

In a multi-channel network scenario, sensing devices should be optimally selected to form multiple cooperative spectrum sensing groups. The formed groups should then be optimally scheduled to sense the corresponding channels. Most of the previous works in this area select the sensing devices based on the incumbent user signal strength as in [25, 37, 38]. The work in [39] adds another parameter: the distance of sensing devices to the fusion center, because the closer a sensing device is to the fusion center, the lower the energy required to transmit the sensing report. However, by considering only these two parameters, the same devices will be selected most of the time. Consequently, the lifetime of the network will be shortened where the energy of the always-selected devices will be depleted faster while other devices will still have much remaining energy. In fact, different sensing devices might also have different properties such as communication pattern, expected lifetime and remaining energy. It is crucial that the spectrum sensing load is distributed fairly among the available sensing devices by taking these parameters and properties into consideration.

1.4 Outline and Contributions

In this thesis, we aim at designing a cognitive radio (CR)-based communication system for a home area network (HAN) to sustainably support the ever-rising wireless communication demands in a house. The design will also be based on a connected clustered network topology which will provide scalability and flexibility to the HAN. The details of the proposed design with the corresponding contributions, which basically address the problems listed in the previous section, are presented in the subsequent chapters.

Chapter 2

In this chapter, we present further motivations on the home communication challenges that are addressed in this thesis including some experimental evaluations

on typical and possible communication scenarios in a HAN. We also motivate the solution that we are going to explore, which is based on cognitive radio technology and clustered based topology. We derive some equations that are essential to evaluate the performance of several proposed designs in the following chapters.

Part of this chapter and the results presented have also appeared in

- Mohd Adib Sarijari et al., "Experimental Studies of the ZigBee Frequency Agility Mechanism in Home Area Networks", *39th IEEE Conference on Local Computer Networks Workshops (LCN Workshops)*, Edmonton, Canada, pp. 711–717, Sept. 2014;
- Mohd Adib Sarijari et al.,"Coexistence of Heterogeneous and Homogeneous Wireless Technologies in Smart Grid-Home Area Network", *2013 International Conference on Parallel and Distributed Systems (ICPADS)*, Seoul, South Korea, pp. 576–581, Dec. 2013;
- Mohd Adib Sarijari et al., "Interference Issues in Smart Grid Home Area Network to Enable Demand Response And Advanced Metering Infrastructure: Survey And Solutions", *Open International Journal of Informatics (OIJI)*, 2013.

Chapter 3

This chapter presents a throughput demand-based communication scheme for home area networks called TD-CRHAN, which is designed based on a clustered network system and CR technology. In the TD-CRHAN, the total throughput demand is used as an additional parameter that is taken into consideration in the design. This will ensure that the HAN's network throughput demand is satisfied by setting the achievable throughput to be just higher or equal to the total throughput demand instead of maximizing it. The TD-CRHAN is mathematically modeled and the suitable optimization problem with the corresponding constraints is formulated. In doing this, general expressions for the cooperative spectrum sensing performance parameters (i.e., cooperative probability of false alarm, and detection) are considered. This supports a more realistic scenario where the signal-to-noise-ratio (SNR) of the incumbent user is not the same at different sensing devices, and also supports for any fusion rules (i.e., not limited for OR and AND rules only). Finally, we present a thorough analysis on the performance of the TD-CRHAN, numerically and through simulations. The performance is compared with the conventional scheme and the impact of different parameter settings are illustrated.

This chapter has been published as

- Mohd Adib Sarijari et al., "On Achieving Network Throughput Demand in Cognitive Radio-based Home Area Networks", *EURASIP Journal on Wireless Communications and Networking*, Vol. 2015, No. 1, pp. 221, 2015.

Chapter 4

In this chapter, we further work on achieving energy efficiency in cooperative spectrum sensing (CSS) while keeping the home networks' throughput demand satisfied. The CSS scheme is designed based on the proposed cognitive radio-based home area network, which is presented in Chapter 3. In this scheme, the cooperating devices are selected, and the sensing time as well as the detection probability of the corresponding selected devices are jointly determined, based on the average throughput demand and the incumbent user SNRs. The proposed CSS scheme is mathematically modeled and an optimization problem is formulated in which the energy is minimized subject to throughput satisfaction. The problem is then solved using a widely used optimization method called Markov-Chain-Monte-Carlo (MCMC), and we specifically use the reversible-jump sampling algorithm. The performance of the proposed scheme is evaluated and we demonstrate the gain from different parameter settings as compared to a number of alternative schemes.

This chapter has been submitted as

- Mohd Adib Sarijari et al., "Energy and Throughput Efficient Cooperative Spectrum Sensing for Cognitive Radio-based Home Area Network", Submitted to the *IEEE Transactions on Cognitive Communications and Networking*.

Chapter 5

An optimal sensing device grouping and scheduling scheme for multi-channel CSS is presented in this chapter. This scheme will optimally determine the number of channels that should be used for the network and which channels. At the same time, the optimal number of devices for each sensing group and which selected devices will also be determined. Additionally, the formed groups will be scheduled to sense the corresponding selected channels. Subsequently, the optimal spectrum sensing time and the detection probability for each selected device will be determined. The objectives are to minimize the energy consumption from spectrum sensing, a fair distribution of spectrum sensing loads among the available sensing devices, and at the same time ensuring that the throughput demand remains satisfied. A fairness

coefficient will be introduced in this chapter that aims to maximize the lifetime of each sensing device to its expected lifetime. The problem is then mathematically modeled. We indicate a solution to the formulated problem using a combination of exhaustive search and the MCMC algorithm. Finally, the performance of the proposed scheme is evaluated and presented.

Chapter 6

In this chapter, the major results and findings are highlighted and the conclusions of this thesis are presented. We also discuss some future research directions regarding this exciting topic, including some further work that should be considered in order to realized the proposed cognitive radio-based home communication system.

Chapter 2

Home Area Networks: Communication Challenges and Background of the Proposed Solution

In this chapter we motivate further the problems and the proposed solutions which are initially mentioned in the previous chapter, and we present some background information as a preparation to read the rest of the thesis. We begin with discussing home communication scenarios that lead to the interference problem and the need for more spectrum in home area networks (HAN). Then, we present a realistic HAN experiment to better understand the problem, and to come out with the most appropriate solution. Later on, we conceptually introduce our proposed solution which is based on the cognitive radio technology and a clustered network topology. We then derive some equations which will be used to analyze, evaluate and prove various system designs proposed in the following chapters of thesis.

2.1 Heterogeneous Wireless Communication Technology in Home Area Networks

A typical home environment consists of various wireless technologies, in particular WiFi, ZigBee, and Bluetooth which usually operate in the ISM license-exempt

frequency band [3]. The WiFi technology is typically used for home entertainment systems, home security systems and human-centric applications including video streaming, Voice over Internet Protocol (VoIP), and video conferencing. The ZigBee technology, on the other hand, is used for low data-rate applications such as home safety systems, remote controls, and machine-to-machine applications (e.g., home automation). The Bluetooth technology is employed for short-range devices including headphones, hands-free gadgets, mice and keyboards, and it is also useful in eliminating cabling needs between electronic devices and accessories. Additionally, appliances like a microwave oven[1] exist as well in a HAN. Figure 2.1 illustrates a typical HAN which comprises WiFi-based, ZigBee-based and Bluetooth-based devices. It is envisaged that a future HAN consists of a large number of these devices that support many applications including the current ones as the aforementioned, and the forthcoming ones, such as uncompressed high definition video streaming, high speed data transfer (e.g., wireless USB) and smart-grid.

2.2 Interference in Home Area Networks

When many HAN devices with different wireless technologies and applications coexist in a small physical space (i.e., limited by the size of the house) – and so create a dense HAN, they might interfere one another and thus severely limit the quality-of-service (QoS), such as throughput. Worse, it can be harmful, particularly to devices which are based on a low-power communication technology such as ZigBee. These issues are further aggravated in dense cities where a specific HAN also receives interference from neighboring HANs. Hence, towards this end, various interference mitigation techniques have been specified by many wireless communication technology alliances in addition to existing features present in the standards they are based on. For example, the ZigBee Alliance has introduced the Frequency Agility mechanism (functioning at the Network Layer) [40] as an additional interference mitigation technique on top of Direct Sequence Spread Spectrum (at the Physical Layer) and Carrier Sense Multiple Access (at the Medium Access Control Layer (MAC)) that has been defined in the IEEE 802.15.4 standard [41], on which ZigBee is based.

[1] A microwave oven emits electromagnetic radiation to heat and cook food. A typical consumer microwave oven radiates at a center frequency of 2.45 GHz which falls within the 2.4-GHz ISM frequency band.

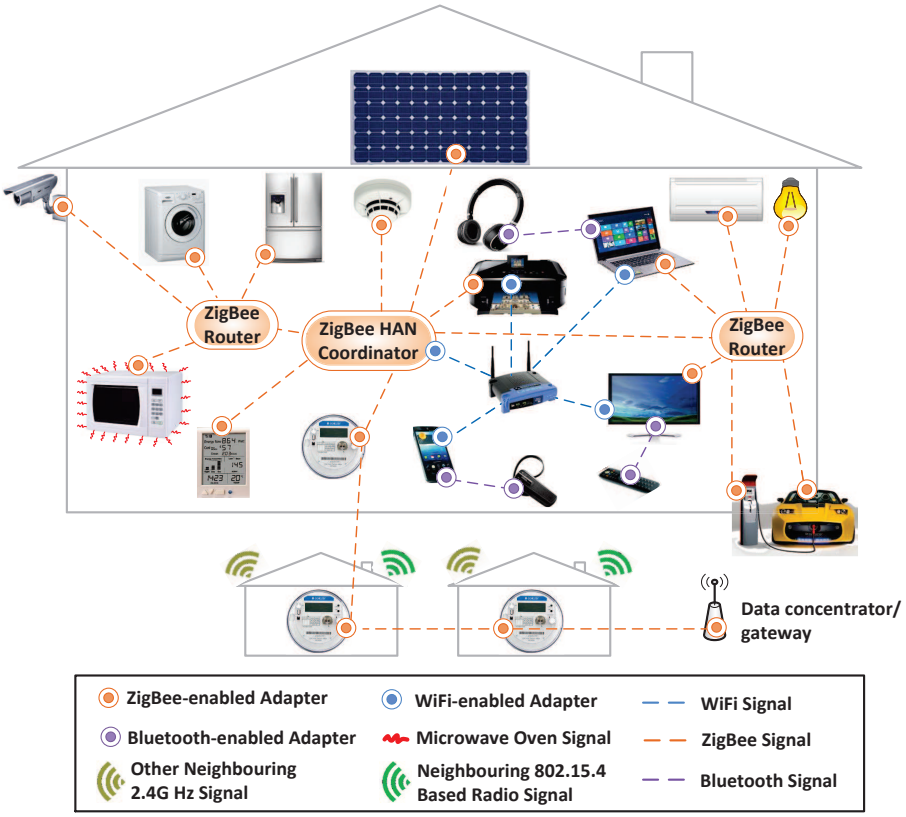

Figure 2.1: Heterogeneous Wireless Technologies in Home Area Network.

2.2.1 ZigBee Frequency Agility Mechanism

The ZigBee Frequency Agility mechanism provides a ZigBee network with the capability to detect interference on the current operating frequency channel, sense other channels in the entire ISM 2.4-GHz band, and switch the network to a new channel that has the least interference level. In essence, the ZigBee Frequency Agility operation can be divided into three phases [40] as shown in Figure 2.2:

i) *Interference Detection*: the ZigBee Coordinator and Router monitor a number of unsuccessful network-layer packets; if the packet error rate (PER), defined as the ratio of unsuccessful packets (*nFail*) to the total number of sent packets (*nSent*), is greater than twenty-five percent, then interference is deduced. For the interference detection mechanism to work, the minimum number of packets sent must be at least twenty.

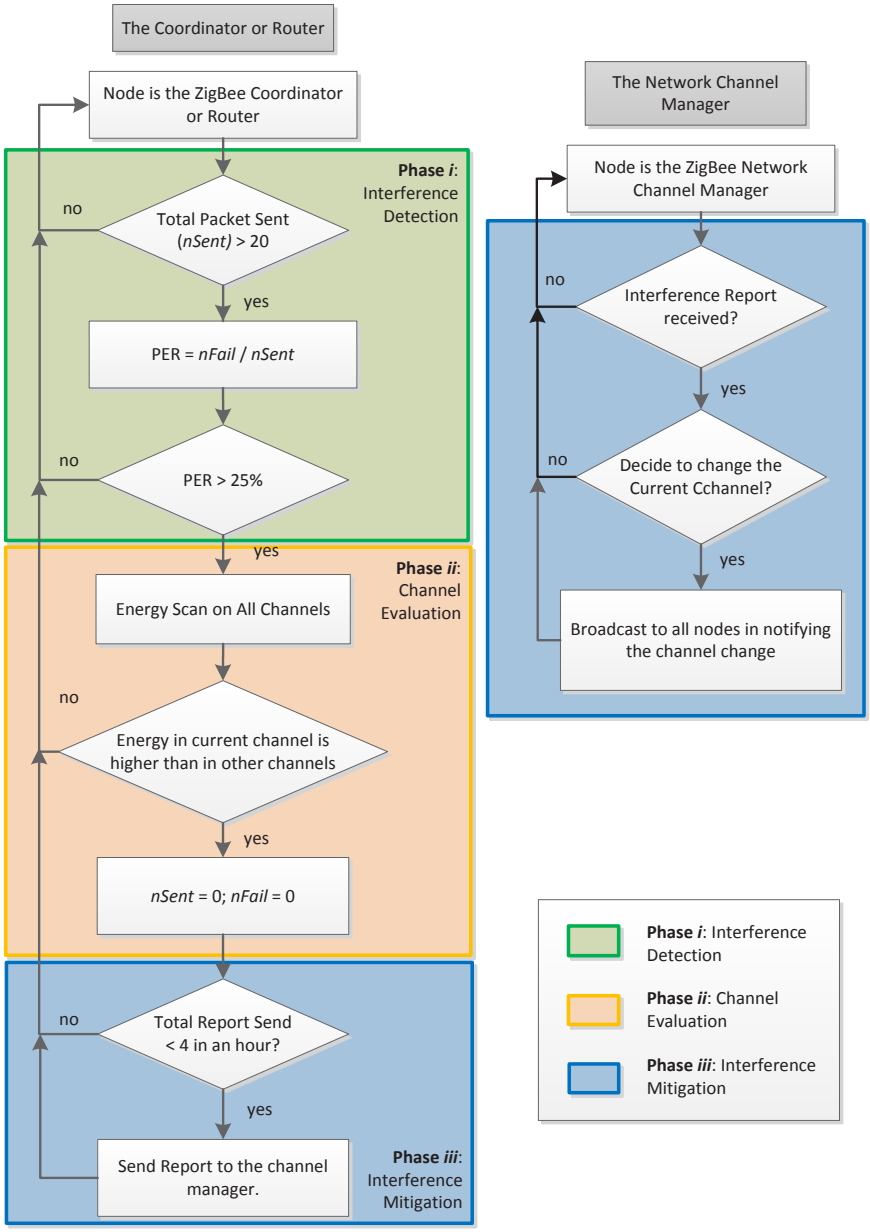

Figure 2.2: ZigBee Frequency Agility operation.

ii) *Channel Evaluation*: once the ZigBee Coordinator or Router has deduced that interference is present in the current frequency channel, then it will scan the energy level present in all the the channels operating in 2.4–2.4835 GHz (the 2.4-GHz band).

iii) *Interference Mitigation*: Upon deciding to switch channel, the ZigBee Coordinator or Router reports to the Network Channel Manager; the default Network Channel Manager is the ZigBee Coordinator. When the interference report is received by the Network Channel Manager, it will decides whether a network channel switch will take place. If the Network Channel Manager makes the decision to switch channel, then it selects the best channel obtained in Phase (ii) and broadcasts that to all nodes in the network.

2.2.2 Experimental Evaluation of ZigBee Frequency Agility Mechanism

In order to gain insight on the ability of the ZigBee Frequency Agility mechanism in mitigating interference in a realistic environment, an experimental HAN testbed in an ordinary home environment with a realistic application traffic (i.e., daily activities of home dwellers) as shown in Figure 2.3 has been setup. The testbed consists of ZigBee-based devices, WiFi-based devices and a microwave oven operating in the 2.4-GHz band. The ZigBee-based devices comprise one ZigBee Coordinator and three ZigBee End-Devices (including a smart TV, a washing machine, and a microwave oven). The ZigBee Coordinator and the End-Devices collectively form a Wireless Personal Area Network (WPAN). The WiFi-based devices constitute a wireless local area network (WLAN) which consists of one WiFi access point, two laptops, two smartphones and the smart TV that is already ZigBee-enabled.

Each ZigBee-based device is equipped with a *Tmote Sky* wireless module [42], realizing the IEEE 802.15.4 Physical and MAC protocols. Each wireless module runs the *TinyOS* [43] operating system. We implemented the ZigBee Frequency Agility mechanism in the ZigBee Coordinator device. The wireless module can operate in one of the 16 orthogonal channels available in the 2.4-GHz band starting with channel 11; channels 1 to 10 are not located in the 2.4-GHz band. The center frequency for each channel is given as follows:

$$f_{\mathrm{c}} = 2.400 + 0.005 \cdot (\mathrm{ChannelNumber} - 10) \ \ \mathrm{GHz} \tag{2.1}$$

For the WLAN, the WiFi technology is based on IEEE 802.11g. There are 13 channels available for 802.11g in 2.4-GHz band with a 20-MHz bandwidth. The

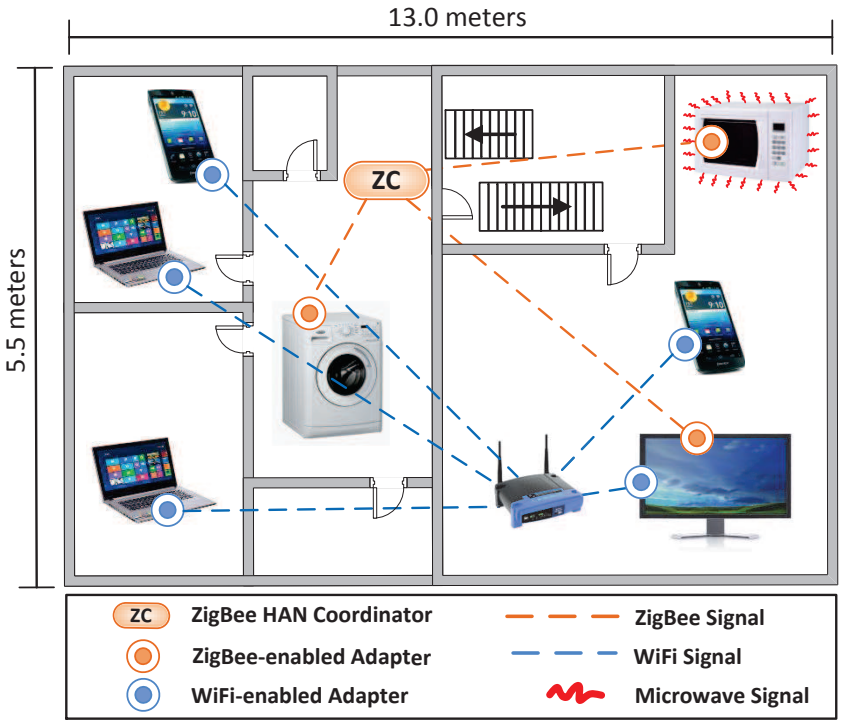

Figure 2.3: A Home Area Networks testbed.

center frequency for each WiFi channel is given as,

$$f_c = 2.407 + 0.005 \cdot \text{ChannelNumber} \ \ \text{GHz} \tag{2.2}$$

For the microwave oven, a Daewoo KOC9Q1TSL with an operating frequency of 2.45 GHz and a maximum transmit power of 900 Watt was used. The microwave oven occupies the entire 2.4-GHz ISM band [44].

Two different experiments were performed, and in all the experiments, the parameter configurations of the ZigBee-based devices were set according to Table 2.1. For WiFi-based devices, the default parameter configuration was used except the WiFi access point was configured to operate at channel 3. Experiment 1 aims at evaluating the ZigBee Frequency Agility mechanism effectiveness under ZigBee normal operation. This is, the ZigBee Coordinator performed an energy scan on all the 16 channels and selected the channel with the lowest received energy level for use during WPAN startup. In order to evaluate the ZigBee Frequency Agility mechanism effectiveness, the ZigBee Coordinator was set to continuously transmit fixed size network-layer packets to each of ZigBee End-Device in a round-robin

Table 2.1: ZigBee parameters and the respective value

ZigBee parameters	Value
Physical layer packet size	50 bytes
Transmission power	0 dBm
MAC Acknowledgement	Enabled
Maximum MAC retransmission	4 times
Channel bandwidth	2 MHz

fashion. Each network-layer packet was generated at an interval of 10 ms. The experiment was run for a period of one day. In addition, the ZigBee coordinator was configured to collect the RSSI values of the channel each time before a packet was transmitted. This is to measure the interference level of the channel throughout the experiment.

Experiment 2 aims at evaluating the capability of the ZigBee Frequency Agility mechanism in detecting and mitigating interference caused by WiFi-based devices and a microwave oven. Thus, the ZigBee WPAN was configured to operate on a particular channel (i.e., channel 15, $f_c = 2.425$ GHz) where its channel bandwidth falls inside the WLAN channel bandwidth. A *YouTube* full high-definition video clip was streamed to the smart TV and the two laptops from the Internet. At a later time, the microwave oven was switched on for a duration of 8 minutes in order to further instill interference to the ZigBee WPAN. Analogous to Experiment 1, network-layer packets were generated and transmitted at a 10-ms interval from the ZigBee Coordinator to the three ZigBee End-Devices in a round-robin manner. The experiment was run for a period of 45 minutes.

2.2.3 Results from the Experiments

The performance metrics used to study the ZigBee Frequency Agility mechanism are as follows:

Packet error rate (PER): the PER is the ratio of unsuccessful received packets to the total number of sent packets. This is calculated at the Network Layer.

Received signal strength indicator (RSSI): the RSSI is the energy which is measured at the radio frequency (RF) pin of the *Tmote Sky*'s radio transceiver chip (CC2420) [30]. It is used to indicate the energy level of the channel or the received packet including the acknowledgment packet.

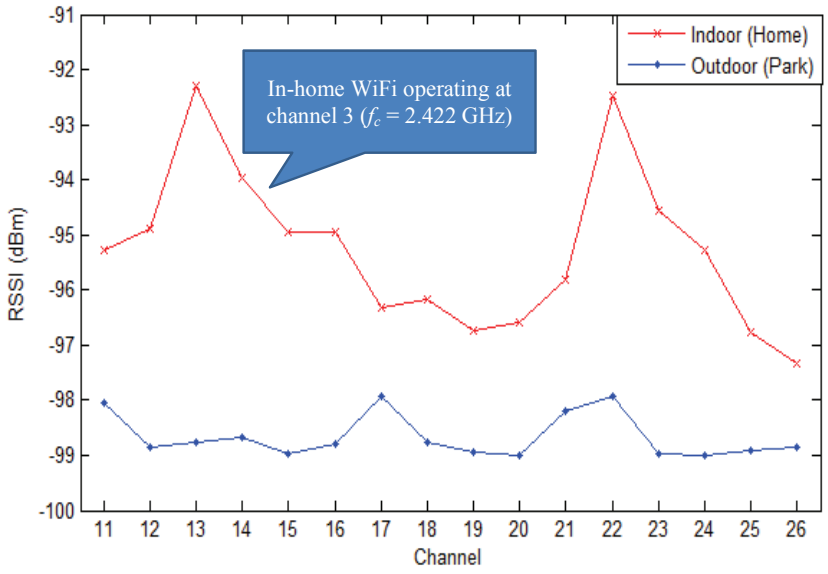

Figure 2.4: RSSI reading at Zigbee Coordinator.

Throughput: The throughput is the amount of correctly received data in bits per second.

Response time: The response time is the amount of time taken for ZigBee Frequency Agility mechanism to mitigate the interference.

Experiment 1

Figure 2.4 plots the RSSI values that were obtained by scanning all the 16 channels using the ZigBee Coordinator at network startup for indoor and outdoor environments. From the outdoor plot, it can be seen that the RSSI levels for all the 16 channels are very low (i.e., less than -97 dBm). This indicates that the area is free from interference. Hence the outdoor plot is used as the reference for comparison with the RSSI level in the presence of interference as well as the RSSI level during the packet reception. For the indoor plot, the curve shows that there are two strong interfering signals at ZigBee channel 13 and 22 at $f_{\mathrm{c}} = 2.415$ GHz and 2.460 GHz, respectively. This is due to the fact that these two ZigBee channels overlap with the WiFi channels 1 and 11 at $f_{\mathrm{c}} = 2.412$ GHz and 2.462 GHz, respectively. This has motivated us to search for WiFi access points which are in the range using a laptop running the *Xirrus WiFi Inspector* [45] software. The laptop was situated

in the same position as the ZigBee Coordinator. As a result of the search, twenty WiFi access points were detected, five of which operated at channel 1 and another five at channel 11. As observed in Figure 2.4, a significantly high RSSI reading is seen at channels 14, 15 and 16 which are due to the WLAN signals of the testbed. From this channel scanning result, the ZigBee Coordinator then selected the channel with the lowest RSSI level which is channel 26, as the best channel and started the ZigBee network.

Figure 2.5 shows the performance of the ZigBee WPAN in terms of PER, throughput and RSSI for a whole day. It can be seen from the top and middle diagrams of this figure, the ZigBee WPAN communication, particularly the smart TV, is significantly degraded at time 1.8 hours and 17.6 hours for a period of approximately two hours and one hour, respectively. This is evidenced by the graph shown in Figure 2.6, which indicates strong interference levels during these two periods, hence corrupting the ZigBee packets. This interference is due to neighboring WiFi access points which operated at channel 13 ($f_c = 2.472$ GHz) in close proximity to the smart TV. This channel overlaps with the selected channel 26 of the ZigBee network. Even though this communication is degraded, the ZigBee Frequency Agility mechanism was not activated because the PER is below the threshold recommended by the ZigBee Alliance, i.e., 25%.

In addition, the bottom diagram of Figure 2.5 shows that the RSSI values of the received acknowledgement packets from the washing machine are significantly higher than the other two devices. This is due to the location of the washing machine which is nearer and in line-of-sight with the ZigBee Coordinator. Furthermore, it also can be seen that the RSSI value of the received acknowledgement packets from each device fluctuates when the interference level is high. This might be caused by the constructive and destructive interference effects to the ZigBee signal. Note that the fluctuation of the RSSI values is not witnessed at around 1.8 hour and 17.6 hours where the interference levels are at maximum and would have corrupted most of the ZigBee packets. This is because the RSSI plot only shows the RSSI values of the successfully transmitted packet (as these RSSI values are acquired from the received acknowledgement packet at the ZigBee Coordinator). This RSSI pattern is significant and can be utilized as additional information for the ZigBee Frequency Agility mechanism in detecting the presence of interference.

Based on these results it can be concluded that, firstly, the ZigBee Frequency Agility interference detection threshold is a crucial parameter that needs to be carefully set in ensuring the effectiveness of the ZigBee Frequency Agility mechanism operation. Secondly, even though the ZigBee Coordinator chooses the best channel

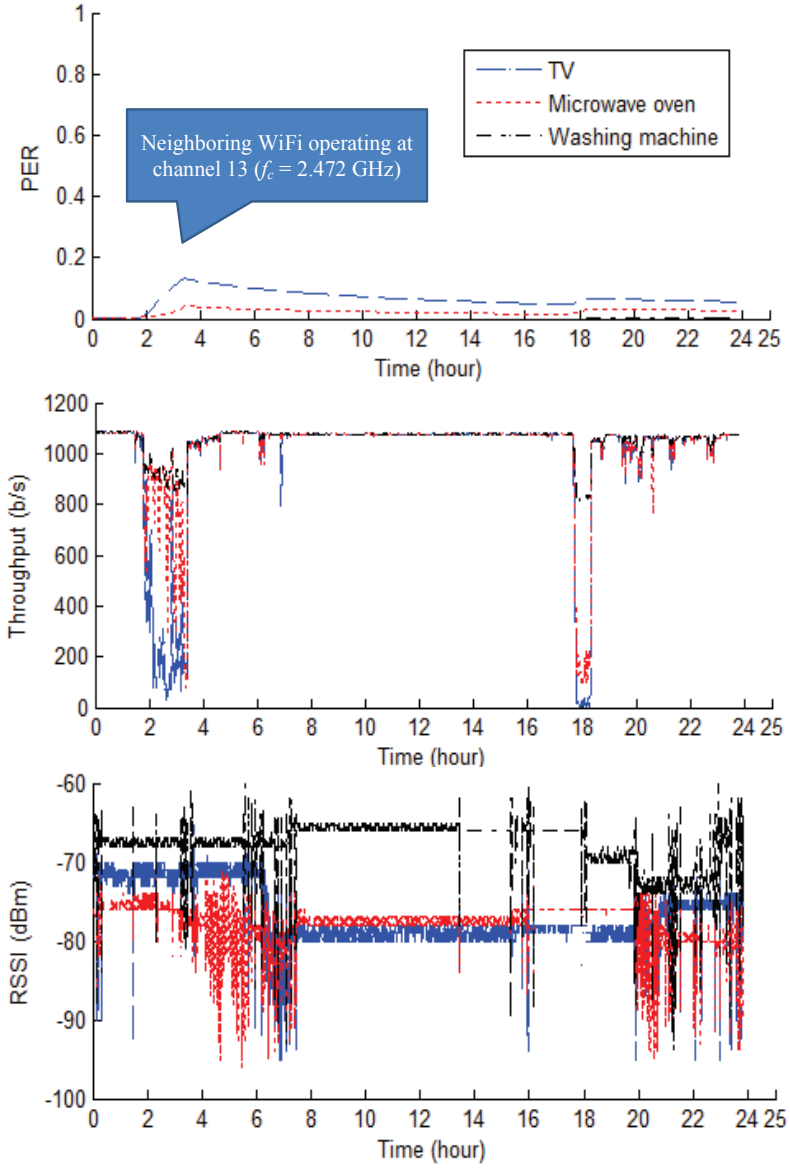

Figure 2.5: ZigBee Frequency Agility mecanism response in a full day ZigBee operation using the best channel among the available 16 channels in HAN.

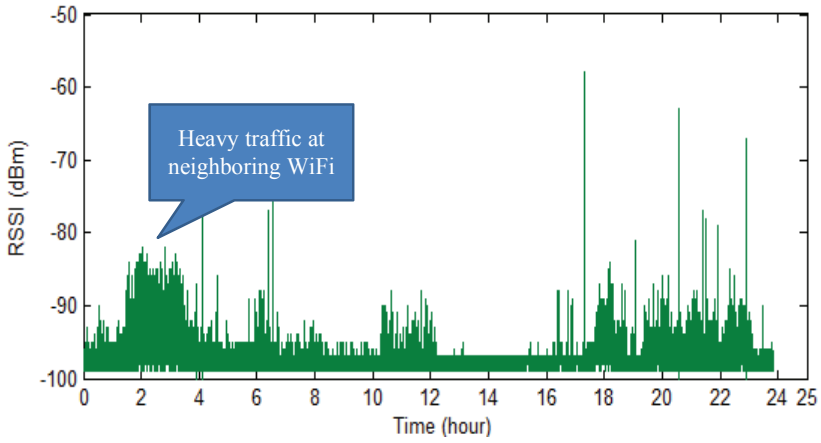

Figure 2.6: Energy level of ZigBee channel 26 before each packet transmission during Experiment 1.

for the ZigBee network operation, this does not guarantee that the chosen channel is the best channel for every ZigBee End-Device in the house. The reason is that the best channel selected for the ZigBee network operations is only based on the channel scan result of the ZigBee Coordinator while excluding the channel information from the ZigBee End-Devices. Hence, the channel chosen might not be the best channel for all ZigBee End-Devices; particularly in this case, the smart TV. Therefore, it is promising if the channel information from all devices are included during the channel selection in order to obtain a better common best channel. The drawback of this is that all ZigBee End-Devices also need to scan the channel each time interference is detected within the network. This will raise the problem of energy efficiency.

Furthermore, it is difficult to find a common best channel for all ZigBee devices in the network. The best channel for some devices might not be the best channel for the others. Therefore, it is interesting if the network could operate using more than one channel, forming a distributed multi-channel network. Hence, the channel can be selected based on the local best channel. Moreover, the distributed multi-channel network feature could also reduce the energy efficiency problem in including the information from each ZigBee device for channel selection where only the channel information from the devices which are in the affected area need to be acquired.

Experiment 2

The performance of the ZigBee Frequency Agility mechanism in mitigating WiFi and microwave oven interference is illustrated in Figure 2.7. As can be seen, the PER of all ZigBee End-Devices increases progressively due to the WiFi signal from the video streaming application. Once the PER of one of the ZigBee End-Devices exceeds 0.25, in this case the smart TV, the Frequency Agility mechanism responded by switching to a better channel, which in this case is channel 26 at $f_{\mathrm{c}} = 2.480$ GHz. As observed, ZigBee WPAN communication improves significantly after the Frequency Agility mechanism initiated a switch of frequency. From the results, it can be concluded that the ZigBee Frequency Agility mechanism performs effectively in mitigating WiFi interference.

Next, we turn on the microwave oven at around 10.5 minutes after the start of the ZigBee network. It can be seen that the microwave oven signal only affects the ZigBee communication of the microwave oven while the other ZigBee End-Devices maintain the PERs at around zero. When the PER of the microwave oven reaches the Frequency Agility interference detection threshold, the ZigBee Coordinator will evaluate the channel and initiate a channel switch. However, this mechanism does not actually help since the microwave oven signal radiates over the entire ISM 2.4-GHz band, hence changing the channel within the same band will not improve the communication performance. Therefore, the potential of the ZigBee Frequency Agility mechanism to move the network to other bands such as 800 MHz, 900 MHz or the TV Whitespace is very interesting. Finally, the ZigBee network becomes stable after the microwave oven operation ends at around 18.5 minutes.

Notice that in the ZigBee Frequency Agility mechanism, transmission in the downlink (i.e., the ZigBee Coordinator to the End-Devices) is monitored while the uplink packet transmission is ignored. It is important to note that, for some applications (i.e., smart metering) there can be only uplink traffic. Hence, the ignorance of uplink packets failure are unacceptable as this might cause a failure in the ZigBee Frequency Agility mechanism; it fails to detect the presence of interference in the network. In addition, due to the use of a single channel for the whole ZigBee network in a single home, the channel switch made by the ZigBee Frequency Agility mechanism affects all the ZigBee devices including the devices that have a good communication link such as the washing machine. Furthermore, it can be observed that the interference in the HAN is localized in a certain area and only affected certain devices. Therefore, the mechanism used in ZigBee Frequency Agility which is changing the channel of all devices in the network to mitigate a local interference

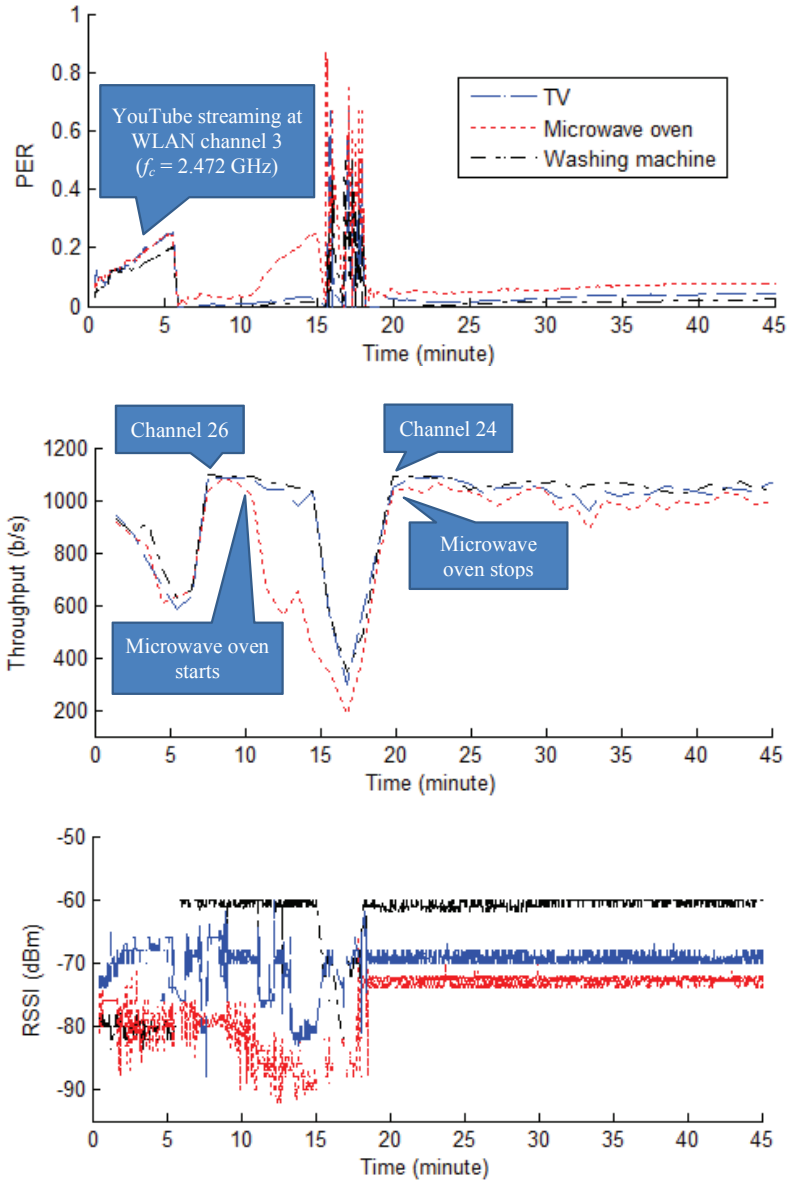

Figure 2.7: ZigBee Frequency Agility mecanism response under harmful WiFi and microwave oven interference.

is inefficient. Again, a distributed multi-channel network is seen as a promising solution.

2.3 Clustered Cognitive Radio-based Communication for Home Area Networks

Wireless communications characteristics in a house might highly vary from one location to another due to different obstacles, layout and size of the house. In addition, the number of devices in a house might also differ from house to house and from room to room. Therefore, clustering is seen as a promising feature in ensuring the scalability and flexibility of HAN communication networks thus ensuring all areas in the house are covered and the devices' demands (e.g., throughput) are satisfied. By clustering, the coverage area can be expanded by deploying a new cluster head (CH), while a high load in a cluster can be reduced by offloading it to another cluster. Besides, from the shown results and the given discussions in Section 2.2.3, it can be concluded that different areas in a house are affected by different neighboring wireless networks in particular for a house that is situated in a dense city. Clustering enables different areas in the house to use different communication parameters (e.g., channel) thus making it easier to find, for example a common idle channel to be used by the HAN devices to communicate.

In addition, it is also shown that the already congested ISM frequency bands are not sufficient to support the communication needs [3], including PER and throughput, of a HAN. The possibility of accessing other bands including the licensed bands (particularly the TV band), would be very beneficial. Cognitive radio (CR) is seen as one of the most promising technologies to enable this feature [3, 6, 7, 9, 34]. CR technology enables the HAN devices to sense and intelligently exploit any idle spectrum for their communications.

In this thesis, we aim at designing an efficient clustered cognitive radio-based communication for heterogeneous and dense home area networks that is situated at a high density residential area, which is conceptually shown in Figure 2.8. This figure shows three adjacent home networks indicated as HAN A, HAN B and HAN C. Each hexagon represent a cluster, which can be set to cover a certain area of the house. For instance, there are five clusters in HAN A, which cover Living Room, Bedroom 1, Bedroom 2, Bathroom and Kitchen. Each cluster will be able to cognitively organize itself in choosing good channel (or channels) for operation. Different areas of the house can utilize different sets of channels. The channels

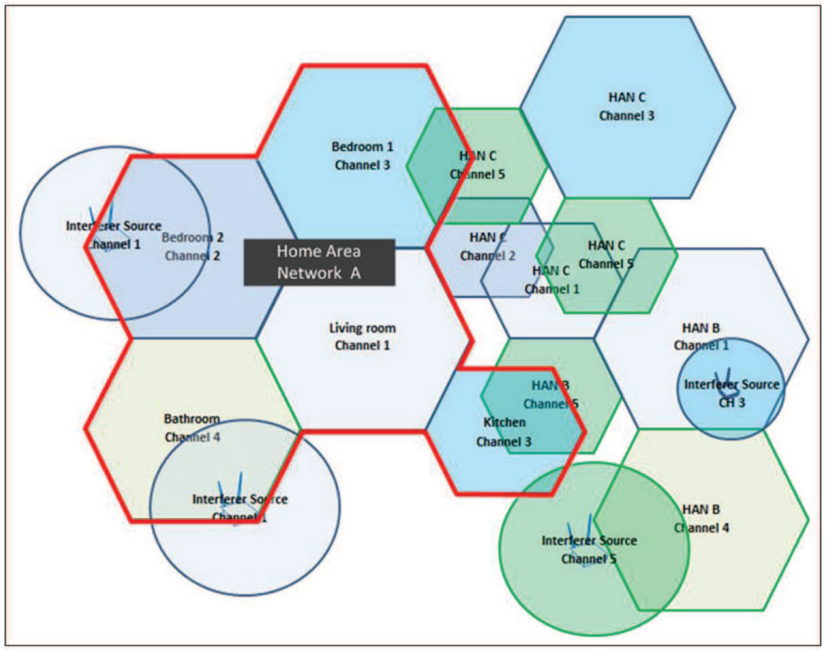

Figure 2.8: The proposed distributed multichannel communication network based on clustered cognitive radio communication technique for heterogeneous and dense HAN situated at a high residential density area in dense cities.

are chosen based on the local environment of the area. For example, Bedroom 2 operates in Channel 2 because there is an interference source that uses Channel 1 within the coverage area; while, Bedroom 1 utilizes Channel 3 because the adjacent cluster (Bedroom 2) is already using Channel 2, and there are two neighbor's (HAN C) clusters operating on Channel 5 and Channel 2. As a result, the proposed scheme enables the HAN to form an efficient multi-channel communication network that mitigates the interference problem and at the same time fulfills the HANs communication needs.

2.4 Wireless Network Categories

In essence, wireless networks can be categorized in licensed and unlicensed networks as illustrated in Figure 2.9. The licensed networks are the wireless networks that operate using dedicated spectrum bands. These bands are allocated by the regulator such as FCC and Ofcom in the United States and the United Kingdom,

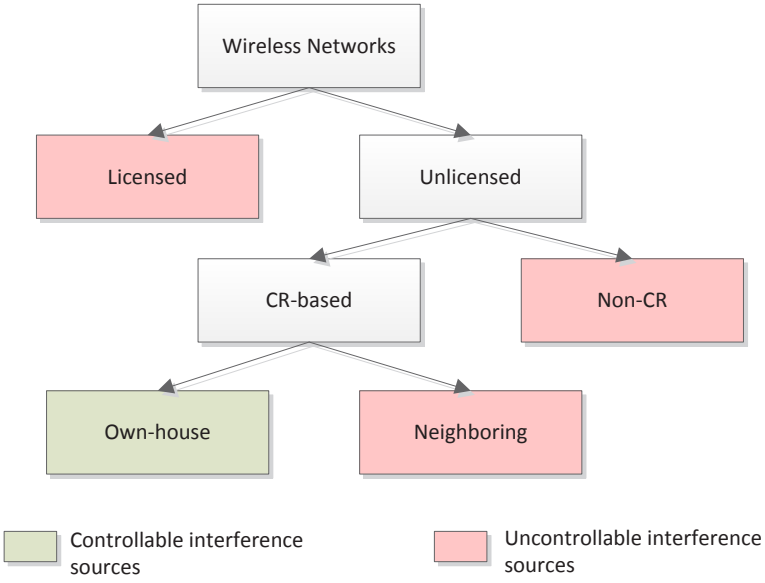

Figure 2.9: Categories of wireless networks.

respectively. Some examples of this type of networks include GSM, TV and Radio broadcasting, and an in-house cellular Femtocell.

On the other hand, unlicensed networks are wireless networks that can access the spectrum freely without any spectrum allocation [46]. This type of networks is further divided into two types: non-CR and CR-based. The non-CR type of unlicensed networks are networks that operate in license-exempted spectrum bands such as the ISM 2.4-GHz and the ISM 5-GHz. Typical examples of this type of networks include WiFi, Bluetooth and ZigBee. Relatively newer, CR-based networks are networks that could operate beyond the license-exempted bands while following certain rules and regulations. Obviously, the proposed networks in this thesis fall under this category i.e., CR-based networks. Additionally, in this thesis, we further classify the CR-based networks into two categories: own-house networks and neighboring networks. The own-house CR-based networks are the CR-based networks which are owned by the house-owner while other networks are classified as neighboring networks.

Among these networks, the own-house CR-based networks are the only type of networks of which we can control its interference using the proposed communication protocol. This is, we could manage the spectrum usage of the networks such that they are only using an interference free spectrum, and at the same time

they do not cause any harmful interference to the others. For the other types of networks, we manage the interference caused to or by them by using CR spectrum sensing methods i.e, we avoid our networks from using the same spectrum as these networks.

2.5 Cognitive Radio Spectrum Sensing

One of the key components for CR-based networks is spectrum sensing, used to reliably identify temporarily unused spectrum which can then be exploited. The significance of spectrum sensing is twofold: protect the band-owner from being interfered by CR-based devices, and ensuring that CR-based devices are communicating in a strongly reduced interference environment. Among the main challenges in spectrum sensing is: longer sensing time is required to produce a more accurate sensing result; however this will decrease the communication throughput and increase the energy overhead. In addition, an individual spectrum sensing measurement suffers from uncertainty due to noise, fading and shadowing [36].

A natural solution in coping with these challenges is through device cooperation, known as cooperative spectrum sensing (CSS). This approach is found to be robust to cope with different channel conditions at different sensing devices. CSS can considerably improve the sensing efficiency, reliability, latency as well as the energy constraint problem of certain sensing devices, by sharing the sensing loads between different network nodes.

In this section we mention some of the key equations regarding the cognitive radio spectrum sensing which will be used in subsequent chapters.

2.5.1 Cooperative Spectrum Sensing

Figure 2.10 shows a general network diagram in CSS. It consists of a fusion center, denoted as FC, and N number of cooperating sensing devices, denoted as $j = 1, 2, \ldots, N$. Each cooperating sensing device will periodically sample the spectrum and send its local spectrum sensing result to the FC (in our case, this is the cluster head (CH)). The FC will combine these local spectrum sensing results using a certain fusion strategy to make the final decision on whether the sensed spectrum is idle or not. In this work, a hard-fusion strategy is considered in which each cooperating sensing device makes a local decision and sends only this decision to the FC. The local decision is a binary hypothesis test: decide whether the sensed channel is idle, given by hypothesis $\mathcal{H}_0$, or occupied, given by hypothesis $\mathcal{H}_1$. Each

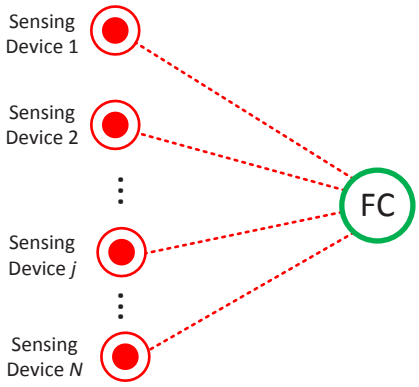

Figure 2.10: General cooperative spectrum sensing network model.

of the spectrum-samples observed by each sensing device j can be modeled as

$$x_j[l] = \begin{cases} w_j[l] & : \mathcal{H}_0 \\ u_j[l] + w_j[l] & : \mathcal{H}_1 \end{cases} \tag{2.3}$$

where $l = 1, 2, \ldots, L_j$. Here, L_j is the total number of observation samples made by sensing device j within the local spectrum sensing period T_{s_j} such that $L_j = {}^{T_{\mathrm{s}_j}}/_{\tau}$, where τ is the sampling period. Further, $u_j[l]$ is the received incumbent signal and $w_j[l]$ is the additive noise signal at device j during the l-th sample. $u_j[l]$ is given by $u_j[l] = s[l] * h_j[l]$, where $s[l]$ is the transmitted incumbent signal and $h_j[l]$ is the impact of the Rayleigh fading channel between the incumbent user and device j. Note that $u_j[l]$ does not contain the impact of additive noise but the additive noise component is taken into account in $w_j[l]$. Both $w_j[l]$ and $u_j[l]$ are assumed to be independent and identically distributed (i.i.d.) random processes with zero mean and variance $\sigma^2_{w_j}$ and $\sigma^2_{u_j}$, respectively.

In this work, energy detection is considered for spectrum sensing where the estimator can be expressed as

$$\hat{E}_j = \frac{1}{L_j} \sum_{l=1}^{L_j} x_j^2[l]. \tag{2.4}$$

$\hat{E}_j$ is the output of the energy detector which is used as input for a binary hypothesis test of the sensing device. In the test, $\hat{E}_j$ is compared to a predefined threshold γ

to decide on hypothesis $\mathcal{H}_0$ or $\mathcal{H}_1$. The performance of this test is characterized by two metrics: the probability of detection (P_{d_j}) and the probability of false alarm (P_{f_j}). The probability that a sensing device decides that the channel is occupied (i.e., $\hat{E}_j > \gamma$) under $\mathcal{H}_1$ is given by

$$P_{\mathrm{d}_j} = P(\hat{E}_j > \gamma \mid \mathcal{H}_1) \tag{2.5}$$

while the the probability that a sensing device decides that the channel is occupied under $\mathcal{H}_0$ is

$$P_{\mathrm{f}_j} = P(\hat{E}_j > \gamma \mid \mathcal{H}_0) \tag{2.6}$$

If the incumbent signal is assumed to be a binary phase shift keying (BPSK) modulated and the noise is modeled as additive white Gaussian noise (AWGN), then from [18, 21], for a targeted $\bar{P}_{\mathrm{d}_j}$, the corresponding probability of false alarm P_{f_j} can be expressed as

$$P_{\mathrm{f}_j}(\bar{P}_{\mathrm{d}_j}, \mathrm{SNR}_{\mathrm{p}_j}, T_{\mathrm{s}_j}) = \mathcal{Q}\left(\mathrm{SNR}_{\mathrm{p}_j}\sqrt{\frac{T_{\mathrm{s}_j}}{2\tau}} + \mathcal{Q}^{-1}(\bar{P}_{\mathrm{d}_j})\sqrt{1+2\mathrm{SNR}_{\mathrm{p}_j}}\right) \tag{2.7}$$

where $\mathcal{Q}(\cdot)$ denotes the statistical Q-function (the tail probability of the standard normal distribution), and $\mathrm{SNR}_{\mathrm{p}_j} := \sigma^2_{u_j}/\sigma^2_{w_j}$ is the signal-to-noise-ratio of the incumbent user at sensing device j. Alternatively, if a target $\bar{P}_{\mathrm{f}_j}$ needs to be achieved, the achievable P_{d_j} can be formulated as [18, 21]

$$P_{\mathrm{d}_j}(\bar{P}_{\mathrm{f}_j}, \mathrm{SNR}_{\mathrm{p}_j}, T_{\mathrm{s}_j}) = \mathcal{Q}\left(\frac{1}{\sqrt{1+2\mathrm{SNR}_{\mathrm{p}_j}}}\left(\mathcal{Q}^{-1}(\bar{P}_{\mathrm{f}_j}) - \mathrm{SNR}_{\mathrm{p}_j}\sqrt{\frac{T_{\mathrm{s}_j}}{2\tau}}\right)\right). \tag{2.8}$$

It can be seen from (2.7) and (2.8) that any pair of $\bar{P}_{\mathrm{f}_j}$ and $\bar{P}_{\mathrm{d}_j}$ can be satisfied if the local spectrum sensing time T_{s_j} is not restricted, i.e.,

$$T_{\mathrm{s}_j}(\mathrm{SNR}_{\mathrm{p}_j}, \bar{P}_{\mathrm{f}_j}, \bar{P}_{\mathrm{d}_j}) = \frac{2\tau}{\mathrm{SNR}^2_{\mathrm{p}_j}}\left(\mathcal{Q}^{-1}(\bar{P}_{\mathrm{f}_j}) - \mathcal{Q}^{-1}(\bar{P}_{\mathrm{d}_j})\sqrt{1+2\mathrm{SNR}_{\mathrm{p}_j}}\right)^2. \tag{2.9}$$

The plot of device j's probability of false alarm P_{f_j} and probability of detection P_{d_j} with respect to the corresponding sensing time T_{s_j} for different incumbent user SNR at device j, i.e., $\mathrm{SNR}_{\mathrm{p}_j}$, is shown in Figure 2.11. In general, it can be seen that a longer T_{s_j} or/and a higher $\mathrm{SNR}_{\mathrm{p}_j}$ give a more reliable sensing outcome (i.e., lower P_{f_j} and higher P_{d_j}).

For CSS with a hard-fusion strategy, the FC makes the final decision and decides $\mathcal{H}_1$ if at least K out of N cooperating sensing devices have decided that

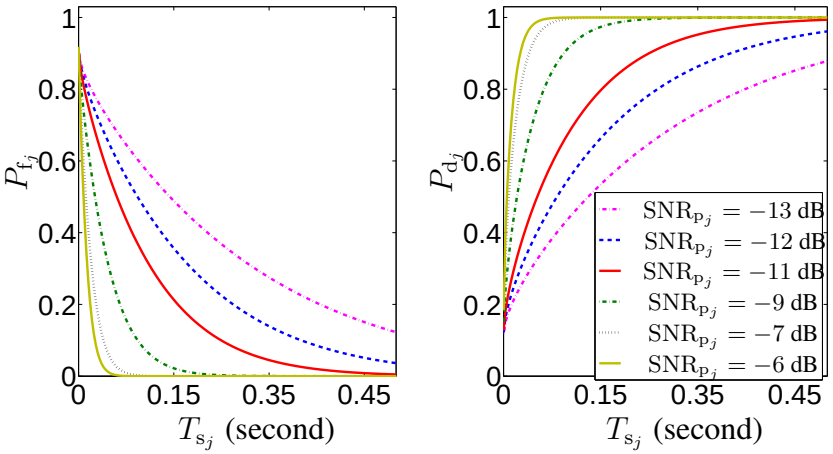

Figure 2.11: Device j's (a) false alarm probability P_{f_j}, and (b) detection probability P_{d_j}, versus T_{s_j} for different $\mathrm{SNR}_{\mathrm{p}_j}$. P_{d_j} is fixed at 0.9 for (a) and P_{f_j} is fixed at 0.1 for (b).

the channel is occupied; otherwise $\mathcal{H}_0$ will be decided. This strategy is known as the K-out-of-N fusion rule. The cooperative probability of detection Q_{d} and false alarm Q_{f} under this fusion rule can be derived using the Poisson-Binomial distribution theorem as [20, 47, 48]

$$Q_{\mathrm{d}} = \sum_{k=K}^{N} \sum_{\mathcal{A}_k^{(a)} \in \mathcal{A}_k} \prod_{g \in \mathcal{A}_k^{(a)}} P_{\mathrm{d}_g} \prod_{h \in \{\mathcal{N} \setminus \mathcal{A}_k^{(a)}\}} (1 - P_{\mathrm{d}_h}) \tag{2.10}$$

$$Q_{\mathrm{f}} = \sum_{k=K}^{N} \sum_{\mathcal{A}_k^{(a)} \in \mathcal{A}_k} \prod_{g \in \mathcal{A}_k^{(a)}} P_{\mathrm{f}_g} \prod_{h \in \{\mathcal{N} \setminus \mathcal{A}_k^{(a)}\}} (1 - P_{\mathrm{f}_h}) \tag{2.11}$$

where

$\mathcal{N} = \{1, 2, \ldots, N\}$ is a set consisting of all cooperating sensing device indices;

$\mathcal{A}_k$ is a set consisting of all possible subsets of k elements of $\mathcal{N}$, representing the k out of N cooperating sensing devices that locally decide that the channel is occupied;

$\mathcal{A}_k^{(a)} \in \mathcal{A}_k$ is one of the sets in $\mathcal{A}_k$, where a is an index such that $a = 1, 2, \ldots, \binom{N}{k}$;

$g, h \in \mathcal{N}$ are cooperating sensing device indices.

There are three special cases in this fusion rule: 1) if $K = 1$, the cooperative detection will become the OR combining rule, 2) if $K = N$, the fusion scheme follows the AND rule, and 3) if $K = \lceil \frac{N}{2} \rceil$, the decision is known as the majority rule (also known as the half-voting rule). In addition, if P_{d_j} (and P_{f_j}), where $j \in \mathcal{N}$, are identical for all devices j (i.e., $P_{\mathrm{d}_j} = P_{\mathrm{d}}$ and $P_{\mathrm{f}_j} = P_{\mathrm{f}}, \forall j$), which can be achieved for example by adapting the sensing time of each sensing device differently according to their $\mathrm{SNR}_{\mathrm{p}_j}$, then (2.10) and (2.11) can be simplified and formulated by using the normal Binomial distribution (instead of Poisson-Binomial), and become

$$Q_{\mathrm{d}} = \sum_{k=K}^{N} \binom{N}{k} P_{\mathrm{d}}^{k} (1 - P_{\mathrm{d}})^{N-k} \tag{2.12}$$

$$Q_{\mathrm{f}} = \sum_{k=K}^{N} \binom{N}{k} P_{\mathrm{f}}^{k} (1 - P_{\mathrm{f}})^{N-k} \tag{2.13}$$

respectively.

In CR, Q_{d} reflects the quality of protection of the band-owner and is determined by the regulator or the standardization body such as the IEEE (for example, in IEEE 802.22, Q_{d} is required to be greater or equal to 0.9, [49]). On the other hand, Q_{f} is important for the CR devices (in our case the CR-based HAN devices). A lower Q_{f} will provide a higher opportunity for the sensing devices to access the spectrum, and hence attain a higher network throughput. Note that IEEE 802.22, which is actually meant for rural areas and to cover large distance, is used as an example because it defines the spectrum sensing specifications (e.g., the probability of detection constraint) that are needed in this thesis. Other newer standards like IEEE 802.11af and IEEE 802.15.4m would be more useful for the home scenarios, but there are no specifications given for the spectrum sensing because they are using a database method instead. In fact, the spectrum sensing parameters (e.g., $Q_{\mathrm{d}} \geq 0.9$ constraint) used in the numerical evaluations and simulations in this thesis are as examples and they can be changed to the desired values.

Figure 2.12 is plotted from equation (2.12) which depict the behavior of the cooperative probability of detection Q_{d} for different local probability of detection P_{d} and minimum number of devices K that decide the channel is occupied. The plot also holds for the cooperative probability of false alarm Q_{f} from the corresponding local probability of false alarm P_{f} that can be produced from equation (2.13). It can be seen that choosing a lower value of K can improve the reliability of detection i.e., higher Q_{d}. On the other hand, this also increases the resulting cooperative false alarm probability Q_{f} which is not of desired. The opposite holds for

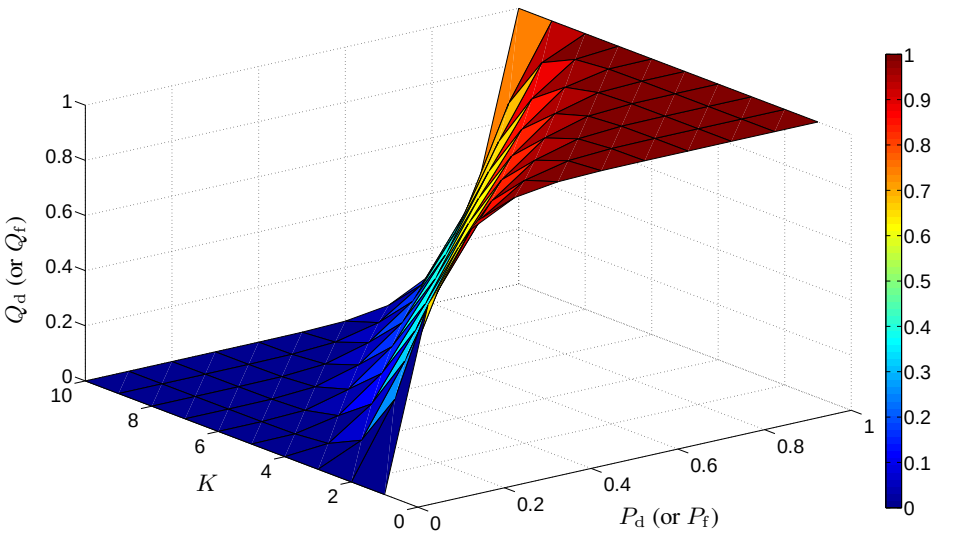

Figure 2.12: The cooperative probability of detection Q_{d} (or false alarm Q_{f}), versus the local probability of detection P_{d} (or false alarm P_{f}) and the minimum number of nodes K that decide the channel is occupied, for $N = 10$.

a higher value of K, in which it produces a better outcome for Q_{f}, but worsen the Q_{d}. Hence, many works in the literature, for example [21, 22, 50], have suggested that the optimal or nearly optimal rule is $K = \lceil \frac{N}{2} \rceil$ i.e., the majority rule.

2.5.2 Channel State Model

We modeled the state of each channel as an ON and OFF alternating renewal process which correspond to $\mathcal{H}_0$ and $\mathcal{H}_1$, respectively. The ON and OFF state are assumed to be independent of each other. This can be expressed using the two-state Markov model that is shown in Figure 2.13. From this, the probability that a channel is idle, which is $\mathcal{H}_0$, can be defined by deriving the steady state probabilities, that is,

$$P(\mathcal{H}_0) = \frac{q}{q+p} \tag{2.14}$$

Whereas, the probability that a channel is occupied (i.e., $\mathcal{H}_1$), which also can be viewed as the utilization of the channel, can be calculated as

$$P(\mathcal{H}_1) = \frac{p}{q+p} = 1 - P(\mathcal{H}_0) \tag{2.15}$$

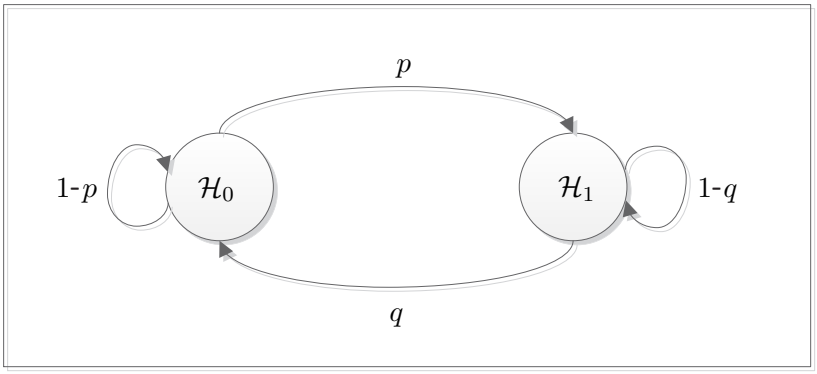

Figure 2.13: Channel state Markov model.

The probabilities $P(\mathcal{H}_0)$ and $P(\mathcal{H}_1)$ can be estimated before the CR network is deployed, i.e., based on a long term measurement or it can be measured online based on, for example, the concept of MAC-layer sensing [26]. In this work, we assume that the value of these probabilities are known.

2.6 Conclusion

In this chapter, we have seen that the communication in future home area network (HAN) will be very challenging, particularly in dense city home environment: i.e., because of the spectrum scarcity and interference problems, and even more challenging, different areas in a house can be affected by different interference sources. As a result, it will be very hard for the current HAN to sustainably support the communication demand that is continuously increasing. In this thesis, we propose a clustered cognitive radio-based communication that can sustainably support the continuously-growing in-house communication (i.e., the HAN) needs. Clustering can provide scalability and flexibility to HAN communication. Moreover, cognitive radio (CR) has been recognized as a technology that is able to intelligently provide more spectrum opportunities, beyond the already crowded unlicensed band, and it is also able to solve the interference problem in wireless communication. The proposed solution results in an efficiently distributed multi-channel communication of a HAN, such that different areas of the house can exploit different communication channels.

We also have mentioned some equations including the local and cooperative detection and false alarm probabilities, the idle and occupied channel probabilities,

and the spectrum sensing time, which will be used later on in following chapters to analyze, evaluate and prove various system designs proposed in this thesis.

In the next chapter, we will present a throughput demand-based cognitive radio solution for home area networks, called TD-CRHAN which aims at tightly satisfying the demanded network throughput by determining the optimal local spectrum sensing time, the number of cooperating sensing devices and the number of active in-band channels needed.

Chapter 3

Meeting the Throughput Demand of Home Area Networks

In the previous chapter, we have mentioned that the cognitive radio technology can be a promising solution to the ever-rising throughput demand, interference, and spectrum scarcity issues of the HAN. In this chapter, we present our proposed throughput demand-based cognitive radio solution for home area networks (TD-CRHAN), aims at effectively and efficiently meet the ever-increasing throughput demand in HAN communication. It is shown numerically and by simulations that a TD-CRHAN can satisfy the requested throughput from the network devices and has high utilization of the available throughput. The analysis further shows that by setting the achievable throughput to be as close as possible to the total demanded throughput (instead of maximizing it), a TD-CRHAN is able to relax the tight cooperative spectrum sensing requirements which significantly improves cooperative spectrum sensing parameters, such as the local spectrum sensing time and the number of cooperative spectrum sensing devices. We then show that these cooperative spectrum sensing parameters can be further improved when additional channels are available.

3.1 Introduction

The growing number of wireless devices for in-house use is causing a more intense use of the spectrum to satisfy the required quality-of-service such as throughput. This has contributed to spectrum scarcity and interference problems particularly in

home area networks (HAN). Cognitive radio (CR) has been recognized as one of the most important technologies which could solve these problems and sustainably meeting the required communication demands by intelligently exploiting temporarily unused spectrum, including licensed spectrum.

A key component of CR-based networks is spectrum sensing, i.e., to reliably identify temporarily unused spectrum which is then exploited. Many existing works on throughput-based spectrum sensing focuses on maximizing the achievable throughput. In [18], the maximum achievable throughput is obtained by optimizing the local spectrum sensing time, subject to a certain level of spectrum owner protection. The work in [20] incorporates the parameters from spectrum sensing (i.e., sensing time and number of cooperating devices that decide the channel is occupied) and spectrum access (i.e., data communication probability), and optimizes those parameters to yield the maximum throughput for a given spectrum set. Further, in [27], the optimal sensing order for the channels is determined based its occupancy history i.e., by correlating the channel availability statistics across time and frequency, in order to maximize the total achievable throughput. In addition, in our previous work [21] and in [22], throughput maximization is achieved by determining the optimal local spectrum sensing time, number of cooperating nodes and fusion strategy. However, aiming at maximizing the achievable network throughput leads to tight requirements on cooperative spectrum sensing parameters (e.g., spectrum sensing time and number of cooperating devices). On the other hand, in practice, every communication network has a certain throughput demand; hence, a maximization of the achievable network throughput without taking into consideration the actual network's needs is inefficient. Throughout this chapter, we refer to this throughput maximization-based solution in spectrum sensing as the conventional case.

In this work, we propose a throughput demand-based cognitive radio communication for home area networks (TD-CRHAN), where instead of maximizing the achievable throughput, the TD-CRHAN seeks to tightly satisfy the network's throughput demand. To the best of our knowledge, this is the first work proposing such an objective for CR-based HAN communication. In the TD-CRHAN, the optimal local spectrum sensing time and number of cooperating devices required for spectrum sensing are determined, and it is shown that these are significantly lower as compared to the values from the conventional scheme. In addition, by taking into consideration the total throughput demand in designing the CR-based HAN, the TD-CRHAN scheme is also able to determine the optimal number of channels needed for the HAN.

We mathematically model the proposed TD-CRHAN scheme and formulate a suitable optimization problem with corresponding constraints. In the derivations, we consider general expressions for the cooperative spectrum sensing performance parameters (i.e., cooperative probability of false alarm, and detection). This supports scenarios in which the signal-to-noise-ratio (SNR) of the incumbent user is not the same at different sensing devices, and supports more general fusion rules, not limited to OR and AND rules only. Note that most of the previous works consider the same incumbent signal strength at all sensing devices and/or only consider OR and AND rules [18, 21, 22, 51] in order to simplify the analytical models and derivations. Assuming the same SNR is not realistic, in particular for indoor environments, due to multipath propagation and because the sensing devices will be located at various locations where for example, devices that are located near the window may receive a relatively strong incumbent user's signal while devices which are located further inside the house will experience a very low signal strength.

Finally, we thoroughly analyze the performance of the TD-CRHAN, numerically and through simulations, where we compare the performance with the conventional scheme, illustrate the impact of different parameter settings, and demonstrate the significant gains obtained from TD-CRHAN.

The remaining of this chapter is organized as follows. Section 3.2 explains the proposed TD-CRHAN; Section 3.3 presents the derivation of the considered system model and the cooperative spectrum sensing, as well as the formulation of the problem and the proposed solution; the numerical analysis and the simulation results are presented in Section 3.4 and 3.5, respectively; and the conclusions are in Section 3.6.

3.2 Throughput Demand-based Cognitive Radio Home Area Network (TD-CRHAN)

3.2.1 TD-CRHAN Topology

The proposed TD-CRHAN topology is based on a network of clustered CR devices as shown in Figure 3.1. It consists of a HAN gateway (G), a cognitive HAN controller (C), a number of cognitive cluster heads (CHs) and many CR-based HAN devices. In such a network, the cognitive HAN controller is connected to the HAN gateway with a fixed connection while the CHs are linked to the cognitive HAN controller through wireless multi-hop links. The CHs are deployed such that each area of the house is covered. The communication among CHs is in a meshed man-

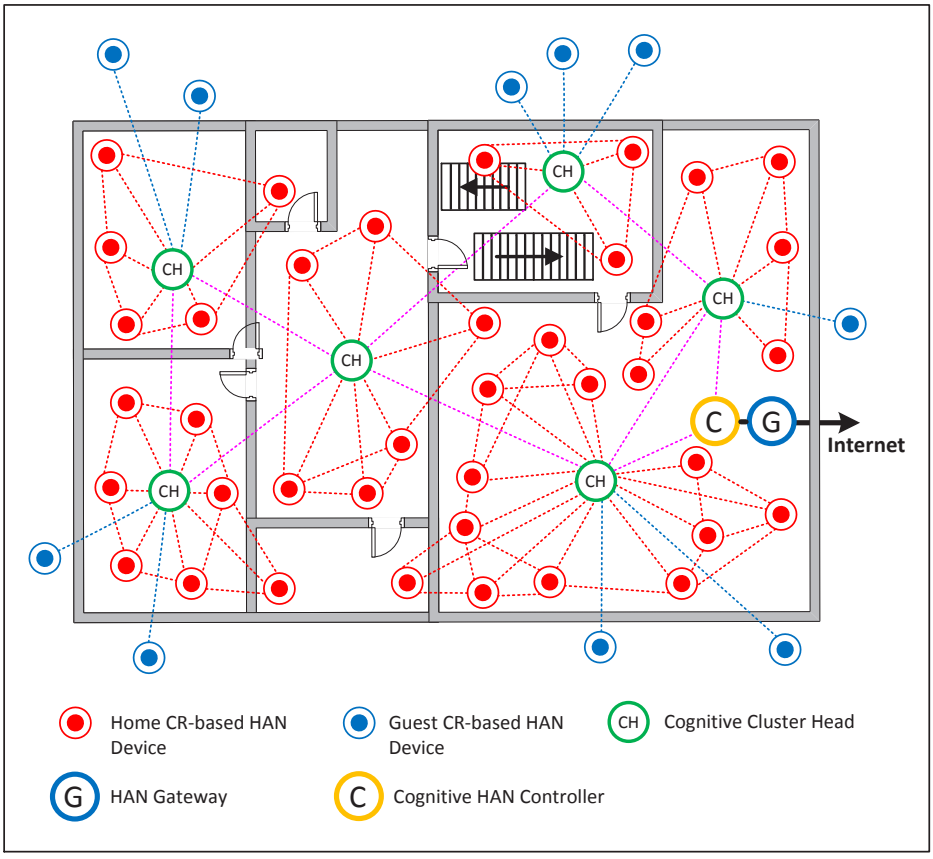

Figure 3.1: The proposed network topology of TD-CRHAN.

ner. Each CH will form a network cluster. The CR-based HAN devices will need to connect to one of the clusters in order to communicate with or through the HAN network.

The functionalities of each network component are further described as follows.

The HAN gateway is the communication gateway for the HAN network to the outside world (i.e., the internet). Normally, the HAN gateway is connected to the internet service provider (ISP) for internet access through an Ethernet or Optical Fiber cable. The other possible connection is via a wireless link e.g., the WiMAX or LTE network.

The cognitive HAN controller is the device that is responsible to manage and coordinate the spectrum usage of the HAN. For this, the cognitive HAN controller needs to construct a spectrum map database for the particular HAN environment. This database consists of a list of channels that the CH can use in their cluster, and the condition of each channel i.e., the statistics of the channel activities including channel utilization. It is constructed from the information fed by the CHs using for example the concept of MAC-layer sensing [26]. From this database, the cognitive HAN controller will provide the CHs with the channels that they could scan and utilize for their cluster. Therefore, the channels that the CHs are going to exploit are optimal and not random. In addition, in this way, the cognitive HAN controller also knows which channels are being utilized by which CHs and which are still unallocated. In this work, the channels that are allocated to the CHs are called in-band channels while the channels that are not allocated are called candidate channels. This concept is illustrated as in Figure 3.2.

The cognitive cluster head (CH) is responsible to manage the usage of the clusters in-band channels including sensing and access. A CH can request for more channels from the cognitive HAN controller if the current in-band channels are not enough to support its network cluster demand. Each CH will utilize different channels from the other CHs creating a distributed multi-channel network in the HAN. In addition, a CH is also responsible for selecting and grouping the CR-based HAN devices that are connected to it to perform the cooperative spectrum sensing (CSS) task. Besides, it also needs to schedule and distribute the selected and grouped CR-based HAN devices on when and where to sense, respectively. For CSS, a CH also acts as the

fusion center where the local sensing results from the sensing devices will be reported to and the decision of spectrum availability will be made. Last but not least, from the CSS results, a CH is required to report the channel utilization and occupancy to the cognitive HAN controller periodically in order for the controller to construct and keep the spectrum map database up to date.

CR-based HAN devices are the devices that carry out various HAN applications including smart grid, security and safety, and home automation. These devices will connect to one of the clusters to get access and communicate with or through the HAN network. Besides performing the communication for its application, CR-based HAN devices also need to execute the spectrum sensing task. We consider two types of CR-based HAN devices: home and guest devices. Home devices are devices which belong to the HAN-owner, while guest devices do not belong to the HAN-owner. An example of a guest device is a neighbor's device which needs to off-load its traffic, e.g., due to congestion in its own HAN network. Another example is a device that passes through the house and wants to connect to the internet through the HAN network. For the home CR-based HAN devices, the communication topology within the cluster is in a mesh. However, the guest devices are only allowed to connect to the CH.

3.2.2 TD-CRHAN Operation

In TD-CRHAN, CR-based HAN devices need to be connected to one of the clusters in order to get access and communicate with or through the HAN network. For this, any cluster joining mechanism such as listed in [52] can be applied. One of the simple mechanisms is as employed in the IEEE 802.22 standard [49]. In this standard, the CH transmits a beacon at the beginning of each frame in each of the in-band channel. Alternatively, this beacon can be sent in one of the highest quality in-band channels. A CR-based HAN device will search for one of these beacons at its start-up and connect to the corresponding CH's cluster once the beacon is found. If the CR-based HAN device can hear beacons from multiple CHs, it may choose to join either one cluster based on for example the signal strength and/or the signal quality of the received beacons [52].

Figure 3.3 illustrates the TD-CRHAN operation for one network cluster. In a TD-CRHAN, the bandwidth of the cluster is adaptable, it can be expanded or shrunk depending on the total throughput demand of the network cluster. In the

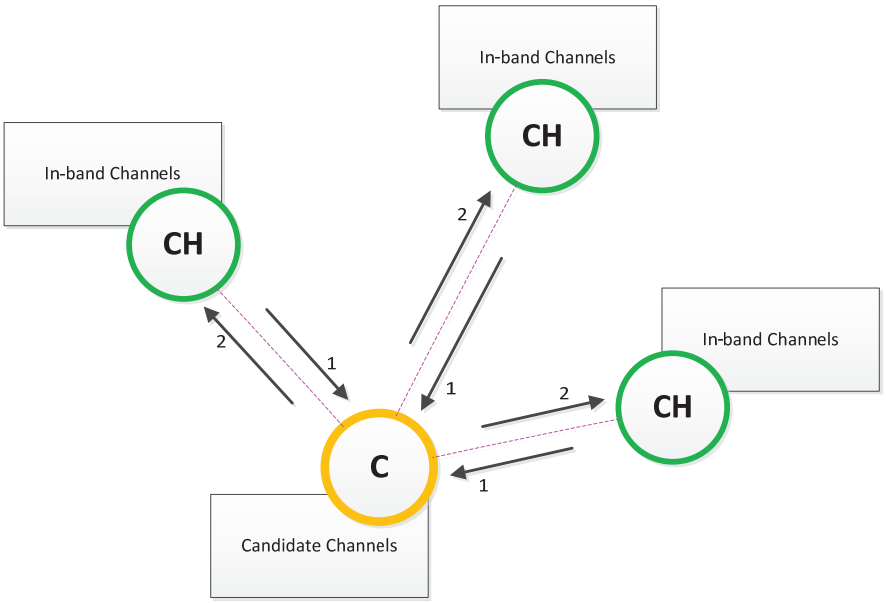

Figure 3.2: The proposed spectrum management in TD-CRHAN.

example in the figure, at time t_0, the cluster only uses one in-band channel i.e., channel B. When the cluster needs more bandwidth i.e., at time t_1 and t_4, for example due to a new connected device, the number of in-band channels is increased to two channels with the addition of channel A, and to three channels with the addition of channel C, respectively. Note that in CR, each channel has to be first sensed before it can be used for any data transmission. Hence, data transmission using channel A and C only can be done after t_2 and t_5, respectively. This additional in-band channels are obtained from the pool of candidate channels at the cognitive HAN controller. This process is illustrated by the arrows labeled 2 in Figure 3.2. The cognitive HAN controller will provide the cluster with the best candidate channels it has. These channels will be passed on to the CH.

In addition, at time t_{10}, the cluster shrinks its bandwidth by releasing one of its in-band channels that is channel D due to a decrease in the network demand e.g., due to a device leaving the cluster. The released channel is selected from the lowest quality channels among the in-band channels. This channel will be returned to the cognitive HAN controller and becomes a candidate channel that can be used

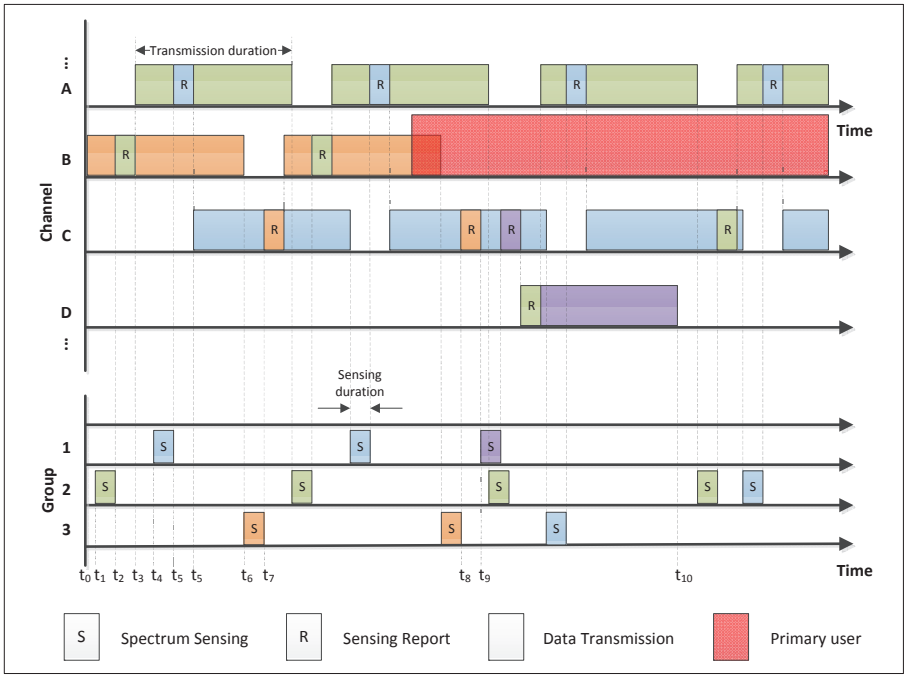

Figure 3.3: An example of TD-CRHAN operation.

by other clusters. This process is illustrated by the arrows labeled 1 in Figure 3.2.

During typical CR operation, spectrum sensing will be executed first before any channel can be used for data communication. In this work, the CSS method is considered. Therefore, the sensing operations will consist of spectrum sensing and reporting segments. For this, the CR-based devices will be grouped together forming multiple spectrum sensing groups in the cluster. For instance, in Figure 3.3, three sensing groups are formed: group $1, 2$ and 3. The CH will schedule and distribute the spectrum sensing tasks among these groups. In doing so, the CH has to ensure as much as possible that the group which is scheduled for sensing does not have any group member involved in active communication during this sensing period.

The CH also acts as the CSS's fusion center. Unlike in conventional CSS where the sensing results are transmitted either at the same sensed channels as in [21, 22] or by using a dedicated common control channel as in [20, 28], in TD-CRHAN, the sensing results are transmitted in one of the active data communication slots of the in-band channels as shown in Figure 3.3. For this, the CH will inform the sensing groups on which channel the sensing reports should be transmitted and when. This information can be broadcast by the CH through the beacons. In this way, the sensing reporting transmission will not interfere with the incumbent user of the channel, and the quality of the reporting channels is also ensured. Note that the sensing report information is very crucial, hence it needs to be highly reliable [53]. In case the dedicated common control channel is used, a dedicated channel will be required and the reporting transmission could cause this channel to become congested, and thus it may become the bottleneck of the network [28].

If the CSS results show that a channel is highly occupied (often busy), the CH will withdraw this channel from its in-band channels' list and return it to the HAN gateway. In the meantime, the CH can request for an additional in-band channel from the HAN controller to overcome throughput degradation due to this highly occupied in-band channel. This scenario is illustrated at times t_8 and t_9 in Figure 3.3 where the returned channel is channel B and the new channel is channel D, respectively. In this example, the channel is returned to the HAN controller after one time it is sensed to be occupied.

In the next sections, we consider schemes to satisfy the TD-CRHAN network throughput demand with high resource (available throughput) utilization, and we determine the optimal local spectrum sensing time, the number of cooperating sensing devices and the number of active in-band channels needed.

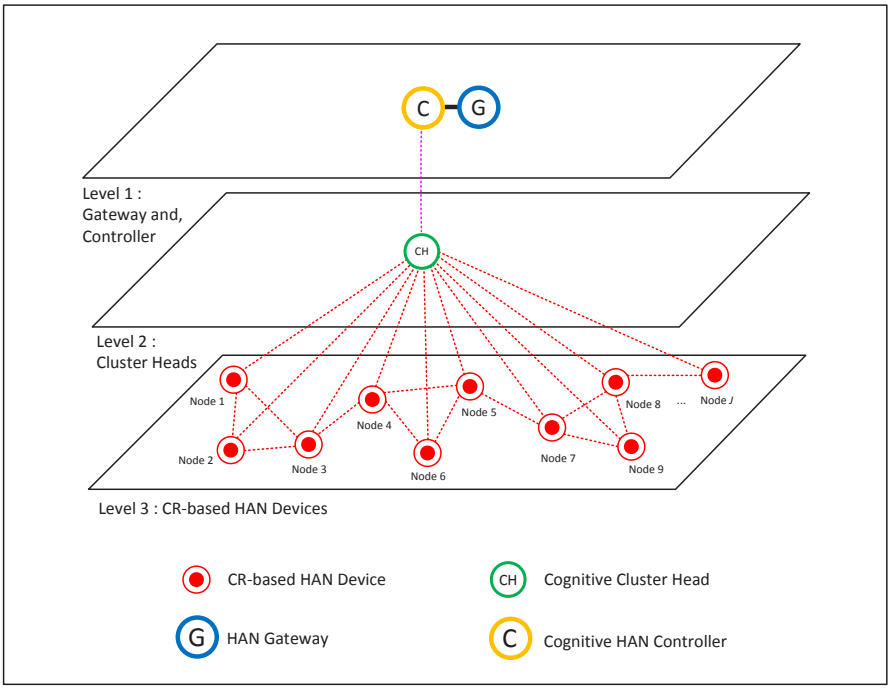

Figure 3.4: Network model diagram for a single TD-CRHAN cluster.

3.3 System Model

A simple network model (one cluster) of the proposed TD-CRHAN network is shown in Figure 3.4. It consists of a HAN gateway (G), a cognitive HAN controller (C), a cluster head (CH) and J CR-based HAN devices indicated as $j, j \in \mathcal{J} = 1, 2, \ldots, J$. Every CR-based HAN device is equipped with a half-duplex radio that can be tuned to any combination of I channels for data communication and reception. This can be done by using, for example, the non-contiguous OFDM (NC-OFDM) technology [54]. Besides data communication, each CR-based HAN device is also able to perform narrow-band spectrum sensing in which the sensed bandwidth is equal to the bandwidth of a single channel.

3.3.1 Problem Formulation

Figure 3.5 shows the timing diagram of a single channel operation where the sensing-transmit task alternates in time. In this figure, T_{sf} is the time duration of a super-

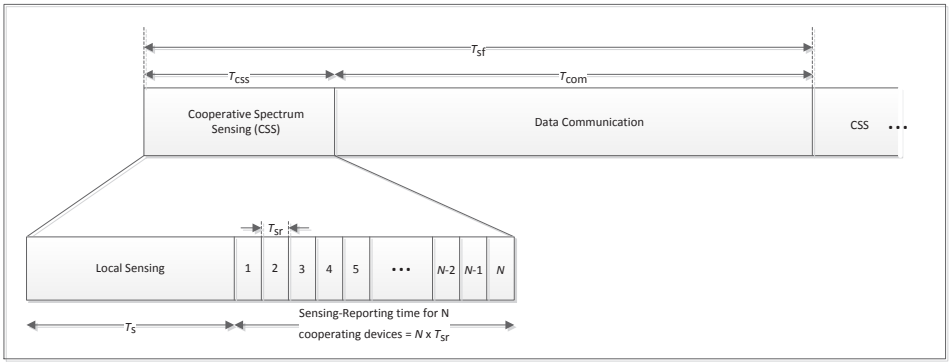

Figure 3.5: TD-CRHAN superframe time for a single channel.

frame which is a constant, and it comprises two sub slots: a sub slot for cooperative spectrum sensing $T_{\rm css}$, and sub slot for data communication $T_{\rm com}$. The former is further divided into two parts namely: a time for local spectrum sensing T_s and the time required to send the sensing result to the CH $T_{\rm sr}$. For reporting the local spectrum sensing result, a TDMA-based channel access scheme is employed, that is: the first CR-based device sends its decision in the first time slot, the second device in the second time slot and so on (the same scheme is considered in [22]); thus, the total reporting time required for N cooperating devices is $N \cdot T_{\rm sr}$.

Note that we have

$$T_{\rm sf} = T_{\rm css} + T_{\rm com} \tag{3.1}$$

$$T_{\rm css} = T_{\rm s} + NT_{\rm sr}. \tag{3.2}$$

In addition, if the data communication's transmission uses rectangular signal pulses, then the maximum data rate for a single channel can be calculated as

$$C = \frac{mW}{2} \quad \text{(bit/second)}. \tag{3.3}$$

where W is the null-to-null bandwidth of the channel, and $m = \log_2(M)$ (bit/symbol) is the modulation order of the transmission when M modulation levels are used.

In cognitive radio, each channel in the spectrum is periodically sensed and may only be utilized for data communication if it is sensed idle, i.e., $\hat{E} < \gamma$ as discussed in Section 2.5.1. This may happen under both $\mathcal{H}_0$ and $\mathcal{H}_1$. Let the achievable throughput under scenario $\mathcal{H}_0$ be R_0. This throughput is smaller than C by a factor $(1 - Q_{\rm f})$, the probability that the channel is correctly detected as idle. Likewise under $\mathcal{H}_1$ the achievable throughput R_1 is smaller than C by a factor $(1 - Q_{\rm d})$,

which is the probability that the occupied channel is wrongly-detected as idle. This probability is significant in case the incumbent signal is weak (e.g., due to the distance from the incumbent node to the CR network).

We also need to consider that for both scenarios the throughput is scaled by a factor $\alpha = T_{\mathrm{com}}/T_{\mathrm{sf}}$, the fraction of time within a superframe that data is transmitted. Using (3.1) and (3.2), we can write α as a function of the sensing time T_s and number of sensing devices N as

$$\alpha(T_{\mathrm{s}}, N) = 1 - \frac{(T_{\mathrm{s}} + NT_{\mathrm{sr}})}{T_{\mathrm{sf}}}. \tag{3.4}$$

Overall, this gives

$$R_0 = \alpha(T_{\mathrm{s}}, N)(1 - Q_{\mathrm{f}})C \tag{3.5}$$

$$R_1 = \alpha(T_{\mathrm{s}}, N)(1 - Q_{\mathrm{d}})C, \tag{3.6}$$

The achievable throughput of a single channel can then be formulated as

$$R = P(\mathcal{H}_0)R_0 + P(\mathcal{H}_1)R_1 \tag{3.7}$$

where $P(\mathcal{H}_0)$ and $P(\mathcal{H}_1)$ are the a-priori probabilities that the channel is idle and occupied, respectively. These probabilities can be estimated before the CR network is deployed based on a long term measurement or it can be measured online based on for example, the concept of MAC-layer sensing [26]. Substituting (3.7) in (3.5) and (3.6) gives

$$R = \alpha(T_{\mathrm{s}}, N)C\left(P(\mathcal{H}_0)(1 - Q_{\mathrm{f}}) + P(\mathcal{H}_1)(1 - Q_{\mathrm{d}})\right). \tag{3.8}$$

Let $R^{(i)}$ be the achievable throughput for channel i, then the total achievable throughput for a cluster with I simultaneously active channels can be calculated as

$$\begin{aligned} R_{\mathrm{t}} &= \sum_{i=1}^{I} R^{(i)} \\ &= \sum_{i=1}^{I} \left[\alpha(T_{\mathrm{s}}^{(i)}, N^{(i)})C\ \left(P(\mathcal{H}_0^{(i)})(1 - Q_{\mathrm{f}}^{(i)}) + P(\mathcal{H}_1^{(i)})(1 - Q_{\mathrm{d}}^{(i)})\right)\right]. \end{aligned} \tag{3.9}$$

where $N^{(i)}$ is the total number of devices used to sense channel i.

Suppose that CR-based HAN device j has a throughput demand of d_j. Then the total throughput demand in a cluster, coming of J CR-based HAN devices, becomes

$$D_{\mathrm{t}} = \sum_{j=1}^{J} d_j \tag{3.10}$$

This information can be acquired by the CH from each connected CR-based HAN device, for example at the time that the device is requesting to join the cluster, or updated by the CR-based HAN device to the CH whenever there is a change in its throughput demand.

Let $\varepsilon = R_{\mathrm{t}} - D_{\mathrm{t}}$ be the difference between R_{t} and D_{t}. Using (3.8)(3.10), we can write ε as

$$\varepsilon(I,\alpha(T_{\mathrm{s}}^{(i)}, N^{(i)})) = \sum_{i=1}^{I} \left[\alpha(T_{\mathrm{s}}^{(i)}, N^{(i)}) C \left(P(\mathcal{H}_0^{(i)})(1 - Q_{\mathrm{f}}^{(i)}) + P(\mathcal{H}_1^{(i)})(1 - Q_{\mathrm{d}}^{(i)})\right)\right] - D_{\mathrm{t}}\,. \tag{3.11}$$

For the CR's spectrum sensing, a cooperative spectrum sensing with energy detection and hard-fusion strategy is considered. The formula for device j's probability of false alarm P_{f_j}, probability of detection P_{d_j}, spectrum sensing time T_{s_j}, and the cooperative probability of false alarm Q_{f} and cooperative probability of detection Q_{d} is given by (2.7)-(2.13), respectively.

3.3.2 Throughput demand-based CR communication

It is important to ensure that the difference between R_{t} and D_{t} is as small as possible. A positive value of ε means that the available throughput of the active channels in the cluster is underutilized while a negative value means that the QoS of the throughput demand is not fulfilled. Notice that in a TD-CRHAN, in case that a cluster's demand is higher than the capacity of a single channel i.e., $D_{\mathrm{t}} > R_{\mathrm{t}}$, the CH in the particular cluster should ask for additional channels from the cognitive HAN controller until the demand is met.

Theoretically, if the number of channels I is unlimited, then the TD-CRHAN scheme can support any amount of throughput demand. With a higher number of channels, we can reduce T_{s} and N (c.f., (3.9)). However, activating more channels will consume more bandwidth. Hence, optimal values of I, T_{s} and N, that can give

the minimum ε should be determined. This optimization problem can be written as

$$\begin{aligned} \min_{I,T_{\mathrm{s}}^{(i)},N^{(i)}} \quad & \varepsilon = R_{\mathrm{t}}(I, T_{\mathrm{s}}^{(i)}, N^{(i)}) - D_{\mathrm{t}} \\ \text{s.t.} \quad & 0 \leq T_{\mathrm{s}}^{(i)} \leq T_{\mathrm{sf}}\,, \quad \forall i \\ & (T_{\mathrm{s}}^{(i)} + N^{(i)} T_{\mathrm{sr}}) \leq T_{\mathrm{sf}}\,, \quad \forall i \\ & Q_{\mathrm{d}}^{(i)} \geq \beta^{(i)}\,, \quad \forall i \\ & \varepsilon \geq 0 \\ & 1 \leq I \leq I_{max} \end{aligned} \tag{3.12}$$

where $T_{\mathrm{s}}^{(i)}$ and $N^{(i)}$ are respectively the spectrum sensing duration and the number of cooperating nodes involved in CSS for channel i; $I_{\max}$ is the maximum number of channels available to be exploited; $Q_{\mathrm{d}}^{(i)}$ is the cooperative probability of detection for channel i and $\beta^{(i)}$ is a lower bound on this. The constraint $\varepsilon \geq 0$ is included to ensure that the throughput demand is met.

It is shown in [19] that the optimal solution for (3.12) can be achieved when constraint $Q_{\mathrm{d}}^{(i)} \geq \beta^{(i)}\ , \forall i$ is satisfied with equality. When this constraint is at equality and for a chosen fusion threshold K (in this chapter, we consider $K = \lceil \frac{N}{2} \rceil$), the corresponding device's probability of detection P_d can be found from $Q_{\mathrm{d}}^{(i)}$ using Equation (2.12). Notice that to use this equation, it is required that the probability of detection P_{d} is the same for all sensing devices, while the effect of different $\mathrm{SNR_p}$ is absorbed by the device's probability of false alarm P_{f} (c.f. Equation (2.7)). Although the simplified equation (2.12) is used to find the probability of detection P_{d}, the general equation (2.11) is used to calculate the cooperative false alarm Q_{f}. In addition, notice that finding the optimal T_{s} and N is equivalent to finding the optimal α (i.e., maximizing α will minimize T_{s} and N); hence, we also can write (3.12) as

$$\begin{aligned} & \min\ \varepsilon(I, \alpha(T_{\mathrm{s}}^{(i)}, N^{(i)})) \\ \text{s.t.,} \quad & 0 \leq T_{\mathrm{s}}^{(i)} \leq T_f \quad , \forall i \\ & (T_{\mathrm{s}}^{(i)} + N^{(i)} T_{\mathrm{sr}}) \leq T_{\mathrm{sf}} \quad , \forall i \\ & \varepsilon > 0 \\ & 1 \leq I \leq I_{\max} \\ & 0 \leq \alpha(T_{\mathrm{s}}^{(i)}, N^{(i)}) \leq 1 \quad , \forall i \end{aligned} \tag{3.13}$$

For this optimization problem, we propose to find the solution by using a two-dimensional search method.

3.4 Numerical Analysis

In this section, we numerically analyze the performance of the TD-CRHAN and compare it with the conventional solution. For this section, let us assume that the $\mathrm{SNR}_{\mathrm{p}_j}^{(i)} = \mathrm{SNR}_{\mathrm{p}}$ and $P(\mathcal{H}_0^{(i)}) = P(\mathcal{H}_0)$ i.e. are the same, for all i and j, and we note that these parameters will be randomized based on a uniform distribution during the simulation analysis (Section 3.5). The following values are considered and fixed throughout this section in which most of them are also used in [22]: $T_{\mathrm{sf}} = 105$ μs, $T_{\mathrm{sr}} = 4$ μs, $\beta^{(i)} = 0.9$ and $W^{(i)} = 5$ MHz, for all i. Moreover, in this work, the majority fusion rule is considered for the CSS as this has been found to be optimal or nearly optimal [21, 22, 50]. For the solution of the optimization problem, we consider $T_{\mathrm{s}}^{(i)} = T_{\mathrm{s}}$ and $N^{(i)} = N$ for all i.

Graphs of ε versus the total number of in-band channels I and a) the data communication time coefficient α, and b) the duration required for local spectrum sensing T_s, are shown in Figure 3.6(a) and (b) respectively, where $\mathrm{SNR}_{\mathrm{p}} = -7$ dB, $P(\mathcal{H}_0) = 0.7$, $N = 6$ and $D_{\mathrm{t}} = 3.5$ Mb/s. Note that, all points on the graphs satisfy every constraint given in (3.13). It is seen that, for each value of $I, \varepsilon(T_{\mathrm{s}})$ and $\varepsilon(\alpha)$ are both concave functions in which the peak points of these functions are the maximum achievable throughput of the cluster. In the conventional CR, these points are considered as optimal. However, it is seen from these graphs that there is an excess throughput (i.e., $\varepsilon > 0$), which is then not going to be used by the network. This throughput underutilization becomes larger with increasing the number of in-band channels I. In contrast, TD-CRHAN tries to find the lowest point of this graph which is the minimum possible ε and at the same time satisfies all the constrains listed in (3.13). By doing this, TD-CRHAN can relax the required local spectrum sensing time T_{s} and the number of cooperating nodes N of the CR system.

From Figure 3.6, the optimal points of the conventional and the proposed TD-CRHAN are taken out and the normalized ε is plotted in Figure 3.7(a), and the corresponding normalized sensing time T_{s} (i.e., fraction of time used for spectrum sensing in a frame) is plotted in Figure 3.7(b). It is seen that ε is linearly proportional to the number of in-band channels I for the conventional case. This is because the total achievable throughput R_{t} for this case is equal to the maximum achievable throughput of each channel multiplied by the total number of in-band channels i.e., $R_{\mathrm{t}} = R \cdot I$ (due to the above assumptions, we have $R^{(i)} = R, \ \forall i$); hence, the larger I, the higher ε irrespective of the D_{t}. On the other hand, in a TD-CRHAN, R_{t} is adjusted as near as possible to D_{t}, which is actually the mini-

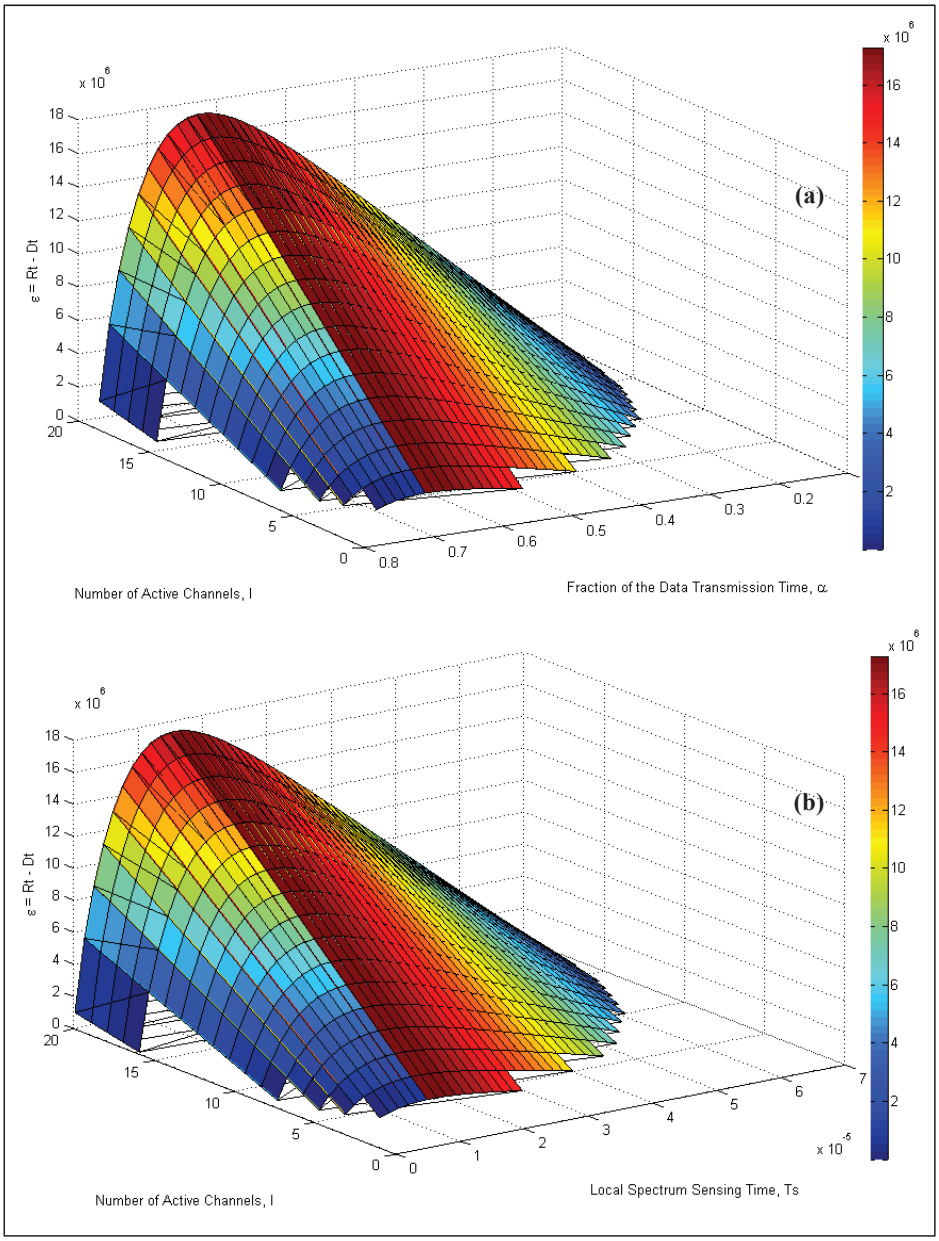

Figure 3.6: The difference between the total achievable- and demanded- throughput (i.e. ε) versus (a) I and α, and (b) I and T_{s}, with $Q_{\mathrm{d}} = \beta$, $D_{\mathrm{t}} = 3.5$ Mb/s, $N = 6$.

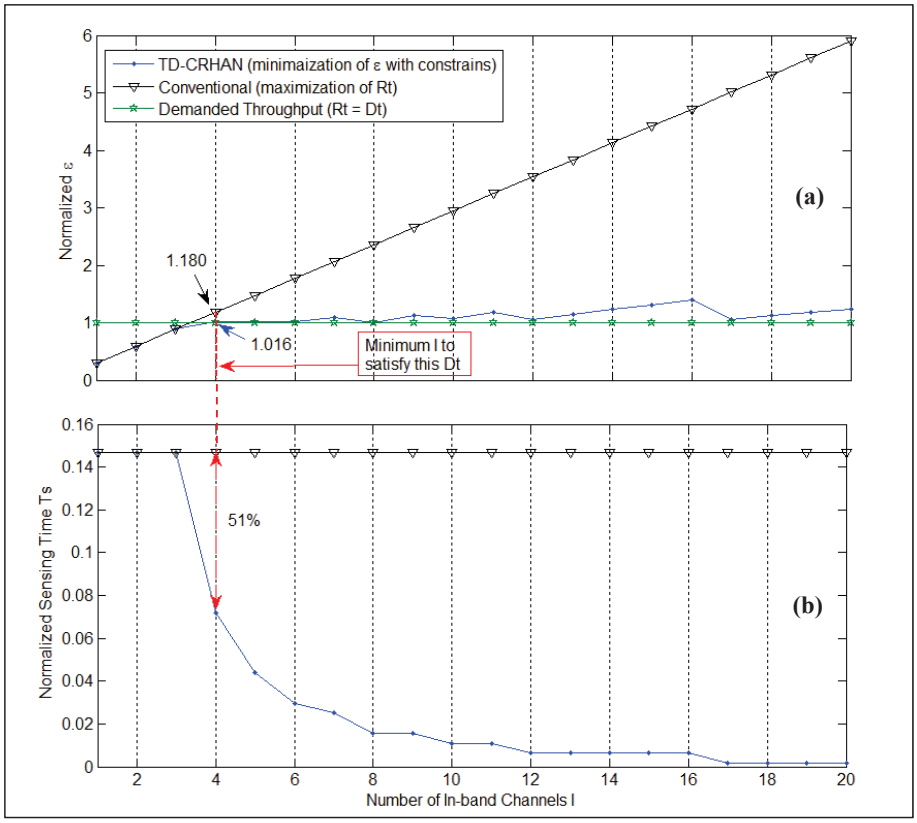

Figure 3.7: Effects of different total number of in-band channels I on (a) normalized $\varepsilon = \frac{\varepsilon}{D_{\mathrm{t}}}$, and (b) fraction of time used for spectrum sensing (i.e., normalized sensing time $= \frac{T_{\mathrm{s}}}{T_{\mathrm{sf}}}$). This is a comparison between TD-CRHAN and the conventional scheme. For this, D_{t} is fixed at 3.5 Mb/s and $N = 6$

mization of ε with constraints. As a result, it can be seen that with a TD-CRHAN scheme, ε is maintained as low as possible, and the spectrum sensing time T_{s} is significantly relaxed as compared to the conventional scheme (as shown in Figure 3.7(b)). These gains become larger as I becomes higher. It is also denoted in Figure 3.7(a) that the minimum I required to satisfy D_{t} is 4. Projecting this point to Figure 3.7(b) (as depicted by the red arrows) shows that, even at this point, TD-CRHAN obtains around 51% gain on the required T_{s} in comparison with the conventional case.

Further, the impact of the number of cooperative sensing devices N on the proposed TD-CRHAN is analyzed as depicted in Figure 3.8. In general, it can be seen that, the higher N, the lesser the T_{s} required, which means a higher N will reduce the burden of sensing on the individual CR-based HAN device. However, it can be noticed that T_{s} is saturated and then becomes constant after a certain I (in this case $I > 6$); thus, at this point, an increase of N or I would not reduce T_s anymore, hence it will increase the value of ε as witnessed in Figure 3.7(a).

Next, with the same setting, we analyze the the performance of the proposed TD-CRHAN in comparison with the conventional one for different D_{t}. Three scenarios of the conventional settings are considered: 1) maximization of R_{t} with $I = 7$, 2) maximization of R_{t} with $I = 10$, and 3) maximization of R_{t} with I is set based on the network throughput demand D_{t} such that $R_{\mathrm{t}} \geq D_{\mathrm{t}}$. Figure 3.9(a) shows that the TD-CRHAN scheme satisfies the throughput demand at all times and has least throughput underutilization compared to other schemes, in particular for the cases that R_{t} is maximized without D_{t} consideration. Worse, the conventional plot without D_{t} consideration (i.e., scenario 1 and 2) are unable to satisfy the demanded throughput after a certain point (for instance, in this case: scenario 1 could not satisfy the demand for $D_{\mathrm{t}} > 9.3$ Mb/s as the number of in-band channels is fixed to 7). In contrast, in principle the proposed TD-CRHAN can support an unlimited D_{t} if I is unlimited.

We then numerically analyze the impact of the channel conditions i.e. $\mathrm{SNR}_{\mathrm{p}}$ and $P(\mathcal{H}_0)$, on the performance of TD-CRHAN as well as the three conventional schemes of which the results are shown in Figure 3.10 and 3.11, respectively. It is witnessed that, for the proposed TD-CRHAN scheme, D_{t} will always be satisfied at minimum ε for almost any $\mathrm{SNR}_{\mathrm{p}}$ or $P(\mathcal{H}_0)$ values (as shown in Figure 3.10(a) and 3.11(a)). This is because, a TD-CRHAN allows for an adaptive number of active in-band channels I (refer to Figure 3.10(b) and 3.11(b)) and local spectrum sensing duration T_s (refer to Figure 3.10(c) and 3.11(c)) where these values are optimized such that the resultant achievable throughput R_{t} is very close to the corresponding

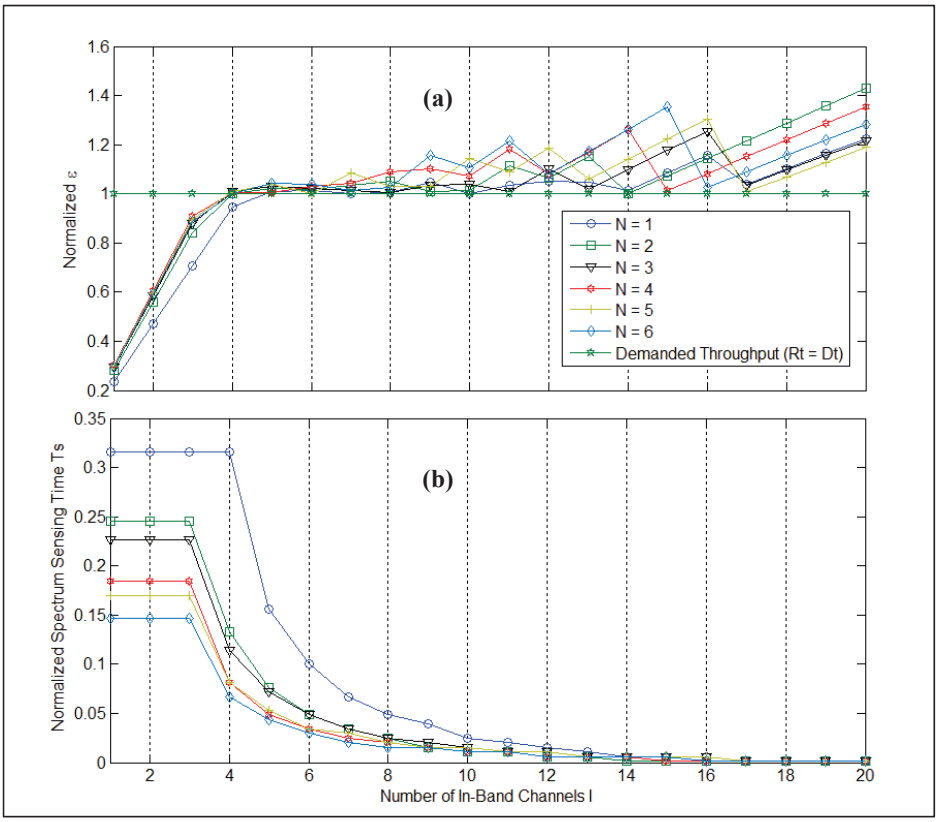

Figure 3.8: Impact of varying number of cooperating sensing devices N on (a) normalized $\varepsilon = \frac{\varepsilon}{D_t}$, and (b) fraction of time used for spectrum sensing (i.e., normalized sensing time $= \frac{T_s}{T_{sf}}$). For this, $D_t = 3.5$ Mb/s.

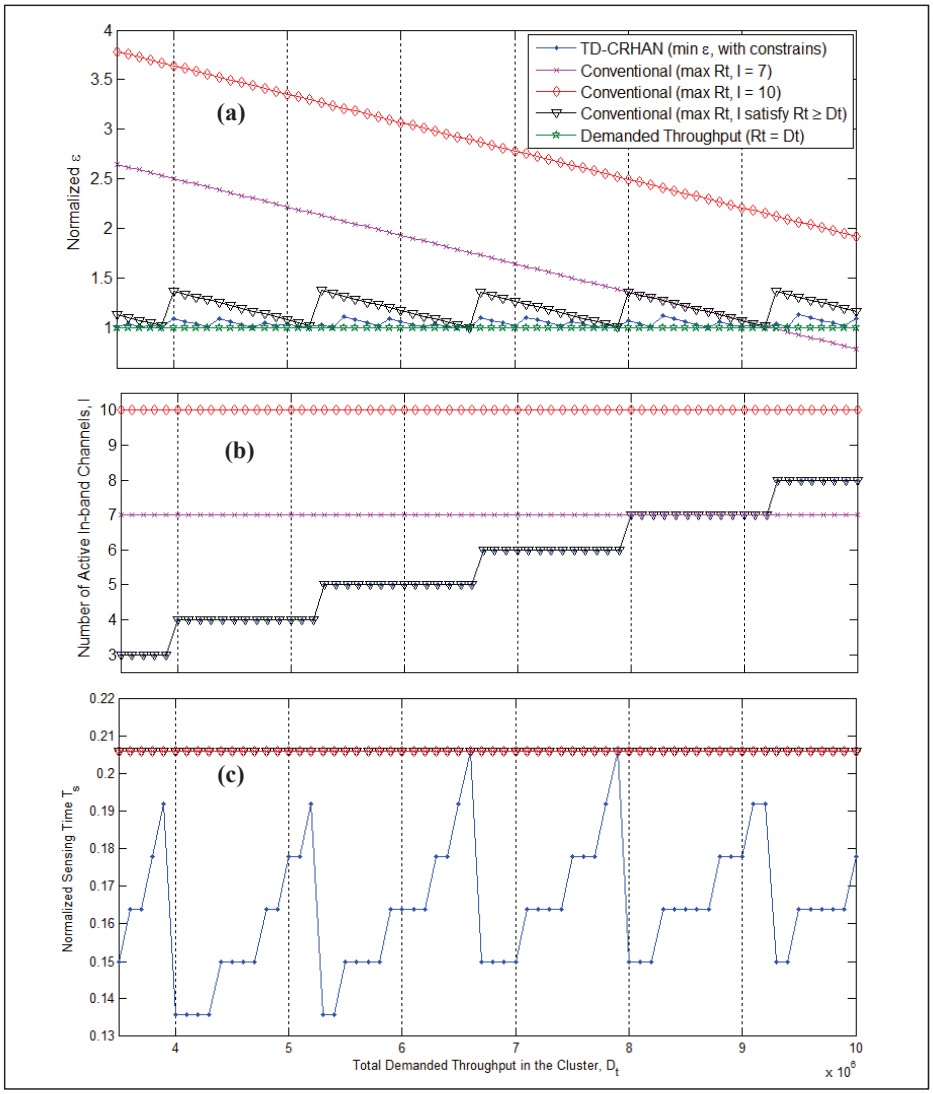

Figure 3.9: Effects of different cluster's throughput demand, D_{t} on (a) normalized $\varepsilon = \frac{\varepsilon}{D_{\mathrm{t}}}$, **(b)** number of in-band channels I used, and **(c)** fraction of time used for spectrum sensing (i.e., normalized sensing time $= \frac{T_{\mathrm{s}}}{T_{\mathrm{sf}}}$). This is a comparison between TD-CRHAN and the conventional schemes. For this, we take $\mathrm{SNR}_{\mathrm{p}} = -7$ dB and $N = 6$.

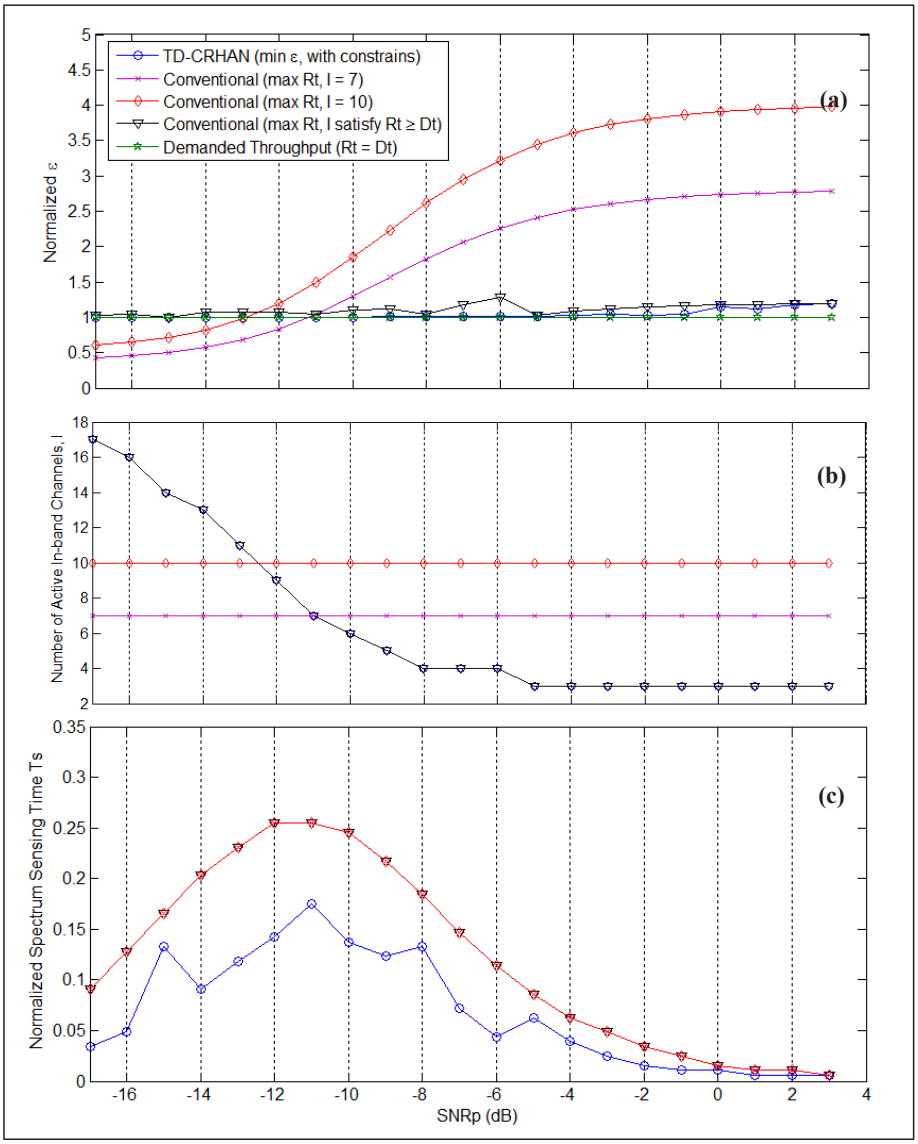

Figure 3.10: Performance of TD-CRHAN in comparison with the conventional schemes for different $\mathrm{SNR_p}$ conditions. The performance is measured in term of **(a)** normalized $\varepsilon = \frac{\varepsilon}{D_t}$, **(b)** number of in-band channels I used, and **(c)** fraction of time used for spectrum sensing (i.e., normalized sensing time $= \frac{T_s}{T_{sf}}$), with $P(\mathcal{H}_0)$ fixed at 0.7.

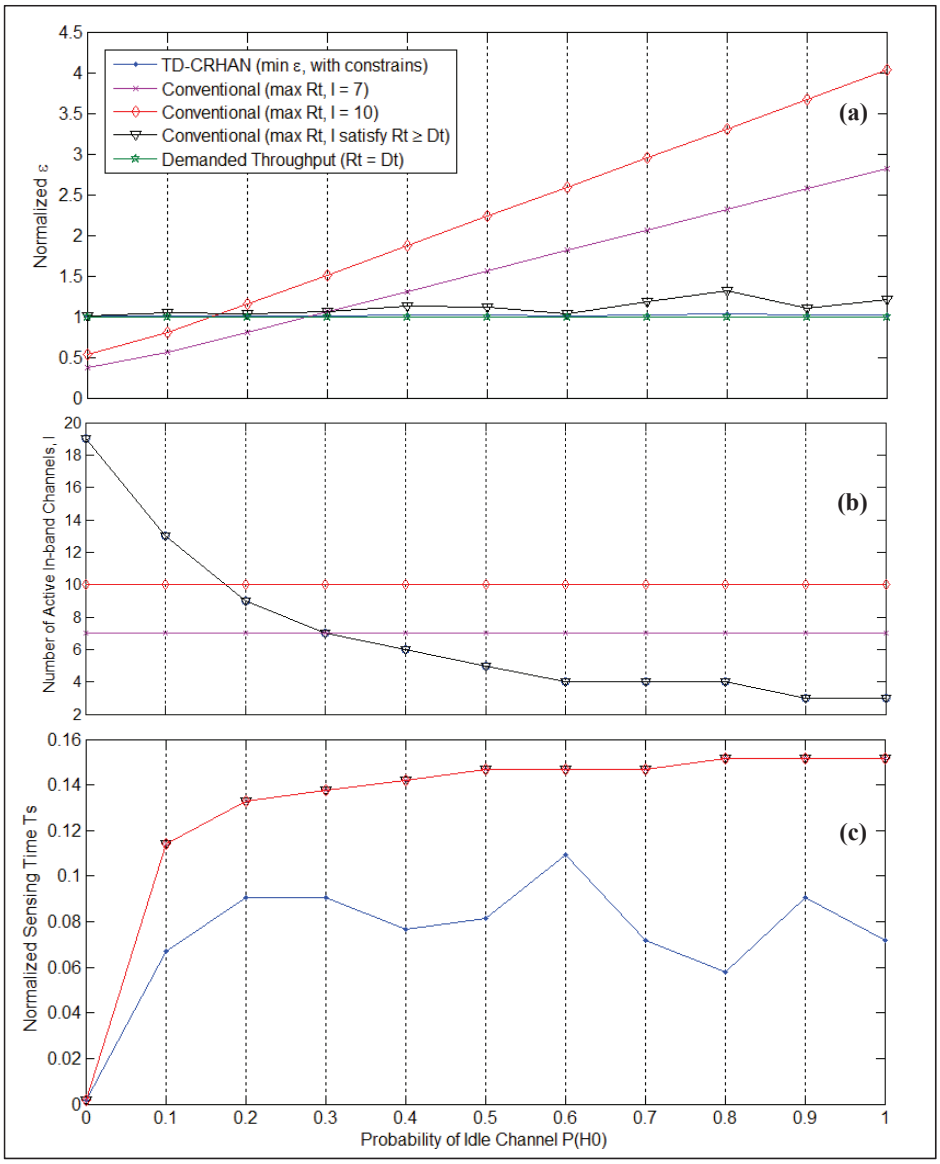

Figure 3.11: Performance of TD-CRHAN in comparison with the conventional schemes for different $P(\mathcal{H}_0)$ conditions. The performance is measured in term of **(a)** normalized $\varepsilon = \frac{\varepsilon}{D_t}$, **(b)** number of active in-band channels I used, and **(c)** fraction of time used for spectrum sensing (i.e., normalized sensing time $= \frac{T_s}{T_{sf}}$), with SNR_p fixed at -7 dB.

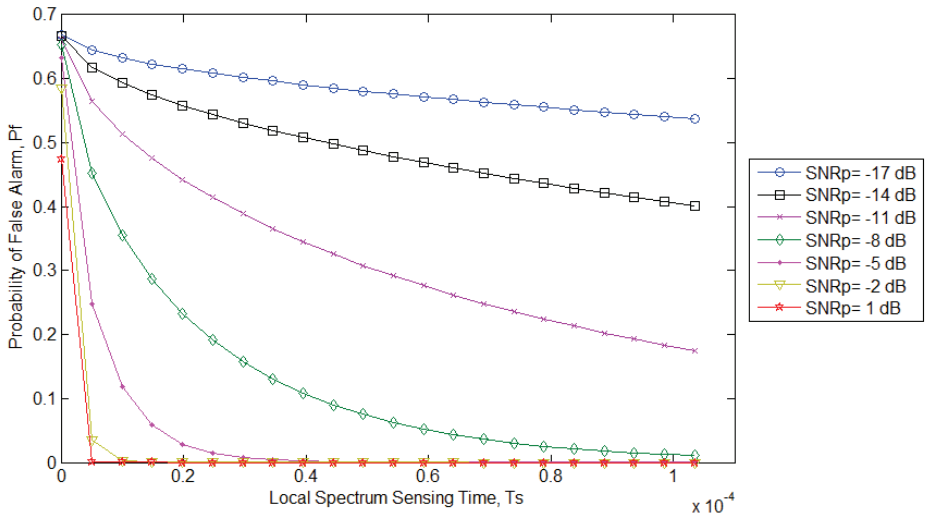

Figure 3.12: P_{f} versus T_{s} for different $\mathrm{SNR}_{\mathrm{p}}$ with P_{d} fixed at 0.9.

demand D_{t}. Specifically, for I, at a very low $\mathrm{SNR}_{\mathrm{p}}$ or $P(\mathcal{H}_0)$, its value will be increased while it will be reduced to the minimal at a high $\mathrm{SNR}_{\mathrm{p}}$ or $P(\mathcal{H}_0)$. Notice that D_{t} is still satisfied even for $P(\mathcal{H}_0) = 0$ in which the network throughput at this point is acquired from the $P(\mathcal{H}_1)$ part (i.e., at the expense of a high I). For T_{s}, it is seen in Figure 3.10(c) that it is adjusted to a lower value at a very low $\mathrm{SNR}_{\mathrm{p}}$. This is because at this point, ε (and R_{t}) is influenced more by T_{s} but less by P_{f} (and Q_{f}) as at a very low $\mathrm{SNR}_{\mathrm{p}}$, a high T_{s} does not provide a significant reduction to P_{f} (i.e., this can be seen from (2.7), as plotted in Figure 3.12). On such a case, a lower T_{s} is more favorable in order to satisfy the demanded throughput D_{t} and meet the $\varepsilon \geq 0$ constraint. However, P_{f} (and Q_{f}) become more dominant with the increase of $\mathrm{SNR}_{\mathrm{p}}$ up to a certain point, but yet it is dominated by T_{s} when P_{f} becomes saturated; this can be observed in Figure 3.10(c). Similarly with Figure 3.11(c), that is at a very low $P(\mathcal{H}_0), T_{\mathrm{s}}$ will be set to a lower value as a high T_{s} is not beneficial because at this instance most of the R_{s} comes from $P(\mathcal{H}_1)$ (c.f., (3.8)). Note that in (3.8) a higher T_{s} leads to a lower Q_{f} and therefore a higher R_{t}; at a very low $P(\mathcal{H}_0)$, a lower Q_{f} does not help because this part of R_{t} is suppressed by the value of $P(\mathcal{H}_0)$ itself, and vice versa.

3.5 Simulation Results and Analysis

In this section, we run Monte Carlo simulations on the proposed TD-CRHAN scheme and the three conventional cases, and compare the results with the numerical results. The settings for this simulation are the same as in Section 3.4 except the SNR of the incumbent user (i.e., $\mathrm{SNR}_{\mathrm{p}_j}$) is randomly set for each CR-based device j based on the Uniform distribution within the range of -11 dB and 3 dB (i.e., $\mathrm{SNR}_{\mathrm{p}_j} \sim \mathcal{U}(-11, 3)$ dB, for all j). We consider this range for this simulation in order to capture the dynamic behavior of the sensing qualities (i.e., P_{d} and P_{f}) and observe the impact of different sensing time T_{s} values. For $\mathrm{SNR}_{\mathrm{s}}$ higher than 3 dB, only a few samples with single device sensing (without cooperation) are required to obtain an already very high probability of detection P_d and very low probability of false alarm P_{f}. For low $\mathrm{SNR}_{\mathrm{p}}$ used i.e., -11 dB and less, an increase of the sensing time does not really give significant improvement of the sensing qualities. We repeat the simulation $1,000$ times and the results are averaged. It can be seen from Figure 3.13 that, in general, the patterns of the simulation results are similar with the graphs from the Numerical Analysis (refer to Figure 3.7). However, notice that the optimal sensing time in the simulation is less than in the numerical analysis which is caused by the possible high value of the incumbent user signal strength in the simulation (i.e., between -11 and 3 dB as compared to a fix -7 dB, respectively). In addition, Figure 3.14 shows that the corresponding cooperative and the individual false alarm probabilities, i.e., Q_{f} and $P_{\mathrm{f}_j}, \forall j$, respectively, of the proposed TD-CRHAN varies according to the number of in-band channels I available. In TD-CRHAN, for the same total throughput demand D_{t}, an increase of the number of in-band channels I will decrease the required achievable throughput $R^{(i)}$ of each channel i, hence this reduces the required Q_{f} and the corresponding $P_{\mathrm{f}_j}, \forall j$. This then further reduces the required sensing time T_{s}, as can be seen in Figure 3.7. Besides, it can be observed from Figure 3.14(a) that the probability of false alarm P_{f_j} of sensing device j depends on its $\mathrm{SNR}_{\mathrm{p}_j}$: a lower $\mathrm{SNR}_{\mathrm{p}_j}$ device has a higher P_{f_j}.

Finally, a Monte Carlo simulation is executed in which all network parameters are uniformly randomized (i.e., $D_{\mathrm{t}} \sim \mathcal{U}(3.5, 10)$ Mb/s, $\mathrm{SNR}_{\mathrm{p}_j}^{(i)} \sim \mathcal{U}(-11, 3)$ dB and $P(\mathcal{H}_0^{(i)}) \sim \mathcal{U}(0, 1),\ \forall i, j$) to evaluate the performance of the TD-CRHAN in a more practical scenario. The graphs of the normalized ε and sensing time T_{s}, versus the number of in-band channel I for $N = 1, 2, \ldots, 6$ are plotted as shown in Figure 3.15. Similarly, it is observed that with the proposed TD-CRHAN scheme, the network throughput demand D_{t} is satisfied at all times for all N. However, it

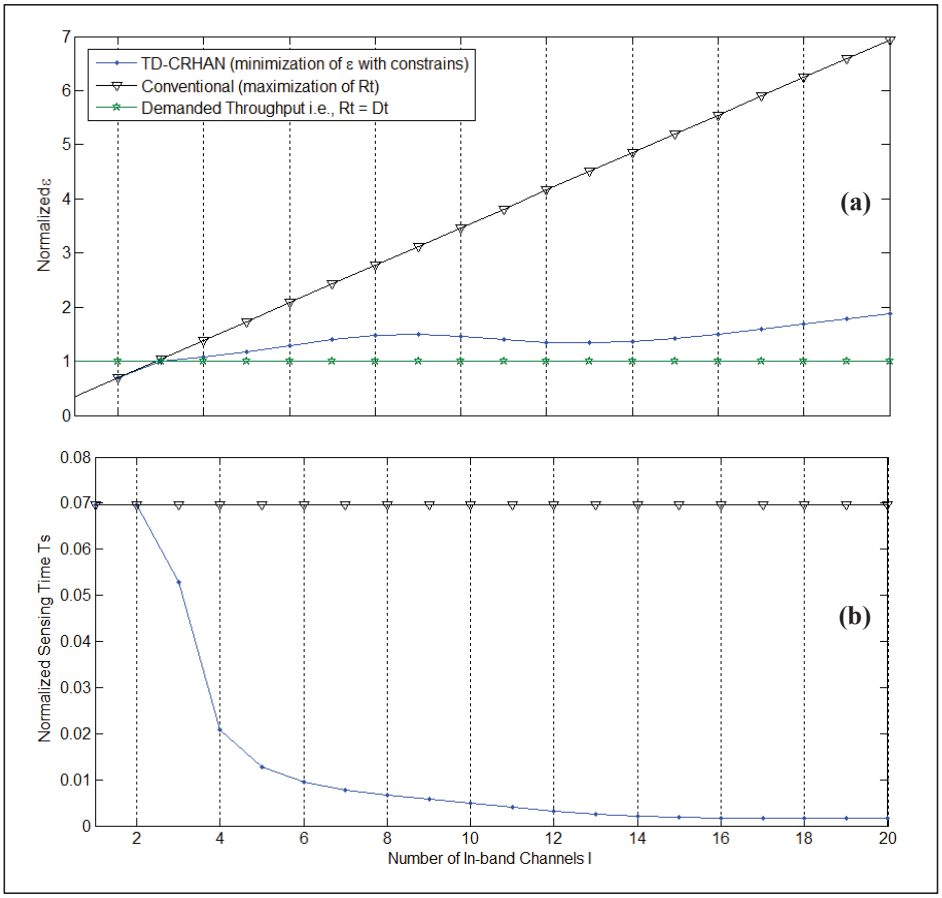

Figure 3.13: Simulation results on the effects of using different total number of in-band channels I on **(a)** normalized $\varepsilon = \frac{\varepsilon}{D_{\mathrm{t}}}$, and **(b)** fraction of time used for spectrum sensing (i.e., normalized sensing time $= \frac{T_{\mathrm{s}}}{T_{\mathrm{sf}}}$). This is a comparison between TD-CRHAN and the conventional schemes. For this, $\mathrm{SNR}_{\mathrm{p}_j}$ is chosen randomly between -11 dB and 3 dB for all j.

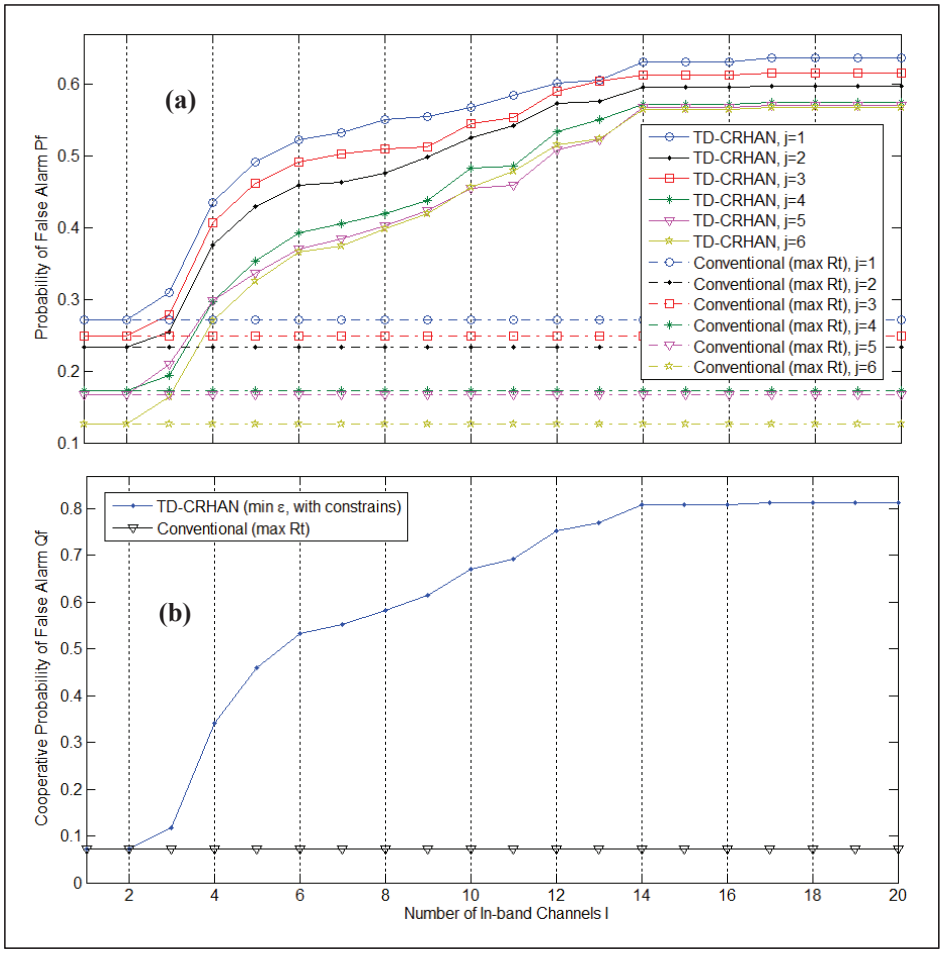

Figure 3.14: The corresponding (a) false alarm probability P_{f_j} of each device j, and (b) cooperative false alarm probability Q_{f}, from the simulation of which the incumbent $\mathrm{SNR}_{\mathrm{p}_j}$ are different at each sensing device j. In the simulation, the random generated $\mathrm{SNR}_{\mathrm{p}_j}, \forall j$ are as the following: $\{\mathrm{SNR}_{\mathrm{p}_j}\} = \{-6.5\ \mathrm{dB}, -5.3\ \mathrm{dB}, -5.9\ \mathrm{dB}, -3.9\ \mathrm{dB}, -3.5\ \mathrm{dB}, -3.2\ \mathrm{dB}\}$ for $j = \{1, 2, \ldots, 6\}$, respectively.

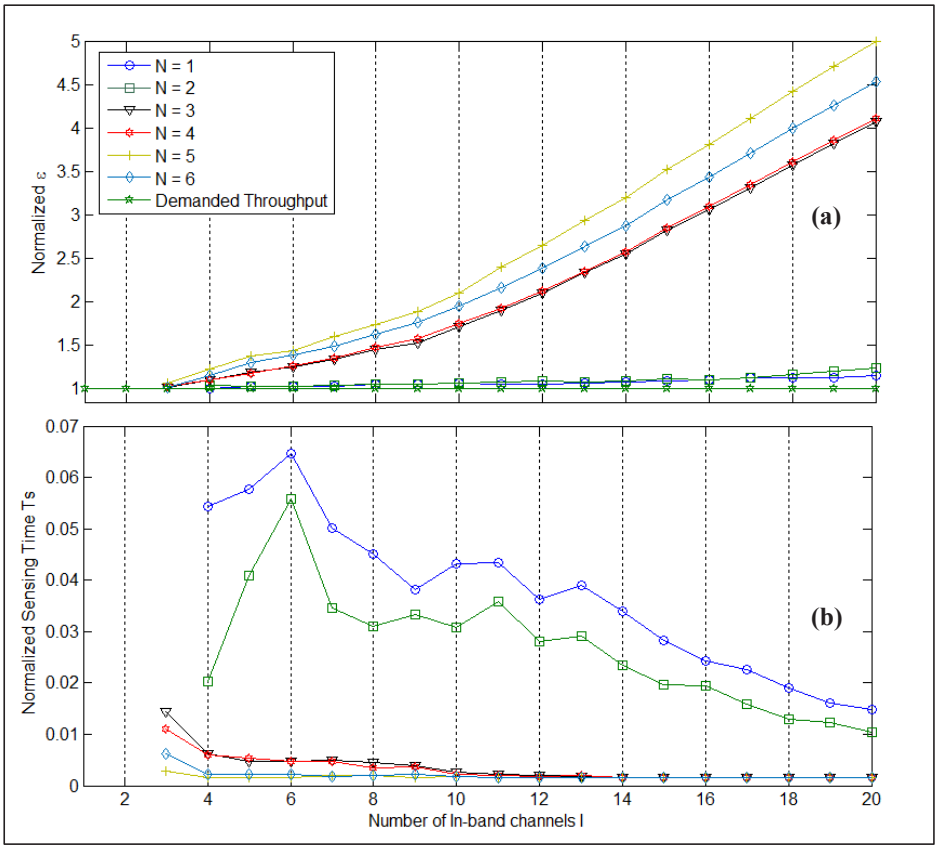

Figure 3.15: Simulation results of the total number of active channels I versus: **(a)** normalized $\varepsilon = \frac{\varepsilon}{D_{\mathrm{t}}}$, and **(b)** fraction of time used for spectrum sensing (i.e., normalized sensing time $= \frac{T_{\mathrm{s}}}{T_{\mathrm{sf}}}$). This is for different number of cooperating devices i.e., $N = 1, 2, \ldots, 6$ with more practical scenario in which all network parameters are randomly chosen i.e., $D_{\mathrm{t}} \sim \mathcal{U}(3.5, 10)$ Mb/s, $\mathrm{SNR}_{\mathrm{p}_j}^{(i)} \sim \mathcal{U}(-11, 3)$ dB and $P(\mathcal{H}_0) \sim \mathcal{U}(0, 1)$, for all i and j.

is seen that a lower number of cooperating sensing devices N will require a higher sensing time T_{s}, and moreover at a certain point, a higher number of channels I is even required (i.e., in this case, $I \geq 4$ for $N = 1$ and 2 compared to $I \geq 3$ for $N = 3, 4, 5$ and 6).

3.6 Conclusion

To support the ever-rising throughput demand of home area networks (HAN), we have presented a cognitive radio (CR) based communication scheme called TD-CRHAN in this chapter. The TD-CRHAN aims at satisfying the demanded network throughput with equality by determining the optimal local spectrum sensing time, the number of cooperating sensing devices and the number of active in-band channels needed. This leads to an efficient scheme which provides a higher utilization of the occupied channels. It was shown by extensive numerical analysis and through simulations that TD-CRHAN is able to relax the tight cooperative spectrum sensing requirements and provides significant gains on the cooperative spectrum sensing parameters (i.e., spectrum sensing time and number of cooperating devices), compared to the conventional solution. More specifically, TD-CRHAN reduces the required local spectrum sensing time by more than 51%. Furthermore, it was shown that these cooperative spectrum sensing parameters can be further improved with the availability of additional cooperating devices or channels (bandwidth).

Besides throughput, another major issue in using the cognitive radio technology is energy efficiency, i.e., particularly caused by the spectrum sensing which introduces extra energy consumption as compared to the conventional communication. In the next chapter, we will address this issue, and design an energy and throughput efficient cooperative spectrum sensing scheme.

Chapter 4

Energy and Throughput Efficient Cooperative Spectrum Sensing

In the previous chapter, we have presented the proposed cognitive radio based communication for home area networks, in which the main objective is to sustainably meet the ever-rising throughput demand of the network. Besides throughput, another major issue in cognitive radio (CR)-based network is the additional energy consumption caused by spectrum sensing. Hence in this chapter, we present a cooperative spectrum sensing (CSS) strategy for CR-based HANs that takes into account these two important aspects (i.e., energy and throughput). For this, the average throughput demand from the HAN devices is included as one of the constraint parameters in the formulation of the optimization problem. In addition, we also consider the variations of the primary user's signal-to-noise-ratio at each sensing device, which models a more practical scenario of a HAN. In fact, we take advantage of this by jointly optimizing the device selection, the sensing time and the probability of detection. Contrary to existing approaches, we propose that the sensing time and the probability of detection can be set differently at each cooperating device. With the proposed CSS strategy, we show that the sensing energy can be conserved by more than 94% and a 12% higher throughput can be achieved as compared to the conventional scheme.

4.1 Introduction

Cognitive radio is seen as one of the most promising technologies for HAN in meeting the throughput demand, and at the same time addressing the interference and spectrum scarcity issues. However, spectrum sensing which is one of the key component in CR can causes a significant additional energy overhead and degradation of communication throughput. For example, in [22], more than 42% of the frame time is allocated to spectrum sensing. In addition, in a real-world implementation as reported in [29], 170 ms is required to sense a QPSK signal at a signal-to-noise-ratio of -1 dB, which is rather long and thus very costly in terms of throughput and energy. Note that the transmission and the sensing power consumption are commonly (e.g. [30, 22, 24]) considered to be nearly the same. Therefore, it is important to design an efficient spectrum sensing technique that takes both energy consumption and throughput into consideration, minimizing the aforementioned overheads.

Most of the earlier works in spectrum sensing, e.g., [18], focus on optimizing sensing parameters to achieve a maximum throughput. Afterwards, research as in [55] started to work on energy-efficient spectrum sensing; however, throughput efficiency is not included. Among the earliest works that consider both energy and throughput jointly in spectrum sensing design is [23]. In this work, the sensing energy is minimized by optimizing the number of cooperating sensing devices. From the obtained optimizer, the throughput is then maximized by deriving the optimal reporting time. However, maximizing the achievable network throughput by optimizing spectrum sensing parameters without taking into consideration the actual network's needs might introduce a surplus of the available throughput which is then being underutilized, and this also causes a waste of energy. One of the first articles that takes network throughput demand into consideration in designing energy and throughput efficient spectrum sensing is in [24]. However, the impact of different throughput demands on spectrum sensing parameters as well as on spectrum sensing energy consumption is not analyzed there. In addition, to the best of our knowledge, all existing works in this domain assign the same value to the spectrum sensing parameters (e.g., the probability of detection and the sensing time) for all cooperating sensing devices. This turns out to be not optimal for networks that consist of devices that have different incumbent user's signal strengths, which is typically the case for a HAN.

In this work, we propose a cooperative spectrum sensing (CSS) strategy that minimizes the energy consumption and at the same time satisfies the throughput

demand of the network, subject to a targeted cooperative probability of detection. Based on the average throughput demand from the HAN network and the variation of the incumbent user's signal-to-noise-ratio (SNR) at each CR-based HAN device (i.e., latter on will be indicated as HAN devices, but also may be used interchangeably), the proposed scheme selects the cooperating devices and jointly determines the sensing time and the detection probability of each selected sensing device. These values can be different from one device to another. The proposed approach will allow us to reduce the CSS energy consumption significantly and, furthermore, satisfy higher throughput demands.

We mathematically model the proposed CSS scheme and formulate a suitable optimization problem with corresponding constraints. In the derivations, we consider general expressions for the cooperative spectrum sensing performance parameters (i.e., cooperative probability of false alarm, and detection). This supports scenarios in which the SNR of the incumbent user is not the same at different devices. Then, we solve the optimization problem by using the reversible-jump sampling algorithm [56], which is a special case of the widely used methodology of Markov Chain Monte Carlo (MCMC) [57, 58] optimization . The performance of the proposed CSS scheme is evaluated by comparing it with three other practically relevant schemes. We illustrate and discuss the impact of different parameter settings and demonstrate the significant gains obtained.

This chapter is organized as follows. Section 4.2 presents the derivation of the considered system model and the spectrum sensing; the formulation of the problem is described in Section 4.3, and the solution is provided in Section 4.4; Section 4.5 evaluates and discusses the performance of the proposed CSS scheme; and finally, conclusions are presented in Section 4.6.

4.2 System Model

A home area network (HAN) based on connected clusters with CR technology as proposed in Chapter 3 is considered. The diagram of HAN with a single cluster as shown in Figure 3.4 is referred.

4.2.1 Cooperative Spectrum Sensing

We consider that each cluster operates in a time-synchronized manner within a superframe where the superframe time is fixed at T_{sf}, as shown in Figure 4.1. Each superframe comprises two sub slots: a sub slot of duration T_{css} for cooperative

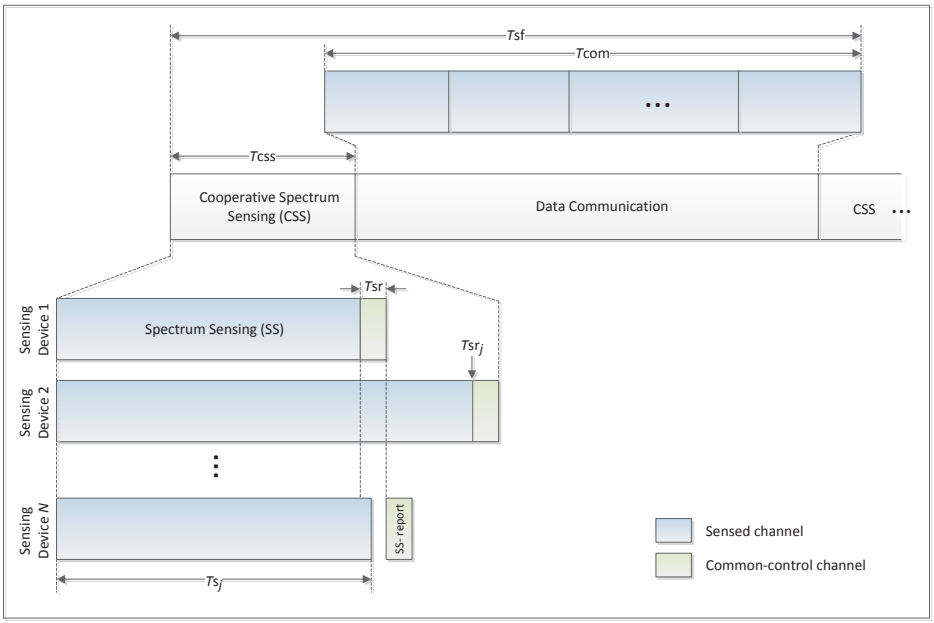

Figure 4.1: Superframe structure for a single channel.

spectrum sensing, and a sub slot of duration T_{com} for data communication. In the former slot, each cooperating sensing device j executes spectrum sensing for a duration of T_{s_j}, and then reports its sensing outcome to the CH at time T_{tsr_j} for a duration of T_{sr}.

In this work a cooperative spectrum sensing with energy detection and hard-fusion strategy is considered. The equation for device j's probability of false alarm P_{f_j}, probability of detection P_{d_j}, spectrum sensing time T_{s_j}, and the cooperative probability of false alarm Q_{f} and cooperative probability of detection Q_{d} is given by (2.7)-(2.13), respectively.

Our main goal is to determine the optimal number of cooperating devices N and the corresponding optimal sensing time T_{s_j} and probability of detection P_{d_j} for each selected cooperating device $j \in \mathcal{N}$, such that the targeted cooperative probability of detection Q_{d} and the demanded throughput of the cluster (denoted by D) is satisfied with the least amount of energy. We consider the scenario that the incumbent user SNR i.e. $\mathrm{SNR}_{\mathrm{p}_j}$ may be different at each cooperating device j; hence, the optimal T_{s_j} and P_{d_j} can also vary with j.

For the sensing-report, we consider that it is transmitted through a channel that

is different from the sensed channel (e.g., through a common control channel). In this way, the sensing-report transmission will not interfere with the incumbent user of the channel, and the quality of the reporting channel is also ensured. Note that the sensing report information is very crucial, hence needs to be highly reliable [53]. Consequently, the sensing-report of each device can be transmitted directly after the corresponding sensing time (i.e., $T_{\mathrm{tsr}_j} = T_{\mathrm{s}_j}$), as long as it does not fall within the active reporting duration of the other cooperating devices, such that $\{T_{\mathrm{tsr}_j}, (T_{\mathrm{tsr}_n} + T_{\mathrm{sr}})\} \cap \{T_{\mathrm{tsr}_p}, (T_{\mathrm{tsr}_j} + T_{sr})\} = \emptyset, \forall j, p$, where $j, p \in \mathcal{N}$, and T_{tsr_j} and T_{tsr_p} are the starting time of the sensing-report transmission of device j and p, respectively. Consequently, the CSS duration T_{css} for set $\mathcal{N}$ of cooperating devices can be expressed as

$$T_{\mathrm{css}} = \max\{T_{\mathrm{tsr}_j}, j \in \mathcal{N}\} + T_{\mathrm{sr}}. \tag{4.1}$$

4.2.2 Throughput

From 4.1, the normalized average achievable throughput for a channel can be formulated as

$$R = \frac{T_{\mathrm{sf}} - T_{\mathrm{css}}}{T_{\mathrm{sf}}} P(\mathcal{H}_0)(1 - Q_{\mathrm{f}}) \tag{4.2}$$

where $P(\mathcal{H}_0)$ is the a-priori probability that the channel is idle. This probability can be estimated before the CR network is deployed based on long term measurements or it can be measured online based on, for example, the concept of MAC-layer sensing [26]. Substituting (4.1) into (4.2), we have

$$R = \left(1 - \frac{\max\{T_{\mathrm{tsr}_j}, j \in \mathcal{N}\} + T_{\mathrm{sr}}}{T_{\mathrm{sf}}}\right) P(\mathcal{H}_0)(1 - Q_{\mathrm{f}}) \tag{4.3}$$

4.2.3 Energy Consumption of Cooperative Spectrum Sensing

Let P_{s} and P_{tx} denote the power for local spectrum sensing and sensing-report transmission, respectively, which are assumed to be the same for all devices. Then, the total energy consumed by the set $\mathcal{N}$ of cooperating HAN devices in performing a CSS in a channel can be expressed as

$$E_{\mathrm{css}} = \sum_{j \in \mathcal{N}} (P_{\mathrm{s}} T_{\mathrm{s}_j} + P_{\mathrm{tx}} T_{\mathrm{sr}}). \tag{4.4}$$

4.3 Energy and Throughput Efficient Cooperative Spectrum Sensing Scheme

4.3.1 Sensing-Throughput Tradeoff

From (4.3), it can be seen that a lower Q_{f} will give a higher achievable throughput R. For a given $\mathrm{SNR}_{\mathrm{p}_j}$ and a required P_{d_j} for $j \in \mathcal{N}$, the lower $Q_{\mathrm{f}}(\{P_{\mathrm{f}_j}, j \in \mathcal{N}\})$ can be obtained by extending the sensing time T_{s_j} for $j \in \mathcal{N}$ (c.f., (2.7) and (2.11)). However, extending the sensing time will increase $\max\{T_{\mathrm{tsr}_j}, j \in \mathcal{N}\}$, hence decreasing the achievable throughput R. Thus, when other parameters are fixed, there exists a maximum throughput $R_{\max}$ that cannot be surpassed by varying T_{s_n}. Conversely, for a given normalized average throughput demand $D \leq R_{\max}$ there is a range of values of T_{s_j} that achieve $R \geq D$. The throughput demand D can be acquired by the CH from each connected HAN device, for example at the time that the device is requesting to join the cluster, or updated by the HAN device to the CH whenever there is a change in its throughput demand. In this work, we require only that $R \geq D$, and we show in Section 4.5 that this gives a significant energy efficiency improvement as compared to maximizing R.

4.3.2 Flexibility on Device's Sensing Time and Probability of Detection

In most of the presented research, the sensing time T_{s_j} and the probability of detection P_{d_j} are taken the same for all cooperating devices. However, this is not optimal when the incumbent user's SNRs vary significantly from device to device (i.e., more than 1 dB [59, 22]).

In general, a longer T_{s_j} is favorable as this will provides a more reliable sensing outcome (i.e., lower P_{f_j} and higher P_{d_j}). However, P_{f_j} and P_{d_j} will be saturated beyond a certain T_{s_j} where the rate of saturation depends on $\mathrm{SNR}_{\mathrm{p}_j}$, as can be seen in Figure 2.11 in Chapter 2. Beyond this saturation point, extending T_{s_j} does not give a significant improvement to the P_{f_j} and P_{d_j} and causes an unworthy higher energy consumption. Thus, it is better if different sensing times T_{s_j} are assigned to different j, depending on the corresponding $\mathrm{SNR}_{\mathrm{p}_j}$.

From the receiver operating curve shown in Figure 4.2, it can be seen that lowering the expected probability of detection P_{d_j} will also lower the corresponding probability of false alarm P_{f_j}, and vice versa. As shown by the cooperative probability of detection Q_{d} of equation (2.10), a different P_{d_j} can be assigned to a different cooperating device j as long as the required cooperative probability of

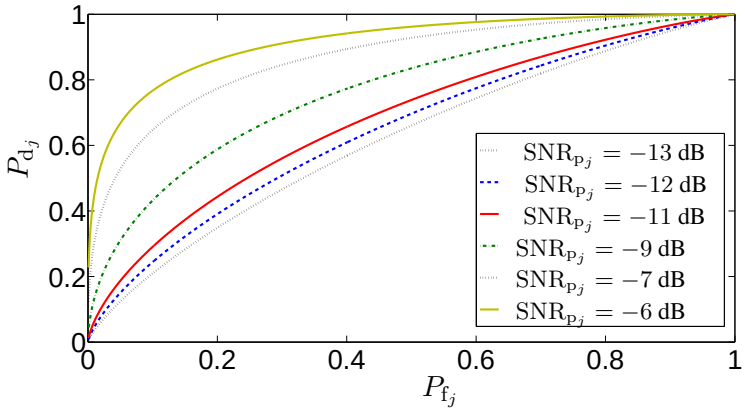

Figure 4.2: The receiver operating curve P_{d_j} versus P_{f_j} for $\mathrm{SNR}_{\mathrm{p}_j}$ between -13 and -6 dB. T_{s_j} is fixed at 15 ms.

detection constraint $\bar{Q}_{\mathrm{d}}$ is met. For devices which have a high $\mathrm{SNR}_{\mathrm{p}_j}$, it is easy to obtain a high P_{d_j} even with a low T_{s_j}. Therefore, if we can have a high P_{d_j} for a certain device j, then we are able to tolerate and assign a relatively lower P_{d_j} for the others, particularity for those that have a low $\mathrm{SNR}_{\mathrm{p}_j}$, hence a lower P_{f_j} can be obtained for these low-$\mathrm{SNR}_{\mathrm{p}_j}$ devices. Consequently in return, the expected minimum throughput $R(\{P_{\mathrm{f}_j}, j \in \mathcal{N}\})$, i.e., $R \geq D$, can be achieved at a lower $E_{css}(\{T_{\mathrm{s}_j}, j \in \mathcal{N}\})$.

4.3.3 Optimization Problem Formulation

Our goal is to find the optimal T_{s_j} and P_{d_j} for each cooperating device j by taking the corresponding $\mathrm{SNR}_{\mathrm{p}_j}$ into account such that the CSS energy consumption E_{css} is minimized. For a dense HAN where there are many devices in a cluster, it is obvious that using all available devices in the cluster for a CSS, i.e. taking $\mathcal{N} = \mathcal{J}$, will cause a high sensing overhead, including the sensing energy consumption. On the other hand, more cooperating devices do not necessarily provide a better sensing performance [60]. Hence, in a heterogeneous $\mathrm{SNR}_{\mathrm{p}_j}$ environment, an optimal set of cooperating devices $\mathcal{N} \subseteq \mathcal{J}$ needs to be found.

To achieve this, our optimization problem can be formulated as

$$\min_{\mathcal{N},\mathbf{P}_{\mathrm{d}},\mathbf{T}_{\mathrm{s}}} \{E_{\mathrm{css}}\} : E_{\mathrm{css}} = \sum_{j \in \mathcal{N}} \left(P_{\mathrm{s}} T_{\mathrm{s}_j} + P_{\mathrm{tx}} T_{\mathrm{sr}}\right) \tag{4.5}$$

$$\text{s.t.,} \qquad Q_{\mathrm{d}}(\mathbf{P}_{\mathrm{d}}) \geq \bar{Q}_{\mathrm{d}} \tag{4.6}$$

$$R\left(\mathbf{T}_{\mathrm{s}}\right) \geq D \tag{4.7}$$

where $\mathbf{P}_{\mathrm{d}} \triangleq [P_{\mathrm{d}_j}]_{j\in\mathcal{N}}$ and $\mathbf{T}_{\mathrm{s}} \triangleq [T_{\mathrm{s}_j}]_{j\in\mathcal{N}}$ are vectors collecting the probability of detection and sensing time of all cooperating devices, respectively, and $P_{\mathrm{d}_j} \in (0,1)$ and $T_{\mathrm{s}_j} \in \{\tau, 2\tau, \ldots, (T_{\mathrm{css}} - T_{\mathrm{sr}})\},\ \forall j$. The equation to calculate $Q_{\mathrm{d}}(\mathbf{P}_{\mathrm{d}})$ is given by (2.10) in Chapter 2. Note that this scheme assigns the device's sensing parameters value individually, hence it can easily be further extended to takes other device's properties into consideration, such as the residual energy and the expected lifetime.

4.4 Optimal Cooperating Device Selection, and Corresponding Optimal Sensing Time and Detection Probability

In (4.5), it can be seen that selecting the set of optimal cooperating devices is a combinatorial problem with $\binom{J}{N}$ combinations. The problem becomes very complex if J is high (i.e. the case for a dense HAN), since its complexity grows exponentially with J. However, this combinatorial complexity can be avoided in spectrum sensing, since the devices with the highest $\mathrm{SNR}_{\mathrm{p}_j}$ should be used [60]. If we sort the devices in descending order of the $\mathrm{SNR}_{\mathrm{p}_j}$, then the device selection problem can be simplified to the determination of the optimal number of cooperating devices. Let $j = 1, \ldots, J$ denote the indices of the devices ordered with descending $\mathrm{SNR}_{\mathrm{p}_j}$. Then the new optimization problem can be written as

$$\begin{aligned} \min_{N,\mathbf{P}_{\mathrm{d}},\mathbf{T}_{\mathrm{s}}} \{E_{\mathrm{css}}\} : E_{\mathrm{css}} &= \sum_{j=1}^{N} \left(P_{\mathrm{s}} T_{\mathrm{s}_j} + P_{\mathrm{tx}} T_{\mathrm{sr}}\right) = N P_{\mathrm{tx}} T_{\mathrm{sr}} + P_{\mathrm{s}} \sum_{j=1}^{N} T_{\mathrm{s}_j} \\ \text{s.t.,} \quad & Q_{\mathrm{d}}(\mathbf{P}_{\mathrm{d}}) \geq \bar{Q}_{\mathrm{d}} \\ & R\left(\mathbf{T}_{\mathrm{s}}\right) \geq D\,. \end{aligned} \tag{4.8}$$

In order to jointly solve this optimization problem and find the optimal: i) number of cooperating devices N^*, ii) sensing times $\mathbf{T}_{\mathrm{s}}^*$, and iii) detection probabilities $\mathbf{P}_{\mathrm{d}}^*$, we use a Markov Chain Monte Carlo (MCMC) [57, 58] optimization method. The basic idea of this approach is to formulate the optimization problem as the maximization of a distribution of $N, \mathbf{T}_{\mathrm{s}}$ and $\mathbf{P}_{\mathrm{d}}$, hereafter referred to as the *target distribution* $p(N, \mathbf{T}_{\mathrm{s}}, \mathbf{P}_{\mathrm{d}})$, and to solve the maximization based on a population of samples from $p(N, \mathbf{T}_{\mathrm{s}}, \mathbf{P}_{\mathrm{d}})$.

4.4.1 MCMC Problem Formulation

To transform the minimization into a maximization, we multiply the objective function with -1. Furthermore, to obtain an objective function that has the characteristics of a distribution, we apply the exponential operator $\exp(\cdot)$, thus ensuring non-negativity. With these modifications, our optimization problem becomes

$$\max_{N,\mathbf{P}_d,\mathbf{T}_s} V \cdot \exp(-P_{\mathrm{s}} \sum_{j=1}^{N} T_{\mathrm{s}_j}) \tag{4.9}$$

$$\text{s.t.,} \qquad Q_{\mathrm{d}}(\mathbf{P}_{\mathrm{d}}) \geq \bar{Q}_{\mathrm{d}} \tag{4.10}$$

$$R\left(\mathbf{T}_{\mathrm{s}}\right) \geq D \tag{4.11}$$

where $V = \exp(-NP_{\mathrm{tx}}T_{\mathrm{sr}})$. Next, we embed the constraints (4.10) and (4.11) into the objective function in (4.8) by way of a binary indicator function defined as

$$I_{\mathrm{c}}(\mathbf{P}_{\mathrm{d}}, \mathbf{T}_{\mathrm{s}}) = \begin{cases} 1, & \text{for } Q_{\mathrm{d}}(\mathbf{P}_{\mathrm{d}}) \geq \bar{Q}_{\mathrm{d}} \text{ and } R(\mathbf{T}_{\mathrm{s}}) \geq D \\ 0, & \text{otherwise.} \end{cases} \tag{4.12}$$

Using this, we can write (4.9)–(4.11) as

$$\max_{N,\mathbf{P}_{\mathrm{d}},\mathbf{T}_{\mathrm{s}}} \{p(N, \mathbf{P}_{\mathrm{d}}, \mathbf{T}_{\mathrm{s}})\} : p(N, \mathbf{P}_{\mathrm{d}}, \mathbf{T}_{\mathrm{s}}) = V \cdot \exp(-P_{\mathrm{s}} \sum_{j=1}^{N} T_{\mathrm{s}_j}) \cdot I_{\mathrm{c}}(\mathbf{P}_{\mathrm{d}}, \mathbf{T}_{\mathrm{s}})\,. \tag{4.13}$$

Now, the objective function has the form of a distribution of N, $\mathbf{T}_{\mathrm{s}}$ and $\mathbf{P}_{\mathrm{d}}$, up to some unknown normalization constant. The normalization constant is not relevant in the following; we can thus work directly with the non-normalized target distribution $p(N, \mathbf{P}_{\mathrm{d}}, \mathbf{T}_{\mathrm{s}})$ as defined in (4.13).

4.4.2 Sample-Based Maximization

Following the MCMC concept, we solve (4.13) by generating a population of samples distributed according to (the normalized version of) $p(N, \mathbf{P}_{\mathrm{d}}, \mathbf{T}_{\mathrm{s}})$. The samples generated by an MCMC method form a Markov chain whose stationary distribution equals the target distribution. Each iteration of the MCMC method generates a new sample $(N^{(m)}, \mathbf{T}_{\mathrm{s}}^{(m)}, \mathbf{P}_{\mathrm{d}}^{(m)})$, where m is the sample index (or iteration index). As the number of samples increases, the maximum of $p(N^{(m)}, \mathbf{T}_{\mathrm{s}}^{(m)}, \mathbf{P}_{\mathrm{d}}^{(m)})$ over all m will converge towards the maximum of $p(N, \mathbf{T}_{\mathrm{s}}, \mathbf{P}_{\mathrm{d}})$. We can therefore approximate the optimal N, $\mathbf{T}_{\mathrm{s}}$ and $\mathbf{P}_{\mathrm{d}}$ by the sample that achieves the largest

$p(N^{(m)}, \mathbf{T}_{\mathrm{s}}^{(m)}, \mathbf{P}_{\mathrm{d}}^{(m)})$:

$$N^* = N^{(m_{\max})}, \quad \mathbf{P}_{\mathrm{d}}^* = \mathbf{P}_{\mathrm{d}}^{(m_{\max})}, \quad \mathbf{T}_{\mathrm{s}}^* = \mathbf{T}_{\mathrm{s}}^{(m_{\max})}$$

with

$$m_{\max} = \arg\max_m \{p(N^{(m)}, \mathbf{P}_{\mathrm{d}}^{(m)}, \mathbf{T}_{\mathrm{s}}^{(m)})\}.$$

4.4.3 Reversible-Jump Sampler

In the optimization problem (4.8), the number of elements in $\mathbf{T}_{\mathrm{s}}$ and $\mathbf{P}_{\mathrm{d}}$ depends on the number of cooperating devices N. Hence, finding the optimal N^* can be viewed as finding the optimal dimension of $\mathbf{T}_{\mathrm{s}}^*$ and $\mathbf{P}_{\mathrm{d}}^*$, and (4.8) can be categorized as a "trans-dimensional" optimization problem [61]. The algorithm that we propose for solving this problem is based on the reversible-jump sampler concept [56], which is a special case of MCMC that is particularly suited for trans-dimensional problems. In each iteration, the reversible-jump sampler first randomly generates a proposal $(\tilde{N}^{(m+1)}, \tilde{\mathbf{T}}_{\mathrm{s}}^{(m+1)}, \tilde{\mathbf{P}}_{\mathrm{d}}^{(m+1)})$ from some proposal distribution that we can choose freely (under some mild conditions). Based on the proposal distribution and the desired target distribution, the algorithm then calculates an "acceptance" probability for the proposal. If the proposal is accepted, the new sample $(N^{(m+1)}, \mathbf{T}_{\mathrm{s}}^{(m+1)}, \mathbf{P}_{\mathrm{d}}^{(m+1)})$ (where $m+1$ is the iteration index) is chosen equal to the proposal. Otherwise, the new sample is chosen equal to $(N^{(m)}, \mathbf{T}_{\mathrm{s}}^{(m)}, \mathbf{P}_{\mathrm{d}}^{(m)})$, i.e., the sample from the previous iteration. This approach produces samples that are distributed according to the desired target distribution [56].

For generating the proposal $(\tilde{N}^{(m+1)}, \tilde{\mathbf{T}}_{\mathrm{s}}^{(m+1)}, \tilde{\mathbf{P}}_{\mathrm{d}}^{(m+1)})$, we first choose the proposed dimension $\tilde{N}^{(m+1)}$. Given the previous sample $N^{(m)}$, the proposal may either move to one dimension higher (i.e., include one more cooperating device) or move to one dimension lower (i.e., remove one cooperating device) or move within the same dimension (i.e., remain with the current number of cooperating devices). The distribution of $\tilde{N}^{(m+1)}$ given $N^{(m)}$ can be expressed as

$$q(\tilde{N}^{(m+1)} \mid N^{(m)}) = \begin{cases} (N^{(m)}+1) & \text{, with probability } \beta_{\mathrm{N}}^{+} \\ (N^{(m)}-1) & \text{, with probability } \beta_{\mathrm{N}}^{-} \\ N^{(m)} & \text{, with probability } \beta_{\mathrm{N}}^{=} \end{cases} \tag{4.14}$$

where $\beta_{\mathrm{N}}^{+} + \beta_{\mathrm{N}}^{-} + \beta_{\mathrm{N}}^{=} = 1$.

Next, we will discuss how the proposed $\tilde{\mathbf{P}}_{\mathrm{d}}^{(m+1)}$ and $\tilde{\mathbf{T}}_{\mathrm{s}}^{(m+1)}$ are generated, for the three different cases distinguished in (4.14). For the case of moving within the

same dimension, i.e., $\tilde{N}^{(m+1)} = N^{(m)}$, the elements of $\tilde{\mathbf{P}}_{\mathrm{d}}^{(m+1)}$ are generated from the proposal distribution

$$q(\tilde{P}_{\mathrm{d}_j}^{(m+1)} \mid P_{\mathrm{d}_j}^{(m)}) \sim \mathcal{U}\left(\max\{0, P_{\mathrm{d}_j}^{(m)} - \beta_{\mathrm{P_d}}\}, \min\{P_{\mathrm{d}_j}^{(m)} + \beta_{\mathrm{P_d}}, 1\}\right) \quad (4.15)$$

for $j = 1, 2, \ldots, (\tilde{N}^{(m+1)} - 1)$, where $\mathcal{U}(\cdot)$ denotes the continuous uniform distribution and $\beta_{\mathrm{P_d}}$ defines the width of its interval, centered at the previous sample position $P_{\mathrm{d}_j}^{(m)}$. $\min\{\cdot,\cdot\}$ and $\max\{\cdot,\cdot\}$ return the smallest and the largest, respectively, of the arguments. The last element of $\tilde{\mathbf{P}}_{\mathrm{d}}^{(m+1)}$, i.e., $\tilde{P}_{\mathrm{d}_{\tilde{N}^{(m+1)}}}^{(m+1)}$, is chosen deterministically such that the targeted detection probability $\bar{Q}_{\mathrm{d}}$ is satisfied. The deterministic function $\tilde{P}_{\mathrm{d}_{\tilde{N}^{(m+1)}}}^{(m+1)}\left(\bar{Q}_{\mathrm{d}}, \tilde{P}_{\mathrm{d}_1}^{(m+1)}, \ldots, \tilde{P}_{\mathrm{d}_{(\tilde{N}^{(m+1)}-1)}}^{(m+1)}\right)$ can be derived from the cooperative probability of detection Q_{d} formula (cf. (2.10)), yielding

$$\tilde{P}_{\mathrm{d}_{\tilde{N}^{(m+1)}}}^{(m+1)}\left(\bar{Q}_{\mathrm{d}}, \tilde{P}_{\mathrm{d}_1}^{(m+1)}, \ldots, \tilde{P}_{\mathrm{d}_{(\tilde{N}^{(m+1)}-1)}}^{(m+1)}\right) = \frac{\bar{Q}_{\mathrm{d}} - \sum_{k=K}^{(\tilde{N}^{(m+1)}-1)} \psi(k)}{\psi(K)} \quad (4.16)$$

where

$$\psi(k) = \sum\nolimits_{\mathcal{A}_{k,\sim\tilde{N}^{(m+1)}}^{(a)} \subseteq \mathcal{A}_{k,\sim\tilde{N}^{(m+1)}}} \left(\prod\nolimits_{g\in\mathcal{A}_{k,\sim\tilde{N}^{(m+1)}}^{(a)}} \tilde{P}_{\mathrm{d}_g}^{(m+1)}\right) \left(\prod\nolimits_{h\in\{\mathcal{N}\setminus\mathcal{A}_{k,\sim\tilde{N}^{(m+1)}}^{(a)}\}} (1 - \tilde{P}_{\mathrm{d}_h}^{(m+1)})\right). \quad (4.17)$$

Here, $\sim\tilde{N}^{(m+1)}$ means that the respective set does not contain the element corresponding to device $\tilde{N}^{(m+1)}$. The elements of $\tilde{\mathbf{T}}_{\mathrm{s}}^{(m+1)}$ are generated from

$$q(\tilde{T}_{\mathrm{s}_j}^{(m+1)} \mid T_{\mathrm{s}_j}^{(m)}) \sim \mathcal{U}\left\{\max\{\tau, T_{\mathrm{s}_j}^{(m)} - \beta_{\mathrm{T_s}}\}, \min\{(T_{\mathrm{s}_j}^{(m)} + \beta_{\mathrm{T_s}}), (T_{\mathrm{sf}} - T_{\mathrm{sr}})\}\right\} \quad (4.18)$$

for $j = 1, 2, \ldots, \tilde{N}^{(m+1)}$, where $\beta_{\mathrm{T_s}}$ defines the width of the uniform distribution intervals, centered at the previous sample position $T_{\mathrm{s}_j}^{(m)}$.

For the case of moving one dimension higher, i.e., $\tilde{N}^{(m+1)} = (N^{(m)} + 1)$, we consider the following distribution for the elements of $\tilde{\mathbf{P}}_{\mathrm{d}}^{(m+1)}$:

$$q(\tilde{P}_{\mathrm{d}_j}^{(m+1)} \mid P_{\mathrm{d}_j}^{(m)}) = \begin{cases} P_{\mathrm{d}_j}^{(m)} - \dfrac{\varphi_{\mathrm{P_d}}}{\tilde{N}^{(m+1)} - 2} & , \text{for } j = 1, 2, \ldots, (\tilde{N}^{(m+1)} - 2) \\ \varphi_{\mathrm{P_d}} & , \text{for } j = (\tilde{N}^{(m+1)} - 1) \end{cases} \quad (4.19)$$

where $\varphi_{\mathrm{P_d}} \sim \mathcal{U}(0, 1)$. Again, the last element of $\tilde{\mathbf{P}}_{\mathrm{d}}^{(m+1)}$, i.e., $\tilde{P}_{\mathrm{d}_{\tilde{N}^{(m+1)}}}^{(m+1)}$, is chosen deterministically according to $\tilde{P}_{\mathrm{d}_{\tilde{N}^{(m+1)}}}^{(m+1)}\left(\bar{Q}_{\mathrm{d}}, \tilde{P}_{\mathrm{d}_1}^{(m+1)}, \ldots, \tilde{P}_{\mathrm{d}_{(\tilde{N}^{(m+1)}-1)}}^{(m+1)}\right)$. For the

elements of $\tilde{\mathbf{T}}_{\mathrm{s}}^{(m+1)}$, we choose:

$$q(\tilde{T}_{\mathrm{s}_j}^{(m+1)} \mid T_{\mathrm{s}_j}^{(m)}) = \begin{cases} T_{\mathrm{s}_j}^{(m)} - \dfrac{\varphi_{\mathrm{T_s}}}{\tilde{N}^{(m+1)} - 1} & , \text{for } j = 1, 2, \ldots, (\tilde{N}^{(m+1)} - 1) \\ \varphi_{\mathrm{T_s}} & , \text{for } j = \tilde{N}^{(m+1)} \end{cases} \tag{4.20}$$

where $\varphi_{\mathrm{T_s}} \sim \mathcal{U}\{\tau, (T_{\mathrm{sf}} - T_{\mathrm{sr}})\}$ is defined as a discrete uniform distribution on an interval of length τ.

For the case of moving one dimension lower, i.e., $\tilde{N}^{(m+1)} = (N^{(m)} - 1)$, the proposal distribution for the detection probabilities and sensing times are as follows:

$$q(\tilde{P}_{\mathrm{d}_j}^{(m+1)} \mid P_{\mathrm{d}_j}^{(m)}) = P_{\mathrm{d}_j}^{(m)} + \frac{\varphi_{\mathrm{P_d}}}{\tilde{N}^{(m+1)} - 1} \quad , \text{for } j = 1, 2, \ldots, (\tilde{N}^{(m+1)} - 1) \tag{4.21}$$

$$q(\tilde{T}_{\mathrm{s}_j}^{(m+1)} \mid T_{\mathrm{s}_j}^{(m)}) = T_{\mathrm{s}_j}^{(m)} + \frac{\varphi_{\mathrm{T_s}}}{\tilde{N}^{(m+1)}} \quad , \text{for } j = 1, 2, \ldots, \tilde{N}^{(m+1)} \tag{4.22}$$

As in the other two cases, the last element of $\tilde{\mathbf{P}}_{\mathrm{d}}^{(m+1)}$ is chosen deterministically according to $\tilde{P}_{\mathrm{d}_{\tilde{N}^{(m+1)}}}^{(m+1)}(\bar{Q}_{\mathrm{d}}, \tilde{P}_{\mathrm{d}_1}^{(m+1)}, \ldots, \tilde{P}_{\mathrm{d}_{(\tilde{N}^{(m+1)}-1)}}^{(m+1)})$.

The acceptance probability of the proposal is defined as 1 whenever the proposal has a higher probability distribution function $p(N, \mathbf{T}_{\mathrm{s}}, \mathbf{P}_{\mathrm{d}})$ than the previous sample, i.e.,

$$\left.\begin{array}{l} N^{m+1} = \tilde{N}^{(m+1)} \\ \mathbf{T}_{\mathrm{s}}^{(m+1)} = \tilde{\mathbf{T}}_{\mathrm{s}}^{(m+1)} \\ \mathbf{P}_{\mathrm{d}}^{(m+1)} = \tilde{\mathbf{P}}_{\mathrm{d}}^{(m+1)} \end{array}\right\} \text{ for } \begin{array}{c} p(\tilde{N}^{(m+1)}, \tilde{\mathbf{T}}_{\mathrm{s}}^{(m+1)}, \tilde{\mathbf{P}}_{\mathrm{d}}^{(m+1)}) \\ \geq p(N^{(m)}, \mathbf{T}_{\mathrm{s}}^{(m)}, \mathbf{P}_{\mathrm{d}}^{(m)}) \end{array} \tag{4.23}$$

If the probability of the proposal is lower than that of the previous sample, the proposal will still be accepted with a certain probability. From [56, 62], this probability can be derived as

$$\begin{aligned} &\varrho(\tilde{N}^{(m+1)}, \tilde{\mathbf{T}}_{\mathrm{s}}^{(m+1)}, \tilde{\mathbf{P}}_{\mathrm{d}}^{(m+1)}) = \\ &\frac{p(\tilde{N}^{(m+1)}, \tilde{\mathbf{T}}_{\mathrm{s}}^{(m+1)}, \tilde{\mathbf{P}}_{\mathrm{d}}^{(m+1)})}{p(N^{(m)}, \mathbf{T}_{\mathrm{s}}^{(m)}, \mathbf{P}_{\mathrm{d}}^{(m)})} \prod_{j=1}^{\tilde{N}^{(m+1)}-1} \left(\frac{q(P_{\mathrm{d}_j}^{(m)} \mid \tilde{P}_{\mathrm{d}_j}^{(m+1)})\, q(T_{\mathrm{s}_j}^{(m)} \mid \tilde{T}_{\mathrm{s}_j}^{(m+1)})}{q(\tilde{P}_{\mathrm{d}_j}^{(m+1)} \mid P_{\mathrm{d}_j}^{(m)})\, q(\tilde{T}_{\mathrm{s}_j}^{(m+1)} \mid T_{\mathrm{s}_j}^{(m)})} \right) \\ &\times \frac{q(T_{\mathrm{s}_{\tilde{N}^{(m+1)}}}^{(m)} \mid \tilde{T}_{\mathrm{s}_{\tilde{N}^{(m+1)}}}^{(m+1)})}{q(\tilde{T}_{\mathrm{s}_{\tilde{N}^{(m+1)}}}^{(m+1)} \mid T_{\mathrm{s}_{\tilde{N}^{(m+1)}}}^{(m)})} \left| \frac{\partial(\tilde{\mathbf{P}}_{\mathrm{d}}^{(m+1)}, \tilde{\mathbf{T}}_{\mathrm{s}}^{(m+1)}, \boldsymbol{\varphi})}{\partial(\mathbf{P}_{\mathrm{d}}^{(m)}, \mathbf{T}_{\mathrm{s}}^{(m)}, \boldsymbol{\varphi})} \right| \end{aligned} \tag{4.24}$$

where $\boldsymbol{\varphi} \triangleq [\varphi_{\mathrm{P_d}}, \varphi_{\mathrm{T_s}}]$, and the Jacobian determinant $\left|\frac{\partial(\tilde{\mathbf{P}}_{\mathrm{d}}^{(m+1)}, \tilde{\mathbf{T}}_{\mathrm{s}}^{(m+1)}, \boldsymbol{\varphi})}{\partial(\mathbf{P}_{\mathrm{d}}^{(m)}, \mathbf{T}_{\mathrm{s}}^{(m)}, \boldsymbol{\varphi})}\right|$ is defined as

$$\begin{vmatrix} \frac{\partial \tilde{P}_{\mathrm{d}_1}^{(m+1)}}{\partial P_{\mathrm{d}_1}^{(m)}} & \cdots & \frac{\partial \tilde{P}_{\mathrm{d}_1}^{(m+1)}}{\partial T_{\mathrm{s}_1}^{(m)}} & \cdots & \frac{\partial \tilde{P}_{\mathrm{d}_1}^{(m+1)}}{\partial \varphi_{\mathrm{P_d}}} & \frac{\partial \tilde{P}_{\mathrm{d}_1}^{(m+1)}}{\partial \varphi_{\mathrm{T_s}}} \\ \vdots & \ddots & \vdots & \ddots & \vdots & \vdots \\ \frac{\partial \tilde{T}_{\mathrm{s}_1}^{(m+1)}}{\partial P_{\mathrm{d}_1}^{(m)}} & \ddots & \vdots & \ddots & \vdots & \vdots \\ \vdots & \ddots & \vdots & \ddots & \vdots & \vdots \\ \frac{\partial \varphi_{\mathrm{P_d}}}{\partial P_{\mathrm{d}_1}^{(m)}} & \ddots & \vdots & \ddots & \vdots & \vdots \\ \frac{\partial \varphi_{\mathrm{T_s}}}{\partial P_{\mathrm{d}_1}^{(m)}} & \cdots & \frac{\partial \varphi_{\mathrm{T_s}}}{\partial T_{\mathrm{s}_1}^{(m)}} & \cdots & \frac{\partial \varphi_{\mathrm{T_s}}}{\partial \varphi_{\mathrm{P_d}}} & \frac{\partial \varphi_{\mathrm{T_s}}}{\partial \varphi_{\mathrm{T_s}}} \end{vmatrix} . \tag{4.25}$$

It can be shown that, with the chosen settings, this Jacobian is equal to one. If $\varrho(\tilde{N}^{(m+1)}, \tilde{\mathbf{T}}_{\mathrm{s}}^{(m+1)}, \tilde{\mathbf{P}}_{\mathrm{d}}^{(m+1)})$ is greater than some random number $\mathrm{rand} \sim \mathcal{U}(0,1)$, then we accept the proposal. In the converse case, we take the previous values as the next samples, i.e.,

$$\left.\begin{array}{l} N^{m+1} = N^{(m)} \\ \mathbf{T}_{\mathrm{s}}^{(m+1)} = \mathbf{T}_{\mathrm{s}}^{(m)} \\ \mathbf{P}_{\mathrm{d}}^{(m+1)} = \mathbf{P}_{\mathrm{d}}^{(m)} \end{array}\right\} \text{ for } \begin{array}{c} p(\tilde{N}^{(m+1)}, \mathbf{T}_{\mathrm{s}}^{(m+1)}, \tilde{\mathbf{P}}_{\mathrm{d}}^{(m+1)}) \\ < p(N^{(m)}, \mathbf{T}_{\mathrm{s}}^{(m)}, \mathbf{P}_{\mathrm{d}}^{(m)}) \end{array} \tag{4.26}$$

Note that $\varrho(\tilde{N}^{(m+1)}, \tilde{\mathbf{T}}_{\mathrm{s}}^{(m+1)}, \tilde{\mathbf{P}}_{\mathrm{d}}^{(m+1)})$ is always be greater than or equal to one if $p(\tilde{N}^{(m+1)}, \mathbf{T}_{\mathrm{s}}^{(m+1)}, \tilde{\mathbf{P}}_{\mathrm{d}}^{(m+1)}) \geq p(N^{(m)}, \mathbf{T}_{\mathrm{s}}^{(m)}, \mathbf{P}_{\mathrm{d}}^{(m)})$, which leads back to (4.23). The stochastic acceptance rule enables the algorithm to explore the space better and avoid being trapped at a local optimum. By alternating the two steps of generating a proposal and accepting/rejecting it, we generate samples $N^{(m)}$, $\mathbf{T}_{\mathrm{s}}^{(m)}$ and $\mathbf{P}_{\mathrm{d}}^{(m)}$ from the distribution $p(N, \mathbf{T}_{\mathrm{s}}, \mathbf{P}_{\mathrm{d}})$.

The reversible-jump sampler algorithm for finding the optimal number of cooperating devices N^*, sensing times $\mathbf{T}_{\mathrm{s}}^*$ and probability of detections $\mathbf{P}_{\mathrm{d}}^*$ that jointly minimize the energy usage in CSS is shown in Algorithm 1.

Algorithm 1 Optimal number of cooperating devices N^*, sensing times $\mathbf{T}_{\mathrm{s}}^*$ and probability of detections $\mathbf{P}_{\mathrm{d}}^*$

Given set $\mathcal{J}$ of HAN devices in a cluster, with signal-to-noise-ratio of the incumbent user at each sensing device $\mathrm{SNR}_{\mathrm{p}_j}$.
Sort the elements in $\mathcal{J}$ in descending order of the $\mathrm{SNR}_{\mathrm{p}_j}$.
Initialize the first sample $N^{(1)}$, $\mathbf{P}_{\mathrm{d}}^{(1)} \triangleq [P_{\mathrm{d}_j}^{(1)}]_{j\in\{1,2,\ldots,N^{(1)}\}}$ and
$\mathbf{T}_s^{(1)} \triangleq [T_{\mathrm{s}_j}^{(1)}]_{j\in\{1,2,\ldots,N^{(1)}\}}$ with arbitrary values.
repeat
  Get a sample proposal for $N^{(m+1)}$: $\tilde{N}^{(m+1)} \sim q(\tilde{N}^{(m+1)} \mid N^{(m)})$ according to (4.14).
  for each $j \in \{1, 2, \ldots, \tilde{N}^{(m+1)}\}$ **do**
    Get a sample proposal for $T_{\mathrm{s}_j}^{(m+1)}$: $\tilde{T}_{\mathrm{s}_j}^{(m+1)} \sim q(\tilde{T}_{\mathrm{s}_j}^{(m+1)} \mid T_{\mathrm{s}_j}^{(m)})$ according to (4.18), (4.20) or (4.22).
  end for
  for each $j \in \{1, 2, \ldots, (\tilde{N}^{(m+1)} - 1)\}$ **do**
    Get a sample proposal for $P_{\mathrm{d}_j}^{(m+1)}$: $\tilde{P}_{\mathrm{d}_j}^{(m+1)} \sim q(\tilde{P}_{\mathrm{d}_j}^{(m+1)} \mid P_{\mathrm{d}_j}^{(m)})$ according to (4.15), (4.19) or (4.21).
  end for
  Get a sample proposal for $P_{\mathrm{d}_{\tilde{N}^{(m+1)}}}^{(m+1)}$:
  $\tilde{P}_{\mathrm{d}_{\tilde{N}^{(m+1)}}}^{(m+1)} = \tilde{P}_{\mathrm{d}_{\tilde{N}^{(m+1)}}}^{(m+1)}\big(\bar{Q}_{\mathrm{d}}, \tilde{P}_{\mathrm{d}_1}^{(m+1)}, \ldots, \tilde{P}_{\mathrm{d}_{(\tilde{N}^{(m+1)}-1)}}^{(m+1)}\big)$ according to (4.16).
  Calculate the acceptance probability $\varrho(\tilde{N}^{(m+1)}, \tilde{\mathbf{T}}_{\mathrm{s}}^{(m+1)}, \tilde{\mathbf{P}}_{\mathrm{d}}^{(m+1)})$ according to (4.24).
  if $\mathrm{rand} \geq \varrho(\tilde{N}^{(m+1)}, \tilde{\mathbf{T}}_{\mathrm{s}}^{(m+1)}, \tilde{\mathbf{P}}_{\mathrm{d}}^{(m+1)})$ **then**
    $N^{(m+1)} = \tilde{N}^{(m+1)}$, $\mathbf{P}_{\mathrm{d}}^{(m+1)} = \tilde{\mathbf{P}}_{\mathrm{d}}^{(m+1)}$ and $\mathbf{T}_{\mathrm{s}}^{(m+1)} = \tilde{\mathbf{T}}_{\mathrm{s}}^{(m+1)}$.
  else
    $N^{(m+1)} = N^{(m)}$, $\mathbf{P}_{\mathrm{d}}^{(m+1)} = \mathbf{P}_{\mathrm{d}}^{(m)}$ and $\mathbf{T}_{\mathrm{s}}^{(m+1)} = \mathbf{T}_{\mathrm{s}}^{(m)}$.
  end if
until maximum iterations
$N^* = N^{(m_{\max})}$, $\mathbf{P}_{\mathrm{d}}^* = \mathbf{P}_{\mathrm{d}}^{(m_{\max})}$ and $\mathbf{T}_{\mathrm{s}}^* = \mathbf{T}_{\mathrm{s}}^{(m_{\max})}$, with
$m_{\max} = \arg\max_m \{p(N^{(m)}, \mathbf{P}_{\mathrm{d}}^{(m)}, \mathbf{T}_{\mathrm{s}}^{(m)})\}$.

4.5 Performance Evaluation and Discussions

4.5.1 Evaluation Setup

In this section, we evaluate the performance of the proposed CSS scheme denoted by $\min_{\mathcal{N},\mathbf{P}_\mathrm{d},\mathbf{T}_\mathrm{s}} E_\mathrm{css}$, and compare it with three other schemes:

i) $\max_{P_\mathrm{d},T_\mathrm{s}} R$ with $P_{\mathrm{d}_j} = P_\mathrm{d},\ T_{\mathrm{s}_j} = T_\mathrm{s},\ \forall j$, where P_d and T_s are optimized such that the achievable throughput R is maximized; we define this as the conventional scheme;

ii) $\min_{P_\mathrm{d},T_\mathrm{s}} E_\mathrm{css}$ with $P_{\mathrm{d}_j} = P_\mathrm{d},\ T_{\mathrm{s}_j} = T_\mathrm{s},\ \forall j$, where P_d and T_s are optimized such that CSS energy consumption E_css is minimized;

iii) $\min_{\mathbf{P}_\mathrm{d},\mathbf{T}_\mathrm{s}} E_\mathrm{css}$ which is the same as scheme (*ii*)) except that P_{d_j} and T_{s_j} can vary from device to device; in this scheme, all devices in the cluster are used for the CSS and N is not optimized.

The following values are used for the network and kept throughout this section: the superframe duration $T_\mathrm{sf} = 100$ ms, the sensing-report duration $T_\mathrm{sr} = 0.5$ ms, the sampling duration $\tau = 0.1$ ms, the target detection probability $Q_\mathrm{d} = 0.9$ and the probability of idle channel $P(\mathcal{H}_0) = 0.7$. Moreover, in this work, the majority fusion rule $k = \lceil \frac{N}{2} \rceil$ is considered for the CSS as this has been found to be optimal or nearly optimal [22, 21]. The power consumption for transmission and reception of HAN devices are 20 mW and 36.54 mW, respectively, which is also used in [23, 24]. We also considered that the incumbent user's SNR is different at each HAN devices, i.e. between -13.0 dB and -6.0 dB (a range that gives a good dynamic response to the sensing time and probability of detection and false alarm, c.f. Figure 2.11). For consistency, we generate this value once for each device and use it throughout this section.

For the reversible-jump MCMC, we choose: $\beta_\mathrm{N}^{+} = 0.25$, $\beta_\mathrm{N}^{-} = 0.25$, $\beta_\mathrm{N}^{=} = 0.5$, $\beta_{\mathrm{P}_\mathrm{d}} = 0.2$, $\beta_{\mathrm{T}_\mathrm{s}} = 30\tau$. The initial $\mathbf{P}^{(1)}_{\mathrm{d},\sim N^{(1)}}$ and $\mathbf{T}_\mathrm{s}^{(1)}$ are set to 0.8 and 32.0 ms, respectively. Note that the results in this section show the gain for a single superframe of a channel. The cumulative gain will be higher if multiple superframes and channels are taken into consideration.

4.5.2 A Simple Network Case

We first evaluate the energy and throughput efficiency performance of the proposed CSS scheme and the three reference schemes for a simple network setup where

there are only two HAN devices in the cluster such that $j \in \mathcal{J} = \{1, 2\}$ with $\{\mathrm{SNR}_{\mathrm{p}_j}\} = \{-12.3, -9.5\}$ dB, respectively. This is to make the results more readable, particularly for graphs where each device $j \in \mathcal{J}$ is assessed individually, and also to facilitate the discussion of the resulting setting for each cooperating device j in all cases.

Figure 4.3(a) shows that the network throughput demands D are dynamically and closely satisfies with the corresponding achievable throughput R for the $\min E_{\mathrm{css}}$ schemes. At the same time, a smaller sensing energy E_{css} is achieved when the demand is lower, as can be seen in Figure 4.3(b). Maximizing the achievable throughput R regardless of the demand D (i.e., the conventional scheme), on the other hand, causes an unnecessary high sensing energy E_{css} overhead. For example, for $D = 0.1$, over 94% of the sensing energy can be saved. This is intuitive since lower throughput demand D (cf. Figure 4.3(e) and 4.3(f)), which amounts to shorter sensing times (cf. Figure 4.3(c)) and thus, lower sensing energy. In the conventional scheme, more than 30% of the superframe time is used for spectrum sensing at all times, resulting in constantly high in sensing energy even when the demand D is very low.

Moreover, by allowing each cooperating device j to have its individual sensing time T_{s_j} and detection probability P_{d_j}, we are able to further reduce the sensing energy E_{css}, for example by 56% at $D = 0.226$. At low throughput demand D, the proposed scheme achieves even lower E_{css} by excluding unnecessary sensing devices. Here we achieved this by allocating cooperating device 1, which has a lower incumbent user's SNR, with a lower detection probability P_{d_1}. Consequently it can achieve a lower P_{f_1}, hence lower Q_{f} and higher R, without requiring a very long sensing time T_{s_1}. This is shown in Figure 4.3(d). In addition to this, by excluding device 1 in the spectrum sensing during a low D (note that there is no line for $j = 1$ at $D < 0.226$ in Figure 4.3(c)–(e)), we are able to achieve the highest energy efficiency among all schemes. This is because, for satisfying a demand D in this region, including device 1 for spectrum sensing is less energy efficient than prolonging the sensing time of device 2, i.e., T_{s_2}. Recall that E_{css} increases with the total number of cooperating devices N.

For a higher D, on the other hand, an inclusion of device 1 is necessary as it can only be satisfied with a higher cooperation in the spectrum sensing (i.e., more cooperating devices and longer sensing time by all devices). Note that, for $D \geq 0.226$, schemes (*i*)) and (*ii*)) are unable to satisfy the demand D anymore. In other words, the higher throughput can only be achieved by allowing each device j to have different P_{d_j} and T_{s_j}. At $D = 0.254$ the throughput of the proposed scheme

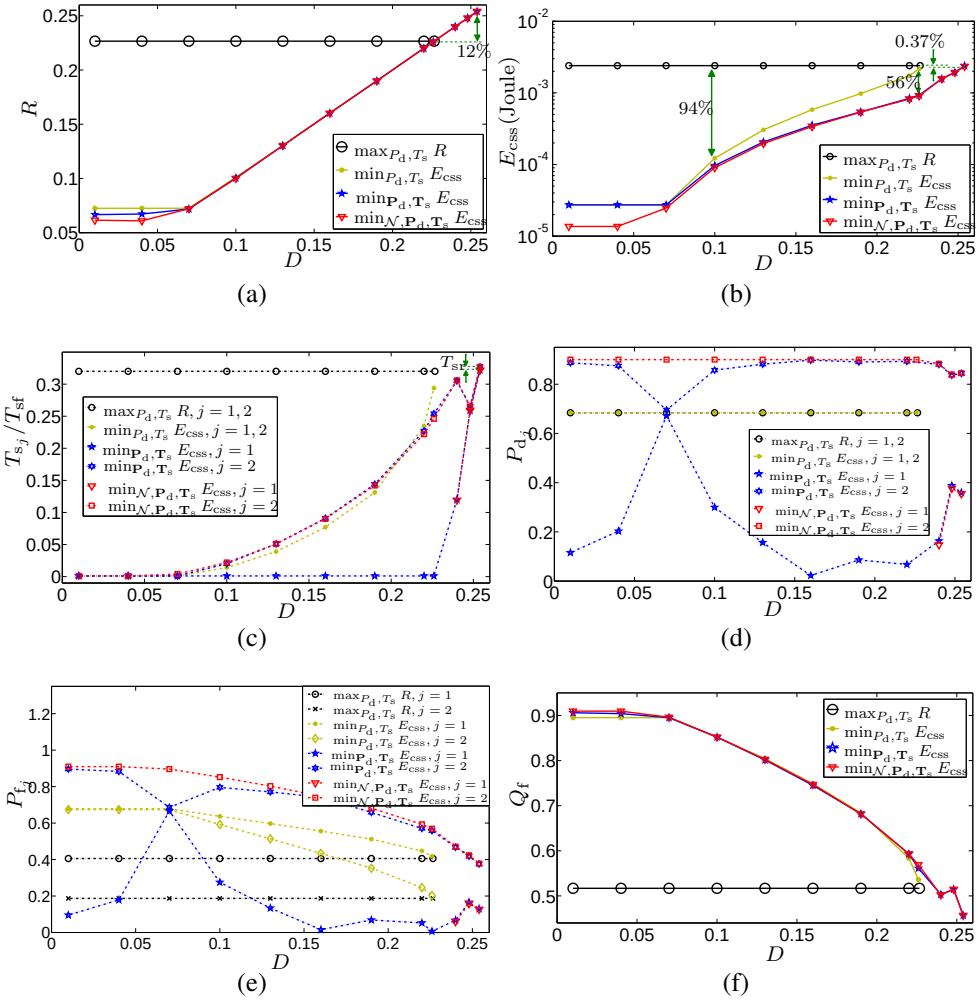

Figure 4.3: Performance evaluation on a simple network model of the proposed CSS scheme and the three reference schemes, in relation with the normalized average network's throughput demand D: (a) the normalized average achievable throughput R, (b) the CSS's energy consumption E_{css}, (c) the sensing time of each cooperating device T_{s_j} normalized to the total superframe time T_{sf}, (d) the detection probability P_{d_j} of each sensing device, (e) the false alarm probability P_{f_j} of each sensing device, (f) the cooperative false alarm probability Q_{f}.

is 12% higher than that of the conventional scheme, and it is achieved with 0.37% less energy. This is attained by utilizing the time available for sensing in CSS to the maximum: device 2 continues sensing until the end of device 1's sensing-report transmission duration, i.e., $T_{\mathrm{s}_2} = T_{\mathrm{s}_1} + T_{\mathrm{sr}}$.

Notice that the cooperative probability of false alarm Q_{f} at throughput demand $D = 0.248$ is higher than at the previous point i.e., $D = 0.24$. This shows that a higher throughput demand need not necessarily be satisfied through a lower cooperative probability of false alarm. Recall that, besides Q_{f}, the achievable throughput $R \geq D$ also depends on the maximum sensing time among all cooperating devices $\max_{j\in\mathcal{N}}\{T_{\mathrm{s}_j}\}$. Algorithm 1 finds the best tradeoff that results in the lowest energy consumption. For $D = 0.248$, a higher Q_{f} and lower $\max_{j\in\mathcal{N}}\{T_{\mathrm{s}_j}\}$ are chosen, compared to D=0.24.

4.5.3 A Many CR-based HAN Devices Case

Now we evaluate the energy and throughput performance of the proposed CSS scheme when many HAN devices available in the cluster, which describes a dense HAN scenario. The performance is compared with scheme (iii) which is the same case as the proposed scheme except that all available devices j in the cluster are included in the spectrum sensing. Let us assumed that $j \in \mathcal{J} = \{1, 2, \ldots, 6\}$ with $\{\mathrm{SNR}_{\mathrm{p}_j}\} = \{-12.3, -9.5, -7.5, -9.5, -6.5, -7.0\}$ dB, respectively. Note that the simulation can also be done for any number of HAN devices. The result shown in Figure 4.4 illustrates that the proposed scheme provides better energy efficiency and can achieve the same (or higher) maximum throughput, which indicates the benefits of selecting the optimal cooperating devices used for spectrum sensing, instead of utilizing all of them.

Figure 4.5 shows the corresponding sensing time T_{s_j} and probability of detection P_{d_j} of all HAN devices j in the cluster for the proposed scheme, which also indicate which cooperating devices are selected for spectrum sensing (i.e., devices for which T_{s_j} and P_{d_j} are shown). Clearly, it can be seen that only a few number of cooperating devices are needed for the spectrum sensing to satisfy the network's throughput demand D, particularly when the demand is low. Even the highest achievable throughput $R = 0.52$ only requires four cooperating devices, which demonstrates that it is not necessary to involve all devices in order to achieve the maximum achievable throughput.

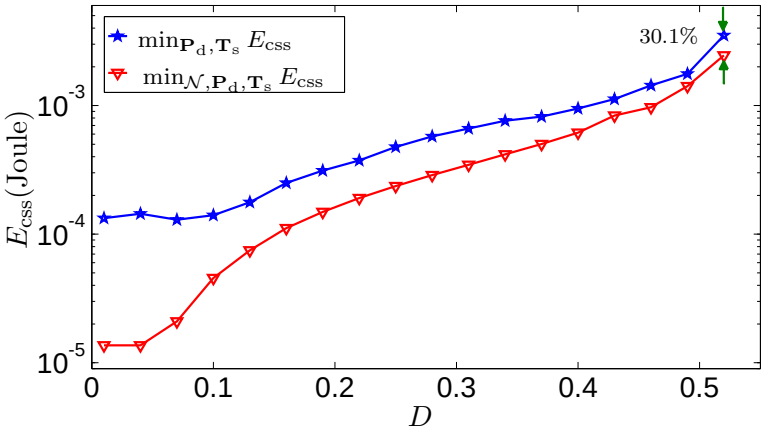

Figure 4.4: The energy consumption of cooperative spectrum sensing with and without device selection, when there are more CR-based HAN devices in the cluster.

4.6 Conclusion

In cognitive radio, it is very important to ensure that the energy consumption in spectrum sensing is minimum, particularly for battery-powered devices, as devices should spend their energy more on executing their actual application. At the same time, it is also important that the demanded throughput of the network is satisfied in an efficient way. In this work, an energy and throughput efficient cooperative spectrum sensing (CSS) scheme for a home area network was proposed, where the demanded throughput of the network and the different signal-to-noise-ratio of the primary user at each sensing device are taken into account. The proposed scheme selects the cooperating devices and jointly determines the sensing time and the detection probability of each selected sensing device were jointly determined. These values can be different from one device to another. We showed that over 94% sensing energy can be saved by considering the throughput demand in optimizing the CSS. In addition, by allowing each cooperating device to have different sensing time and detection probability from one another, the energy consumption was further reduced, for example by 56% at $D = 0.226$. This innovation also allowed us to achieve 12% higher throughput with 0.37% less energy as compared to the conventional scheme. Moreover, when many HAN devices are available in the cluster, it is highly beneficial to select the optimal subset of devices for CSS, rather than utilizing all of them. We showed that, for a case of six HAN devices, more than 30% of the sensing energy can be saved.

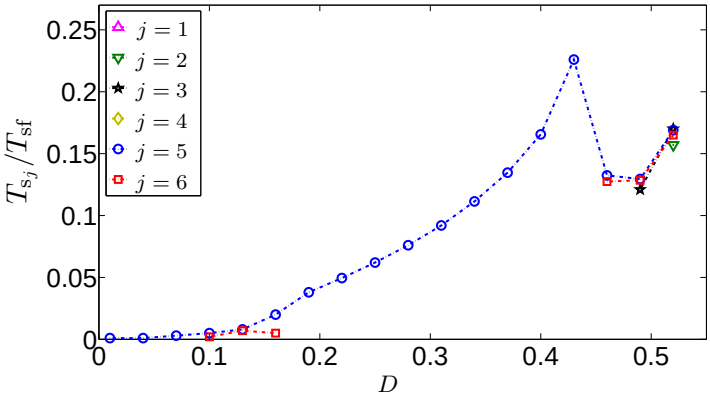

(a)

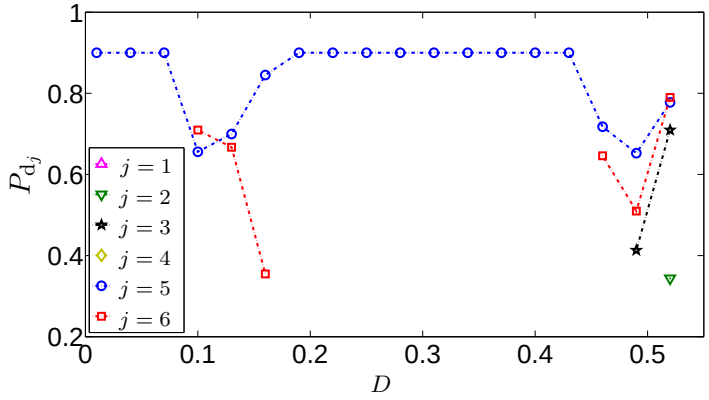

(b)

Figure 4.5: The selected cooperating devices for spectrum sensing form graphs of: (a) the normalized spectrum sensing time, and (b) the detection probability, with respect to the normalized average network's throughput demand.

In the next chapter, we will further work on grouping the selected HAN devices to form multiple spectrum sensing groups. We will then schedule the groups to sense the optimal channels set used by the cluster.

Chapter 5

Sensing Device Grouping and Scheduling for Multi-channel Cooperative Spectrum Sensing

In the previous chapter, we have worked at optimally selecting the cognitive HAN devices for spectrum sensing, such that it gives the lowest cooperative spectrum sensing energy consumption and at the same time satisfies the demanded throughput of the network. The selection is based on the signal-to-noise-ratio of the incumbent user at each device. In this chapter, we will further work at grouping the HAN devices together to form multiple cooperative spectrum sensing groups, and then schedule these groups to sense the selected channels. In doing this, we want to make sure that the energy that will be used for the spectrum sensing is kept to a minimum, the lifetime of each HAN device is maximized, and at the same time, the throughput demand of the network is kept satisfied. For this, we will take the energy condition of each HAN device into consideration, in addition to the signal-to-noise-ratio of the incumbent user.

5.1 Introduction

In a typical cognitive radio-based communication, the CR-based HAN devices (which later on will also be denoted simply as HAN devices) need to sense the spectrum to find idle channels to communicate. In the scenario of a dense HAN, there will exist a large number of HAN devices in a house. Asking all available

devices to sense a channel at the same time will lead to an unnecessary overhead including high spectrum sensing energy consumption and reduce the communication throughput. Hence, in Chapter 4, we determined the optimal subset of HAN devices which should be selected for the spectrum sensing task, and the corresponding optimal spectrum sensing time and detection probability of each of the selected devices, that minimized the cooperative spectrum sensing (CSS) energy consumption and at the same time satisfied the demanded average communication throughput.

However, that particular work is limited to a single channel and a single spectrum sensing group. In this chapter, we will extend the work to multiple channels and multiple CSS groups. Consequently, these HAN devices will be divided into groups leading to multiple CSS groups. These groups are scheduled to sense the active in-band channels in the cluster. In addition, the optimal spectrum sensing time and detection probability of each device will be jointly determined. These will be done with the objective of minimizing the total energy consumption in CSS and at the same time ensuring the average demanded throughput is satisfied. Furthermore, in doing so, we also attempt to fairly distribute the spectrum sensing burden among the available CR-based HAN devices such that the lifetime of each device is optimized to its expected lifetime: this is regarded as CSS load fairness.

5.2 System Model

A CR-based HAN network model as proposed in Chapter 3 is considered. We denote device j's residual energy, expected lifetime, and incumbent user's signal-to-noise ratio at each channel i as E_{res_j}, T_{live_j}, and $\mathrm{SNR}_{\mathrm{p}_j}^{(i)}$, respectively. The initial expected lifetime is defined for example by the device's manufacturer which can be calculated from the energy capacity installed (e.g., battery) and the typical energy consumption of the device. The active in-band channel is denoted as i, where $i \in \mathcal{I}$. The group of devices that is assigned to sense channel i is denoted as $\mathcal{N}^{(i)}$.

Figure 5.1 shows the proposed CR multi-channel and multi-CSS-group operation for one network cluster, and the CSS strategy considered in this chapter. The number of channels used in a cluster is adaptive, i.e. it can be expanded or shrunk depending on the total throughput demand of the network cluster, as mentioned in more detail in Chapter 3.

This figure also illustrates that the superframe of each channel i comprises of two sub slots: a sub slot of duration $T_{\mathrm{css}}^{(i)}$ for cooperative spectrum sensing, and a sub slot of duration $T_{\mathrm{com}}^{(i)}$ for data communication. In the former slot, each sens-

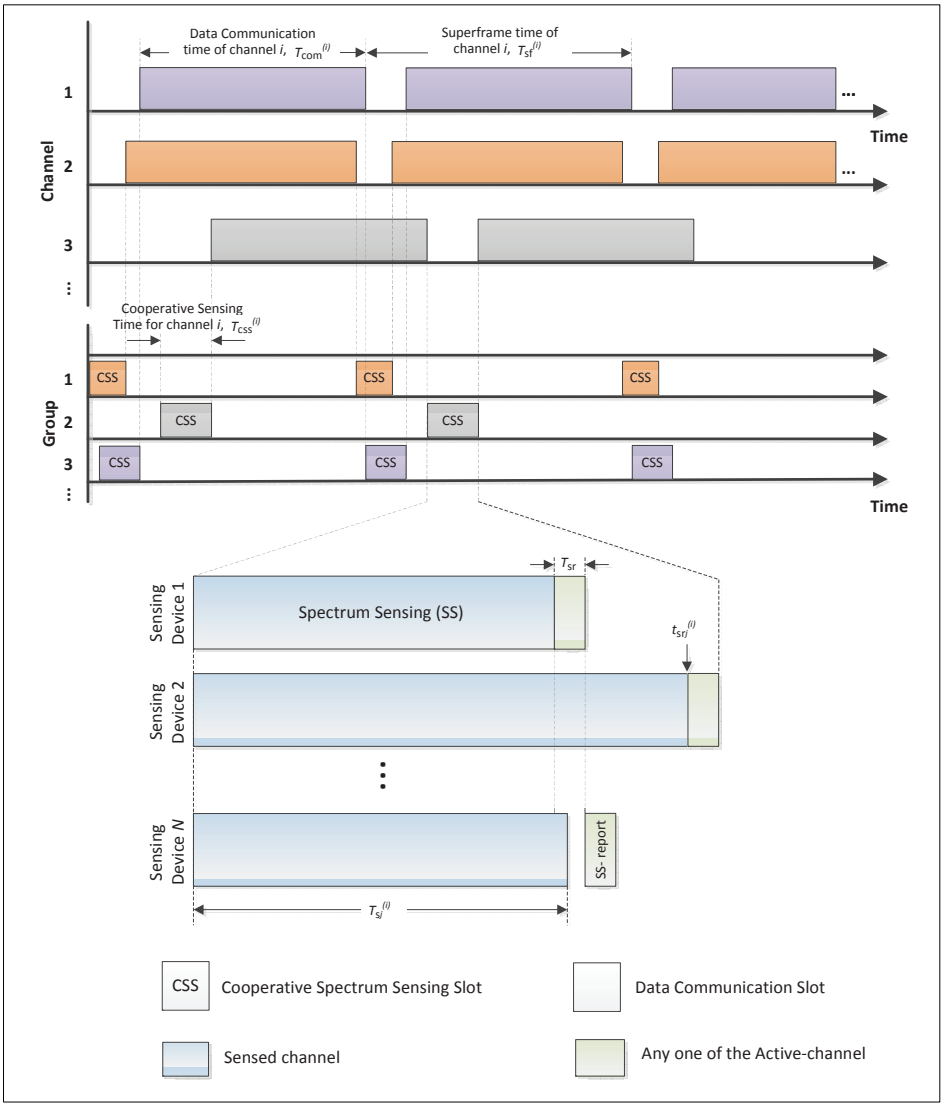

Figure 5.1: An example of the proposed multi-channel and multi-cooperative-spectrum-sensing-group cognitive radio network operation, with the cooperative spectrum sensing strategy considered.

ing device j executes spectrum sensing for a duration of $T_{\mathrm{s}_j}^{(i)}$, and then reports its sensing outcome to the CH at time $t_{\mathrm{tsr}_j}^{(i)}$ for a duration of T_{sr}.

The spectrum sensing is based on energy detection. We use $P_{\mathrm{f}_j}^{(i)}$ and $P_{\mathrm{d}_j}^{(i)}$ to denote the false alarm and the detection probabilities of device j at channel i, respectively. Considering the same assumptions as in Chapter 2, from (2.7), for a targeted $\bar{P}_{\mathrm{d}_j}^{(i)}$ we then have

$$P_{\mathrm{f}_j}^{(i)}(\bar{P}_{\mathrm{d}_j}^{(i)}, \mathrm{SNR}_{\mathrm{p}_j}^{(i)}, T_{\mathrm{s}_j}^{(i)}) = \mathcal{Q}\left(\mathrm{SNR}_{\mathrm{p}_j}^{(i)}\sqrt{\frac{T_{\mathrm{s}_j}^{(i)}}{2\tau}} + \mathcal{Q}^{-1}(\bar{P}_{\mathrm{d}_j}^{(i)})\sqrt{1+2\mathrm{SNR}_{\mathrm{p}_j}^{(i)}}\right) \tag{5.1}$$

Alternatively, if a target $\bar{P}_{\mathrm{f}_j}^{(i)}$ needs to be achieved, from (2.8), the achievable $P_{\mathrm{d}_j}^{(i)}$ can be expressed as

$$P_{\mathrm{d}_j}^{(i)}(\bar{P}_{\mathrm{f}_j}^{(i)}, \mathrm{SNR}_{\mathrm{p}_j}^{(i)}, T_{\mathrm{s}_j}^{(i)}) = \mathcal{Q}\left(\frac{1}{\sqrt{1+2\mathrm{SNR}_{\mathrm{p}_j}^{(i)}}}\left(\mathcal{Q}^{-1}(\bar{P}_{\mathrm{f}_j}^{(i)}) - \mathrm{SNR}_{\mathrm{p}_j}^{(i)}\sqrt{\frac{T_{\mathrm{s}_j}^{(i)}}{2\tau}}\right)\right). \tag{5.2}$$

Consequently, from (5.1) and (5.2) we can write

$$T_{\mathrm{s}_j}^{(i)}(\mathrm{SNR}_{\mathrm{p}_j}^{(i)}, \bar{P}_{\mathrm{f}_j}^{(i)}, \bar{P}_{\mathrm{d}_j}^{(i)}) = \frac{2\tau}{(\mathrm{SNR}_{\mathrm{p}_j}^{(i)})^2}\left(\mathcal{Q}^{-1}(\bar{P}_{\mathrm{f}_j}^{(i)}) - \mathcal{Q}^{-1}(\bar{P}_{\mathrm{d}_j}^{(i)})\sqrt{1+2\mathrm{SNR}_{\mathrm{p}_j}^{(i)}}\right)^2. \tag{5.3}$$

We consider CSS with a hard-fusion strategy, wherein each cooperating CR-based HAN device sends its local decision to the CH. Let $N^{(i)} = |\mathcal{N}^{(i)}|$ be the total number of HAN devices selected to sense channel i. The CH makes the final decision and decides that the channel is occupied, denoted as $\mathcal{H}_1$, if at least K out of $N^{(i)}$ cooperating CR-based HAN devices have decided that the incumbent user is present; otherwise an idle channel, denoted as $\mathcal{H}_0$, will be decided. By considering this, the cooperative probability of detection and false alarm of channel i can be written as

$$Q_{\mathrm{d}}^{(i)} = \sum_{k=K}^{N^{(i)}} \sum_{\mathcal{A}_k^{(a)} \in \mathcal{A}_k} \prod_{g \in \mathcal{A}_k^{(a)}} (P_{\mathrm{d}_g}^{(i)}) \prod_{h \in \{\mathcal{N}^{(i)} \setminus \mathcal{A}_k^{(a)}\}} (1 - P_{\mathrm{d}_h}^{(i)}) \tag{5.4}$$

$$Q_{\mathrm{f}}^{(i)} = \sum_{k=K}^{N^{(i)}} \sum_{\mathcal{A}_k^{(a)} \in \mathcal{A}_k} \prod_{g \in \mathcal{A}_k^{(a)}} (P_{\mathrm{f}_g}^{(i)}) \prod_{h \in \{\mathcal{N}^{(i)} \setminus \mathcal{A}_k^{(a)}\}} (1 - P_{\mathrm{f}_h}^{(i)}) \tag{5.5}$$

where $\mathcal{A}_k$ is a set consisting of all possible subsets of k elements of $\mathcal{N}^{(i)}$, representing the k out of $N^{(i)}$ sensing devices that locally decide that the channel is occupied. $\mathcal{A}_k^{(a)} \in \mathcal{A}_k$ is one of the sets in $\mathcal{A}_k$, where a is an index such that $a = 1, \cdots, \binom{N^{(i)}}{k}$. $g, h \in \mathcal{N}^{(i)}$ are sensing device indices.

We assume that the sensing-reports are transmitted through one of the active in-band channels, i.e., as explained in more details in Chapter 3 and 4. Consequently, the sensing-report of each device can be transmitted directly after the corresponding sensing time (i.e., $t_{\mathrm{tsr}_j}^{(i)} = T_{\mathrm{s}_j}^{(i)}$), as long as it does not fall within the active reporting duration of the other cooperating devices, such that $\{t_{\mathrm{tsr}_j}^{(i)}, (t_{\mathrm{tsr}_j}^{(i)} + T_{\mathrm{sr}})\} \cap \{t_{\mathrm{tsr}_g}^{(i)}, (t_{\mathrm{tsr}_g}^{(i)} + T_{sr})\} = \emptyset, \forall j, g$, where $j, g \in \mathcal{N}^{(i)}$, and t_{tsr_j} and t_{tsr_g} are the starting time of the sensing-report transmission of device j and g, respectively. Consequently, the CSS duration $T_{\mathrm{css}}^{(i)}$ for set $\mathcal{N}^{(i)}$ of cooperating devices can be expressed as

$$T_{\mathrm{css}}^{(i)} = \max\{t_{\mathrm{tsr}_j}^{(i)}, j \in \mathcal{N}^{(i)}\} + T_{\mathrm{sr}}. \tag{5.6}$$

5.3 Problem Formulation

5.3.1 Energy and Throughput Efficiency

Let P_{s} and P_{tx} denote the power for local spectrum sensing and sensing-report transmission, respectively, which are assumed to be the same for all devices. Then, the energy consumption that HAN device j needs to sense channel i can be expressed as

$$E_{\mathrm{css}_j}^{(i)} = P_{\mathrm{s}} T_{\mathrm{s}_j}^{(i)} + P_{\mathrm{tx}} T_{\mathrm{sr}} \tag{5.7}$$

For a cluster that has active in-band channels set $\mathcal{I}$, the total energy consumption for spectrum sensing can now be calculated as

$$E_{\mathrm{css}} = \sum_{i \in \mathcal{I}} \sum_{j \in \mathcal{N}^{(i)}} \left(E_{\mathrm{css}_j}^{(i)}\right). \tag{5.8}$$

In doing this, we also want to ensure that the average demanded throughput D and the targeted cooperative detection probability $Q_d^{(i)}$, for $i \in \mathcal{I}$, are satisfied, i.e., for SU quality-of-service (QoS) and incumbent user protection, respectively. This

problem can be written as

$$\min_{\{\mathcal{N}^{(i)}, i\in\mathcal{I},\}, \{T_{\mathrm{s}_j}^{(i)}, P_{\mathrm{d}_j}^{(i)}, j\in\mathcal{N}^{(i)}, i\in\mathcal{I}\},\, \mathcal{I}} E_{\mathrm{css}} \tag{5.9}$$

$$\text{s.t.,} \quad Q_{\mathrm{d}}^{(i)}\big(\{P_{\mathrm{d}_j}^{(i)}, j\in\mathcal{N}^{(i)}\}\big) \geq \bar{Q}_{\mathrm{d}}, \quad i\in\mathcal{I} \tag{5.10}$$

$$R\big(\{T_{\mathrm{s}_j}^{(i)}, j\in\mathcal{N}^{(i)}, i\in\mathcal{I}\}\big) \geq D \tag{5.11}$$

5.3.2 Lifetime Efficiency for Sensing Device Fairness

Notice that, by focusing only on energy and throughput efficiency, the high $\mathrm{SNR}_{p_j}^{(i)}$ devices will always be loaded with a high sensing burden e.g., always be selected and given a longer sensing time than the relatively lower $\mathrm{SNR}_{p_j}^{(i)}$ devices. As a result, the energy of the always-selected devices will be depleted quickly while the others still have more remaining energy. In addition, in reality, each HAN device is deployed at a different time instant, and it has different communication patterns and expected lifetime. Thus, this results in diverse spectrum sensing energy efficiency requirements for different devices in the cluster. To address this CSS fairness issue, we introduce a fitness coefficient parameter for each HAN device j, denoted as α_j, that indicates the relative level of energy efficiency required by a HAN device as compared to the other devices.

Let E_{onecycle} denotes the expected energy for a single spectrum sensing cycle, which can be estimated based on, for example, a long term measurement. Then, the expected energy to live to the expected lifetime T_{live_j} can be calculated as

$$E_{\mathrm{live}_j} = E_{\mathrm{onecycle}} \frac{T_{\mathrm{live}_j}}{T_{\mathrm{sf}}} \tag{5.12}$$

where $\frac{T_{\mathrm{live}_j}}{T_{\mathrm{sf}}}$ is the total number of expected superframe cycles that device j will go through until the expected lifetime. Based on this definition, the proposed fitness coefficient parameter for device j can be formulated as

$$\alpha_j = \frac{E_{\mathrm{live}_j} - E_{\mathrm{res}_j}}{E_{\mathrm{live}_j}}\,. \tag{5.13}$$

α_j indicates the normalized amount of the remaining energy that a device has as compared to the energy that the device requires to live to the expected lifetime T_{live_j}. A lower value (i.e., less than zero) indicates that the device has more remaining energy, and vice versa. Notice that α_j does not only capture the difference in the amount of energy left at each sensing device, but it also accommodates the difference in the lifetime duration that each device is expected to be in operation.

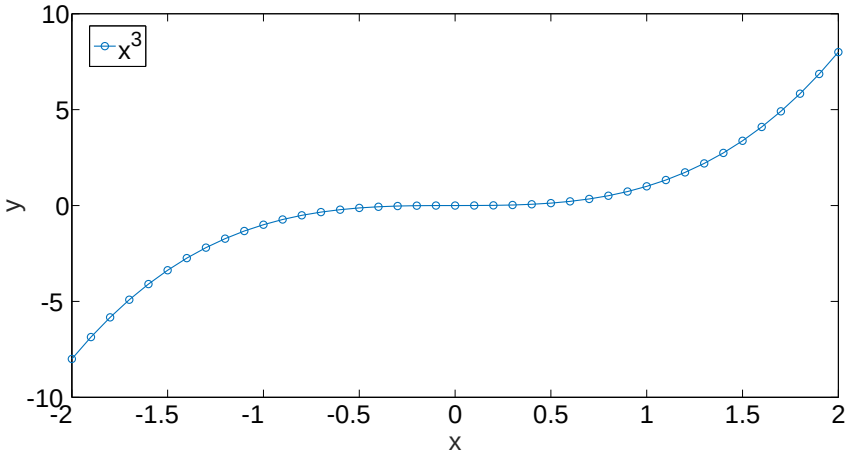

Figure 5.2: Accelerating positive and negative error values by using a cubic function $(\cdot)^3$.

5.3.3 Optimization Function Formulation

By considering the aforementioned discussions, we can derive a cost function that specifies the relative cost of using HAN device j to sense channel i in a particular CSS cycle, i.e.,

$$C_j^{(i)} = \frac{E_{\text{css}_j}^{(i)}}{E_{\text{onecycle}}} + \alpha_j \tag{5.14}$$

where the denumerators E_{onecycle} is the normalization factor for the CSS energy consumption. Both parts can be further adjusted with some coefficient to provide priority, or modification to provide control e.g., accelerating the error correction if it exceeds a certain value. In this work, we apply a coefficient δ to accommodate the priority between energy and lifetime efficiency, while the cubic function i.e., $(\cdot)^3$, can be applied to accelerate the error correction if it is larger than one or lower than negative one, i.e., as shown in Figure 5.2. By this definition, the cost function for device j to sense channel channel i becomes

$$C_j^{(i)} = \delta\Big(\frac{E_{\text{css}_j}^{(i)}}{E_{\text{onecycle}}}\Big)^3 + (1-\delta)\alpha_j^3 \tag{5.15}$$

Further, the total cost of sensing channel set $\mathcal{I}$ with the corresponding sensing device sets $\mathcal{N}^{(i)}, i \in \mathcal{I}$ can be written as

$$C = \sum_{i\in\mathcal{I}} \sum_{j\in\mathcal{N}^{(i)}} C_j^{(i)} . \tag{5.16}$$

5.4 Optimal Grouping and Scheduling for Multi-channel Cooperative Spectrum Sensing

In the previous chapter, we have solved the problem of finding the optimal sensing time and detection probability of each sensing device for a single channel and a single sensing group case by using the Markov-chain Monte-Carlo (MCMC) optimization method. Here we can apply the same method to find the $T_{\mathrm{s}_j}^{(i)}$ and $P_{\mathrm{d}_j}^{(i)}$, for $j \in \mathcal{N}^{(i)}$ and $i \in \mathcal{I}$, by fixing sensing device set $\mathcal{N}^{(i)}, i \in \mathcal{I}$ and the channel set $\mathcal{I}$. We will do this for all possible combinations of elements in $\mathcal{I}$ and $\mathcal{N}^{(i)}, i \in \mathcal{I}$, and obtain the optimal solution i.e., the combination that has the lowest cost C among all combinations. By this, the optimization problem becomes

$$\begin{aligned} \min_{\{T_{\mathrm{s}_j}^{(i)}, P_{\mathrm{d}_j}^{(i)}, j\in\mathcal{N}^{(i)}, i\in\mathcal{I}\}} \quad & C\big(\{\mathcal{N}^{(i)}, i \in \mathcal{I}\}, \mathcal{I}\big) \\ \text{s.t.,} \quad & Q_{\mathrm{d}}^{(i)}\big(\{P_{\mathrm{d}_j}^{(i)}, j \in \mathcal{N}^{(i)}\}\big) \geq \bar{Q}_{\mathrm{d}}, \quad i \in \mathcal{I} \\ & R\big(\{T_{\mathrm{s}_j}^{(i)}, j \in \mathcal{N}^{(i)}, i \in \mathcal{I}\}\big) \geq D \\ & \{\mathcal{N}^{(a)}\} \cap \{\mathcal{N}^{(b)}\} = \emptyset, \quad \forall a, b\,. \end{aligned} \tag{5.17}$$

where $a, b \in \mathcal{J}$. It is assumed in this chapter that for each sensing cycle, each sensing device can be assigned to sense only one channel, i.e., given by the last constraint in (5.17).

5.4.1 MCMC Problem Formulation

As in the previous chapter, we have to first transform the optimization problem (5.17) into a suitable form. Following the same procedure in Chapter 4.4.1, we will arrive at

$$\max_{\{T_{\mathrm{s}_j}^{(i)}, P_{\mathrm{d}_j}^{(i)}, j\in\mathcal{N}^{(i)}, i\in\mathcal{I}\}} \{p(\{T_{\mathrm{s}_j}^{(i)}, P_{\mathrm{d}_j}^{(i)}, j \in \mathcal{N}^{(i)}, i \in \mathcal{I}\})\} \tag{5.18}$$

where

$$\begin{aligned} & p(\{T_{\mathrm{s}_j}^{(i)}, P_{\mathrm{d}_j}^{(i)}, j \in \mathcal{N}^{(i)}, i \in \mathcal{I}\}) \\ & \quad = \exp\Big(-C\big(\{\mathcal{N}^{(i)}, i \in \mathcal{I}\}, \mathcal{I}\big)\Big) \cdot I_{\mathrm{c}}(T_{\mathrm{s}_j}^{(i)}, P_{\mathrm{d}_j}^{(i)}, j \in \mathcal{N}^{(i)}, i \in \mathcal{I}\}) \end{aligned} \tag{5.19}$$

and

$$I_{\rm c}(T_{{\rm s}_j}^{(i)}, P_{{\rm d}_j}^{(i)}, j \in \mathcal{N}^{(i)}, i \in \mathcal{I}\}) = \begin{cases} 1, & Q_{\rm d}^{(i)}\big(\{P_{{\rm d}_j}^{(i)}, j \in \mathcal{N}^{(i)}\}\big) \geq \bar{Q}_{\rm d},\ i \in \mathcal{I} \text{ and} \\ & R\big(\{T_{{\rm s}_j}^{(i)}, j \in \mathcal{N}^{(i)}, i \in \mathcal{I}\}\big) \geq D \\ 0, & \text{otherwise.} \end{cases} \tag{5.20}$$

5.4.2 Metropolis-Hastings Sampler

In this chapter, we use a simpler sampler which is the Metropolis-Hastings sampler [63] instead of the reversible-jump sampler because the problem in (5.17) does not involve any trans-dimension movement, i.e., the channel set $\mathcal{I}$ and the sensing device selection for each channel $i, \mathcal{N}^{(i)}, i \in \mathcal{I}$, are fixed.

The proposed $T_{{\rm s}_j}^{(i)}$ and $P_{{\rm d}_j}^{(i)}$, for $j \in \mathcal{N}^{(i)}, i \in \mathcal{I}$, can be generated in the same way as those are generated in the reversible-jump sampler in the previous chapter, for the case of moving within the same dimension. These are, for each combination of elements in $\mathcal{I} \subset \{i_1, i_2, \ldots, i_I\}$ and $\{\mathcal{N}^{(i)}, i \in \mathcal{I}\} \subset \mathcal{J}$,

$$q(\tilde{T}_{{\rm s}_j}^{(i,m+1)} \mid T_{{\rm s}_j}^{(i,m)}) \sim \mathcal{U}\left\{\max\{\tau, T_{{\rm s}_j}^{(i,m)} - \beta_{\rm T_s}\}, \min\{(T_{{\rm s}_j}^{(i,m)} + \beta_{\rm T_s}), (T_{\rm sf} - T_{\rm sr})\}\right\} \tag{5.21}$$

for $j \in \mathcal{N}^{(i)}, i \in \mathcal{I}$, and

$$q(\tilde{P}_{{\rm d}_j}^{(i,m+1)} \mid P_{{\rm d}_j}^{(i,m)}) \sim \mathcal{U}\left(\max\{0, P_{{\rm d}_j}^{(i,m)} - \beta_{\rm P_d}\}, \min\{P_{{\rm d}_j}^{(i,m)} + \beta_{\rm P_d}, 1\}\right) \tag{5.22}$$

for $j \in \{\mathcal{N}^{(i)} \setminus N^{(i)}\}, i \in \mathcal{I}$ and

$$\tilde{P}_{{\rm d}_{N^{(i)}}}^{(i)}\big(\bar{Q}_{\rm d}, \tilde{P}_{{\rm d}_1}^{(i,m+1)}, \ldots, \tilde{P}_{{\rm d}_{(N^{(i)}-1)}}^{(i,m+1)}\big) = \frac{\bar{Q}_{\rm d} - \sum_{k=K}^{(N^{(i)}-1)} \psi(k)}{\psi(K)} \tag{5.23}$$

where

$$\psi(k) = \sum\nolimits_{\mathcal{A}_{k,\sim N^{(i)}}^{(a)} \subseteq \mathcal{A}_{k,\sim N^{(i)}}} \Big(\prod\nolimits_{g \in \mathcal{A}_{k,\sim \tilde{N}^{(i)}}^{(a)}} \tilde{P}_{{\rm d}_g}^{(i,m+1)}\Big) \Big(\prod\nolimits_{h \in \{\mathcal{N} \setminus \mathcal{A}_{k,\sim \tilde{N}^{(i)}}^{(a)}\}} (1 - \tilde{P}_{{\rm d}_h}^{(i,m+1)})\Big). \tag{5.24}$$

The acceptance probability of the proposal can then be written as

$$\begin{aligned}\varrho(\{\tilde{T}_{\mathrm{s}_j}^{(i,m+1)}, \tilde{P}_{\mathrm{d}_j}^{(i,m+1)}, j \in \mathcal{N}^{(i)}, i \in \mathcal{I}\}) = \\ \frac{p(\{\tilde{T}_{\mathrm{s}_j}^{(i,m+1)}, \tilde{P}_{\mathrm{d}_j}^{(i,m+1)}, j \in \mathcal{N}^{(i)}, i \in \mathcal{I}\})}{p(\{T_{\mathrm{s}_j}^{(i,m)}, P_{\mathrm{d}_j}^{(i,m)}, j \in \mathcal{N}^{(i)}, i \in \mathcal{I}\})} \\ \prod_{i \in \mathcal{I}} \Bigg(\prod_{j \in \{\mathcal{N}^{(i)} \setminus N^{(i)}\}} \left(\frac{q(P_{\mathrm{d}_j}^{(i,m)} \mid \tilde{P}_{\mathrm{d}_j}^{(i,m+1)})\, q(T_{\mathrm{s}_j}^{(i,m)} \mid \tilde{T}_{\mathrm{s}_j}^{(i,m+1)})}{q(\tilde{P}_{\mathrm{d}_j}^{(i,m+1)} \mid P_{\mathrm{d}_j}^{(i,m)})\, q(\tilde{T}_{\mathrm{s}_j}^{(i,m+1)} \mid T_{\mathrm{s}_j}^{(i,m)})} \right) \\ \times \frac{q(T_{\mathrm{s}_{N^{(i)}}}^{(i,m)} \mid \tilde{T}_{\mathrm{s}_{N^{(i)}}}^{(i,m+1)})}{q(\tilde{T}_{\mathrm{s}_{N^{(i)}}}^{(i,m+1)} \mid T_{\mathrm{s}_{N^{(i)}}}^{(i,m)})} \Bigg).\end{aligned} \tag{5.25}$$

Notice that we do not have Jacobian determinant in this equation as compared to (4.24) of the previous chapter because there is no change of variable (number of sensing devices) in this algorithm. The number of sensing devices and which devices, as well as the number of channels and which channels are found by using exhaustive search algorithm.

The algorithm for finding the optimal channels set $\mathcal{I}^*$, sensing group sets for each of the corresponding channel $(\mathcal{N}^{(i)})^*, i \in \mathcal{I}$, and the corresponding sensing time $(T_{\mathrm{s}_j}^{(i)})^*$ and detection probabilities $(P_{\mathrm{d}_j}^{(i)})^*$, for $j \in \mathcal{N}^{(i)}, i \in \mathcal{I}$ that jointly minimize the energy usage and provide fairness in CSS is shown in Algorithm 2. The most part of the algorithm constitutes of the Metropolis-Hastings MCMC algorithm which is given by line 3 until 22. The Metropolis-Hastings MCMC algorithm is repeated for each and every possible combination of elements in set $\mathcal{I}$ and $\mathcal{N}^{(i)}, i \in \mathcal{I}$, as given by the "for" loop of which begins at line 2 and ends at line 24. The optimal solution is given by the combination that gives the lowest cost C i.e., given in line 25.

The complexity of the algorithm is caused by two parts: i) the complexity from the Metropolis-Hastings MCMC algorithm which is linearly proportional to the number of channels, the number of sensing devices, and the maximum number of iterations chosen, and ii) the complexity from the exhaustive search which is exponentially proportional to the number of channels and the number of HAN devices in the network. Basically, the algorithm has to be executed for every CSS cycle because the expected energy to live to the expected lifetime E_{live_j}, and possibly the residual energy E_{res_j}, for $j \in \mathcal{J}$ changes after each CSS cycle. Alternatively, the algorithm can also be executed in a less periodic (e.g., hourly) or only when an event happens (e.g., a new device is deployed), in which this needs to be carefully and optimally further determined.

Algorithm 2 Optimal channels set $\mathcal{I}^*$, sensing group sets for each corresponding channel $(\mathcal{N}^{(i)})^*, i \in \mathcal{I}$, and the corresponding sensing time $(T_{\mathrm{s}_j}^{(i)})^*$ and detection probabilities $(P_{\mathrm{d}_j}^{(i)})^*$ for $j \in \mathcal{N}^{(i)}, i \in \mathcal{I}$

Given the set of possible exploited channels $\{i_1, i_2, \ldots, i_I\}$, set $\mathcal{J}$ of HAN devices in a cluster, and signal-to-noise-ratio of the incumbent user at each sensing device in each channel $\mathrm{SNR}_{\mathrm{p}_j}^{(i)}$.
for each combination of elements in $\mathcal{I} \subset \{i_1, i_2, \ldots, i_I\}$ and $\{\mathcal{N}^{(i)}, i \in \mathcal{I}\} \subset \mathcal{J}$ with $\{\mathcal{N}^{(a)}\} \cap \{\mathcal{N}^{(b)}\} = \emptyset, a, b \in \mathcal{J}$ **do**
  Initialize the first sample $P_{\mathrm{d}_j}^{(i,1)}$ and $T_{\mathrm{s}_j}^{(i,1)}$, for $j \in \mathcal{N}^{(i)}, i \in \mathcal{I}$ with arbitrary values.
  repeat
    for each $i \in \mathcal{I}$ **do**
      for each $j \in \mathcal{N}^{(i)}$ **do**
        Get a sample proposal for $T_{\mathrm{s}_j}^{(i,m+1)}$:
        $\tilde{T}_{\mathrm{s}_j}^{(i,m+1)} \sim q(\tilde{T}_{\mathrm{s}_j}^{(i,m+1)} \mid T_{\mathrm{s}_j}^{(i,m)})$ according to (5.21).
      end for
      for each $j \in \{\mathcal{N}^{(i)} \setminus N^{(i)}\}$ **do**
        Get a sample proposal for $P_{\mathrm{d}_j}^{(i,m+1)}$:
        $\tilde{P}_{\mathrm{d}_j}^{(i,m+1)} \sim q(\tilde{P}_{\mathrm{d}_j}^{(i,m+1)} \mid P_{\mathrm{d}_j}^{(i,m)})$ according to (5.22).
      end for
      Get a sample proposal for $P_{\mathrm{d}_{N^{(i)}}}^{(i,m+1)}$:
      $\tilde{P}_{\mathrm{d}_{N^{(i)}}}^{(i,m+1)} = \tilde{P}_{\mathrm{d}_{N^{i)}}}^{(i,m+1)}\big(\bar{Q}_{\mathrm{d}}, \tilde{P}_{\mathrm{d}_1}^{(i,m+1)}, \ldots, \tilde{P}_{\mathrm{d}_{(N^{(i)}-1)}}^{(i,m+1)}\big)$ according to (5.23).
    end for
    Calculate the acceptance probability
    $\varrho(\{\tilde{T}_{\mathrm{s}_j}^{(i,m+1)}, \tilde{P}_{\mathrm{d}_j}^{(i,m+1)}, j \in \mathcal{N}^{(i)}, i \in \mathcal{I}\}$ according to (5.25).
    if $\mathrm{rand} \geq \varrho(\{\tilde{T}_{\mathrm{s}_j}^{(i,m+1)}, \tilde{P}_{\mathrm{d}_j}^{(i,m+1)}, j \in \mathcal{N}^{(i)}, i \in \mathcal{I}\}$ **then**
      $P_{\mathrm{d}}^{(i,m+1)} = \tilde{P}_{\mathrm{d}}^{(i,m+1)}$ and $T_{\mathrm{s}}^{(i,m+1)} = \tilde{T}_{\mathrm{s}}^{(i,m+1)}$ for $j \in \mathcal{N}^{(i)}, i \in \mathcal{I}$.
    else
      $P_{\mathrm{d}}^{(i,m+1)} = P_{\mathrm{d}}^{(i,m)}$ and $T_{\mathrm{s}}^{(i,m+1)} = T_{\mathrm{s}}^{(i,m)}$ for $j \in \mathcal{N}^{(i)}, i \in \mathcal{I}$.
    end if
  until maximum iterations
  $m_{\max} = \arg\max_m \{p(\{\tilde{T}_{\mathrm{s}_j}^{(i,m+1)}, \tilde{P}_{\mathrm{d}_j}^{(i,m+1)}, j \in \mathcal{N}^{(i)}, i \in \mathcal{I}\})\}$,
  for $j \in \{\mathcal{N}^{(i)}, i \in \mathcal{I}\}, i \in \mathcal{I}$.

22: $P_{\mathrm{d}_j}^{(i)}(\{\mathcal{N}^{(i)}, i \in \mathcal{I}\}, \mathcal{I}) = P_{\mathrm{d}_j}^{(i,m_{\max})}$ and $T_{\mathrm{s}_j}^{(i)}(\{\mathcal{N}^{(i)}, i \in \mathcal{I}\}, \mathcal{I}) = T_{\mathrm{s}_j}^{(i,m_{\max})}$.

23: Calculate $C\big(\{\mathcal{N}^{(i)}, i \in \mathcal{I}\}, \mathcal{I}\big)$ according to (5.16).

24: **end for**

25: $\{\{\mathcal{N}^{(i)}, i \in \mathcal{I}\}_{\min}, \mathcal{I}_{\min}\} =$
$\arg\min_{\{\{\mathcal{N}^{(i)}, i \in \mathcal{I}\}, \mathcal{I}\}} \{C\big(\{\mathcal{N}^{(i)}, i \in \mathcal{I}\}, \mathcal{I}, \forall \text{combinations}\big)\}$,
for $j \in \{\mathcal{N}^{(i)}, i \in \mathcal{I}\}^*, i \in \mathcal{I}^*$.

26: $\{\mathcal{N}^{(i)}, i \in \mathcal{I}\}^* = \{\mathcal{N}^{(i)}, i \in \mathcal{I}\}_{\min}$ and $\mathcal{I}^* = \mathcal{I}_{\min}$.

27: $(P_{\mathrm{d}_j}^{(i)})^* = P_{\mathrm{d}_j}^{(i)}(\{\mathcal{N}^{(i)}, i \in \mathcal{I}\}_{\min}, \mathcal{I}_{\min})$
and $(T_{\mathrm{s}_j}^{(i)})^* = T_{\mathrm{s}_j}^{(i)}(\{\mathcal{N}^{(i)}, i \in \mathcal{I}\}_{\min}, \mathcal{I}_{\min})$.

5.5 Performance Evaluation and Discussions

5.5.1 Evaluation Setup

In this section, we evaluate the performance of the proposed grouping and scheduling scheme. The same values as in the previous chapter, for the superframe duration, the sensing-report duration, the sampling duration, the target detection probability, the transmission and sensing power consumption of HAN devices, and the fusion rule, are used in this section, i.e.,: $T_{\mathrm{sf}} = 100$ ms, $T_{\mathrm{sr}} = 0.5$ ms, $\tau = 0.1$ ms, $Q_{\mathrm{d}} = 0.9$, $P_{\mathrm{tx}} = 20$ mW and $P_{\mathrm{s}} = 36.54$ mW, and $k = \lceil \frac{N}{2} \rceil$, respectively. We set the coefficient $\delta = 0.5$ i.e., the efficiency between energy and lifetime are treated as equally important.

Let us assume that there are two channels available to be exploited i.e., $i \in \{1, 2\}$ with the probability of idle channel $P(\mathcal{H}_0)$ of 0.75 and 0.65 for channel 1 and 2, respectively. There are four HAN devices available in the channel for spectrum sensing i.e., $\mathcal{J} \in \{1, 2, 3, 4\}$. For the SNR of the incumbent user, as in the previous chapter, we consider that it is different at each HAN device, and also different for each channel, i.e. between -13.0 dB and -6.0 dB. For consistency, we generate this value once for each device and use it throughout this section, i.e.,: $[\mathrm{SNR}_{\mathrm{p}_1}^{(1)}, \mathrm{SNR}_{\mathrm{p}_2}^{(1)}, \mathrm{SNR}_{\mathrm{p}_3}^{(1)}, \mathrm{SNR}_{\mathrm{p}_4}^{(1)}] = [-11.17, -10.28, -10.31, -9.33]$ dB for the respective devices for channel 1 and $[\mathrm{SNR}_{\mathrm{p}_1}^{(2)}, \mathrm{SNR}_{\mathrm{p}_2}^{(2)}, \mathrm{SNR}_{\mathrm{p}_3}^{(2)}, \mathrm{SNR}_{\mathrm{p}_4}^{(2)}] = [-7.95, -12.29, -7.07, -7.84]$ dB for the respective devices for channel 2. We also assume that the average sensing time is 14 ms, hence from (5.7) we have the expected energy for one sensing cycle $E_{\mathrm{onecycle}} = 52.16$ mJ. The initial residual energy for each device is set as the following: $[E_{\mathrm{res}_1}, E_{\mathrm{res}_2}, E_{\mathrm{res}_3}, E_{\mathrm{res}_4}] =$

$[1.0E_{\text{live}_1}, 1.25E_{\text{live}_2}, 0.85E_{\text{live}_3}, 0.5E_{\text{live}_4}]$.

For the MCMC, we use the same setting as in the previous chapter: $\beta_{\text{P}_\text{d}} = 0.2$, $\beta_{\text{T}_\text{s}} = 30\tau$, $P_{\text{d}_j}^{(i,1)} = 0.8$, for $j \in \{\mathcal{N}^{(i)} \setminus N^{(i)}\}, i \in \mathcal{I}$, and $T_{\text{s}_j}^{(i,1)} = 0.32$, for $j \in \mathcal{N}^{(i)}, i \in \mathcal{I}$.

5.5.2 Different Throughput Demands

We first evaluate the performance of the proposed scheme as a function of average throughput demand D. Table 5.1 shows the optimal grouping and scheduling of sensing devices in set $\mathcal{J}$ for channel set $\{1, 2\}$, in different throughput demand D. It can be seen from the table that during the lowest demand i.e., $D = 0.1$, the optimal setting is to use only one channel i.e., channel 1, and sense this channel by using only one sensing device i.e., device 2. This can also be seen in the achievable throughput R plot of Figure 5.3(a) and the CSS energy consumption E_{css} plot of Figure 5.3(b) (i.e., only $R^{(i)}$ and E_{css_j} for which channels and devices, respectively, used are shown). For this setting, device 2 is selected because it has the highest excess energy as compared to the other devices. Even though device 4 has the highest incumbent user SNR for channel 1, it is not chosen because it has a very low residual energy E_{res_4} relative to its expected energy E_{live_4}, hence it is very costly to be used for spectrum sensing c.f., (5.15). Besides, only a low achievable throughput R needs to be obtained i.e., ≥ 0.1, hence the sensing requirement, including the Q_f, is also low. Therefore, device 2 can satisfy this with relatively not-a-very-high sensing time $T_{\text{s}_1}^{(1)}$ and hence also $E_{\text{css}_1}^{(1)}$, as shown in Figure 5.4(a) and 5.3(b), respectively. Thus, this setting gives low in both E_{css} and α, hence the lowest cost C. In addition, channel 1 is chosen instead of 2 because the device that is chosen to execute spectrum sensing i.e., device 2 has a better incumbent user SNR for this channel. Besides, channel 1 has a higher channel-idle probability $P(\mathcal{H}_0)$ as compared to channel 2.

For throughput demand $D = 0.2$, a higher cooperation is required to achieve a lower Q_f and obtain a higher R that can satisfy this demand. For this, an addition of device 1 on top of the previous settings, to sense channel 1, is found to be optimal. Device 1 is chosen because it has the second highest good energy condition among the available devices.

Then, when the throughput demand increases to $D = 0.3$, the optimal settings become: use only channel 2 and sense this channel using only device 3, as can be seen in Figure 5.4 (i.e., devices and channels for which $T_{\text{s}_j}^{(i)}$ are shown). Although channel 2 has a lower $P(\mathcal{H}_0)$ as compared to channel 1, and device 3 has a 25%

less residual energy E_{res_3} from its expected E_{live_3}, but the highest incumbent user SNR is at this device for this channel i.e., $\mathrm{SNR}_{\mathrm{p}_3}^{(2)}$. Hence it can produce a good sensing outcome (i.e., high Q_{f}) that can satisfy the demanded throughput, with a reasonable sensing time and thus energy.

The optimal decision to use both channel 1 and 2 begins when the throughput demand becomes $D = 0.4$. At this throughput demand, device 2 and 1 are selected to sense each channel, respectively. Further, an addition of device 3 is required to cooperate with device 2 to sense channel 1 when the demand reached $D = 0.6$.

A full cooperation from all devices and a utilization of all channels are required when the throughput demand becomes relatively very high, i.e., in this case $D \geq 0.8$. The optimal grouping and scheduling at this point are: device 2 and 4 are grouped together to cooperatively sense channel 1, and device 1 and 3 are grouped together to cooperatively sense channel 2. This grouping and scheduling settings are obvious based on the incumbent user SNR of each device for each channel, which could provide the highest achievable throughput R.

In all cases, the throughput demand is always satisfied i.e., as can be seen in Figure 5.3(a). The corresponding probability of detection $P_{\mathrm{d}_j}^{(i)}, j \in \{1, 2, 3, 4\}, i \in \{1, 2\}$ are shown in Figure 5.5.

Table 5.1: Optimal sensing device grouping and scheduling for cooperative spectrum sensing on different throughput demand

Throughput demand D	**Sensing device 1**	**Sensing device 2**	**Sensing device 3**	**Sensing device 4**
0.1	–	Channel 1	–	–
0.2	Channel 1	Channel 1	–	–
0.3	–	–	Channel 2	–
0.4	Channel 2	Channel 1	–	–
0.5	–	Channel 1	Channel 2	–
0.6	Channel 2	Channel 1	Channel 1	–
0.7	–	Channel 1	Channel 2	Channel 1
0.8	Channel 2	Channel 1	Channel 2	Channel 1

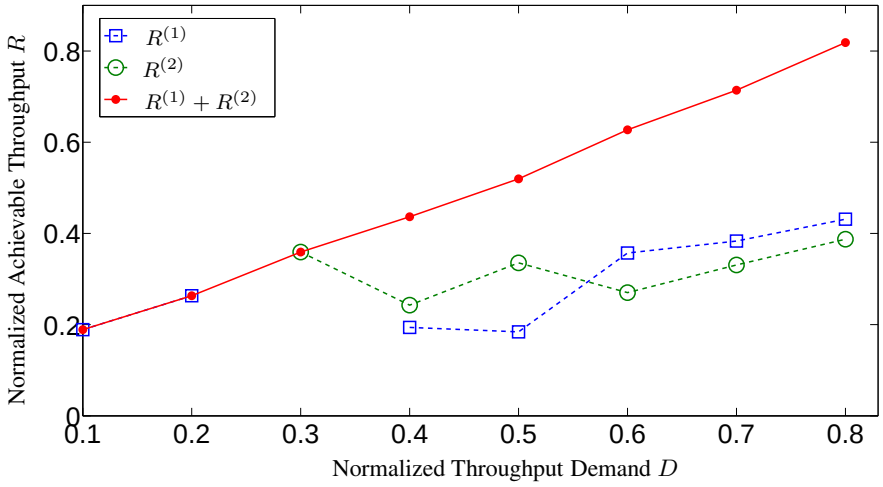

(a)

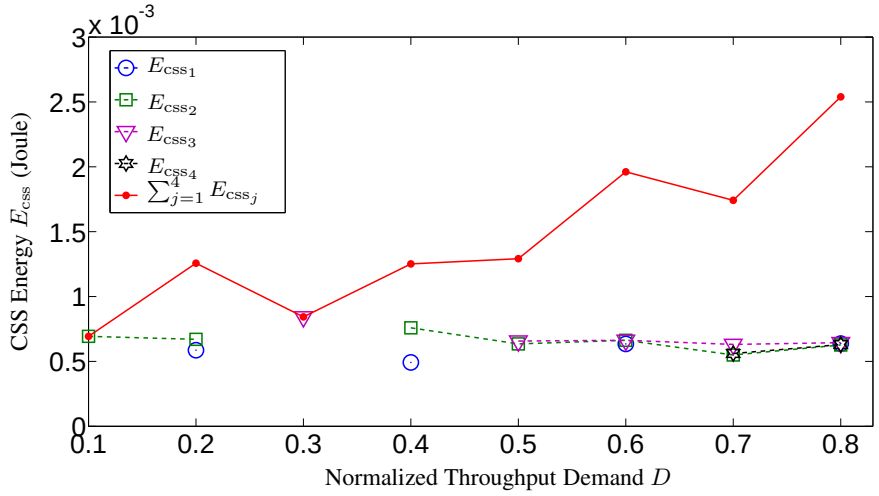

(b)

Figure 5.3: (a) The average throughput demand R, and (b) the cooperative spectrum sensing energy consumption E_{css}, of the proposed sensing device grouping and scheduling of cooperative spectrum sensing on different average normalized throughput demand D.

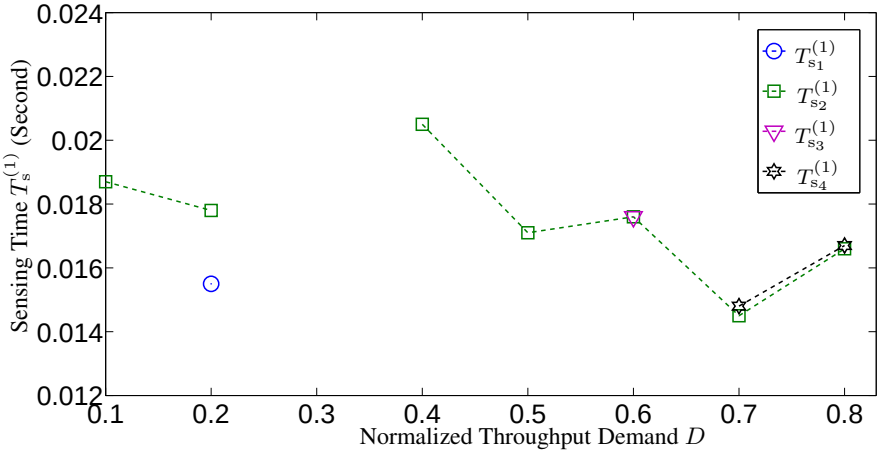

(a)

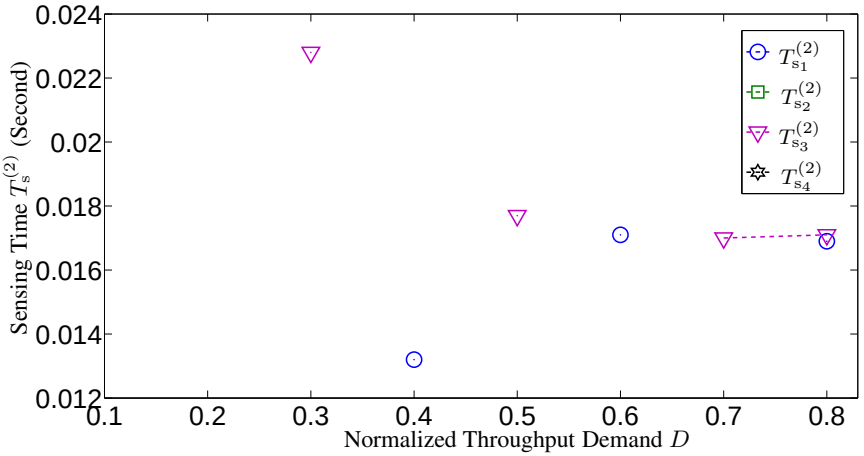

(b)

Figure 5.4: The corresponding optimal spectrum sensing time of each device for (a) channel 1, and (b) channel 2, for different average normalized throughput demand D.

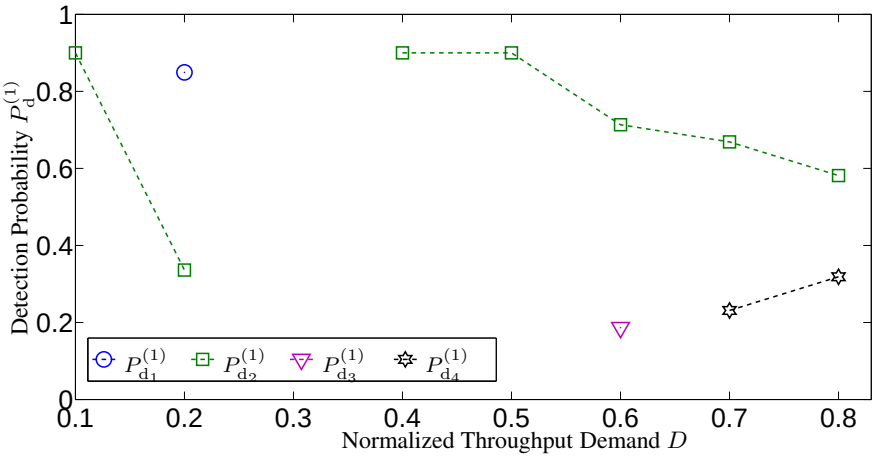

(a)

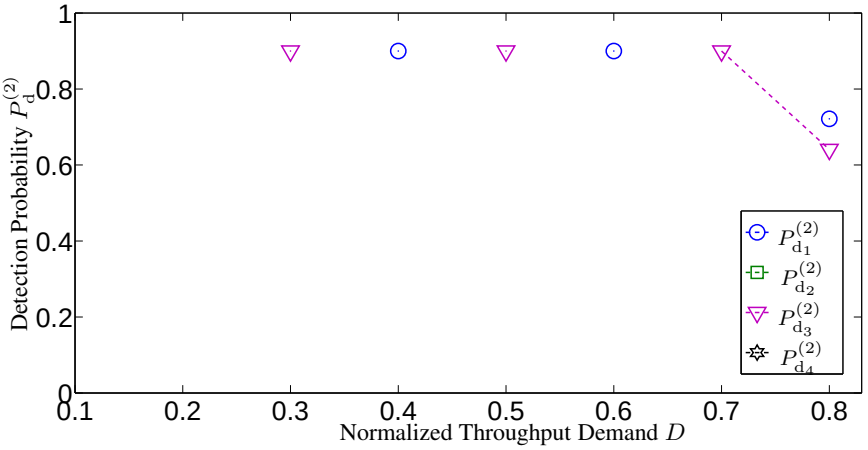

(b)

Figure 5.5: The corresponding optimal detection probability of each device for (a) channel 1, and (b) channel 2, for different average normalized throughput demand D.

5.5.3 Lifetime Performance

We then evaluate the lifetime performance of the network with the proposed CSS sensing device grouping and scheduling scheme. For this, we fixed the throughput demand at $D = 0.6$ and the expected lifetime is set to $1,000$ cooperative spectrum sensing cycles. It is worth to mention here the definition of lifetime that we considered in this thesis. As most commonly defined in the literature [64, 65], it is defined as: the time to the first sensing device failure, which in this case is whenever the residual energy becomes less than the energy required for a single spectrum sensing cycle ($E_{\text{res}_j} < E_{\text{onecycle}}$ for any $j, j \in \mathcal{J}$).

Figure 5.6 shows the residual energy E_{res} of each sensing device after each sensing cycle. The proposed scheme which contains the optimization in device's lifetime that is denoted as "+ live", while the conventional scheme which only considers the CSS energy that is denoted as "- live".

It can be seen from this figure that the lifetime of the cluster's network from the conventional scheme is very short i.e., ended at the 344-th sensing cycle – after device 4 was running out of energy for spectrum sensing. This is because the energy condition of the devices is not taken into consideration in this scheme, hence device 4 is always selected, as can be seen from Figure 5.7, and consequently finished its energy quickly. Note that device 4 has the worst energy condition, i.e., only half that from the required energy, but at the same time, it has a good incumbent user SNR, particularly for channel 2. On the other hand, device 2, which was in excellent energy condition for spectrum sensing, is always being excluded, i.e., as can be seen in Figure 5.7. This is due to its incumbent user SNR which is relatively low as compared to the other devices, particularly for channel 2 (i.e., the lowest available).

With the proposed scheme, it can be seen from Figure 5.6 that the lifetime will be significantly extended almost to the expected lifetime, i.e., 990 CSS cycles from $1,000$ CSS cycles. In contrast with the conventional scheme, as can be seen from Figure 5.8, the proposed scheme excludes device 4 from performing CSS at the beginning of the sensing cycles until the cycle number reaches approximately 306. This is the point where the residual energy of device 4 has become similar with device 3. Device 4 is then used alternately with device 3, and by this, improving the energy condition of both devices. When the residual energy of device 3 and 4 have become closer to the residual energy of device 1, i.e., at CSS cycle number 544, the scheme then reduces the burden of spectrum sensing for device 1 by alternating the sensing task between the three devices, i.e., one device is excluded during each

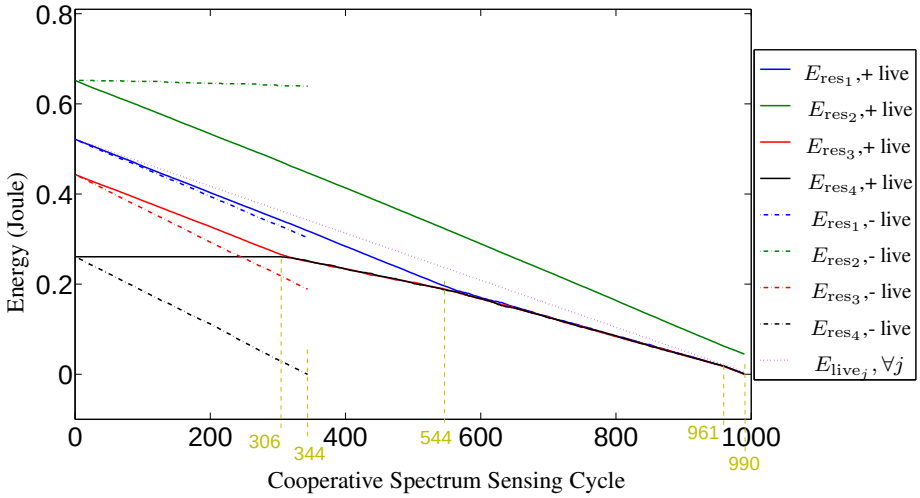

Figure 5.6: The residual energy of each sensing device $E_{\text{res}_j}, \forall j$, from the proposed scheme, denoted as "+ live", and the conventional scheme, denoted by "- live". The throughput demand is fixed at $D = 0.6$, and the expected lifetime is set at $1,000$ cooperative sensing cycles.

cycle. Finally, when the residual energy E_{res} of device 1, 3 and 4 has become very close to the expected energy E_{live}, i.e., at the 961-th CSS cycle, all of the available devices are then used to sense the channel, hence to reduce the required sensing time of all devices to less than the expected (average) sensing time for one sensing cycle, as can be seen in Figure 5.8.

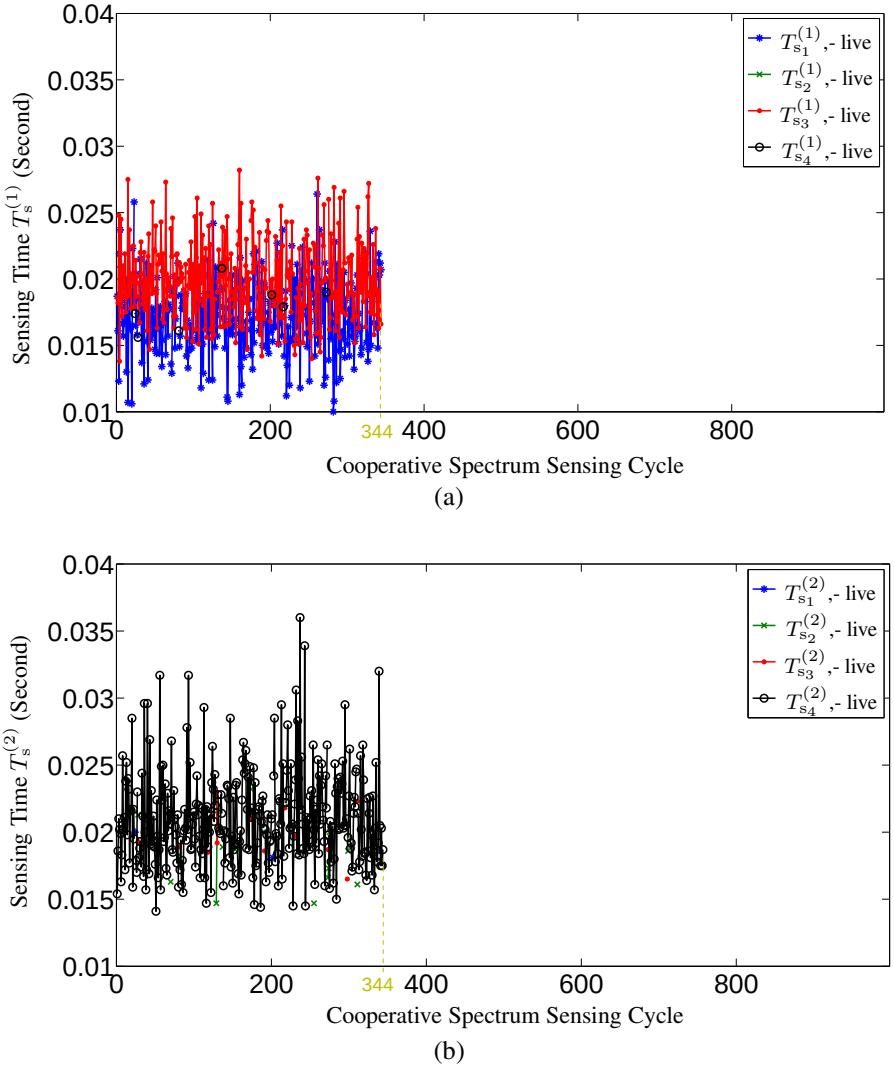

Figure 5.7: The corresponding optimal spectrum sensing time of each device from the conventional scheme, for (a) channel 1, and (b) channel 2, throughout the lifetime of the cluster's network.

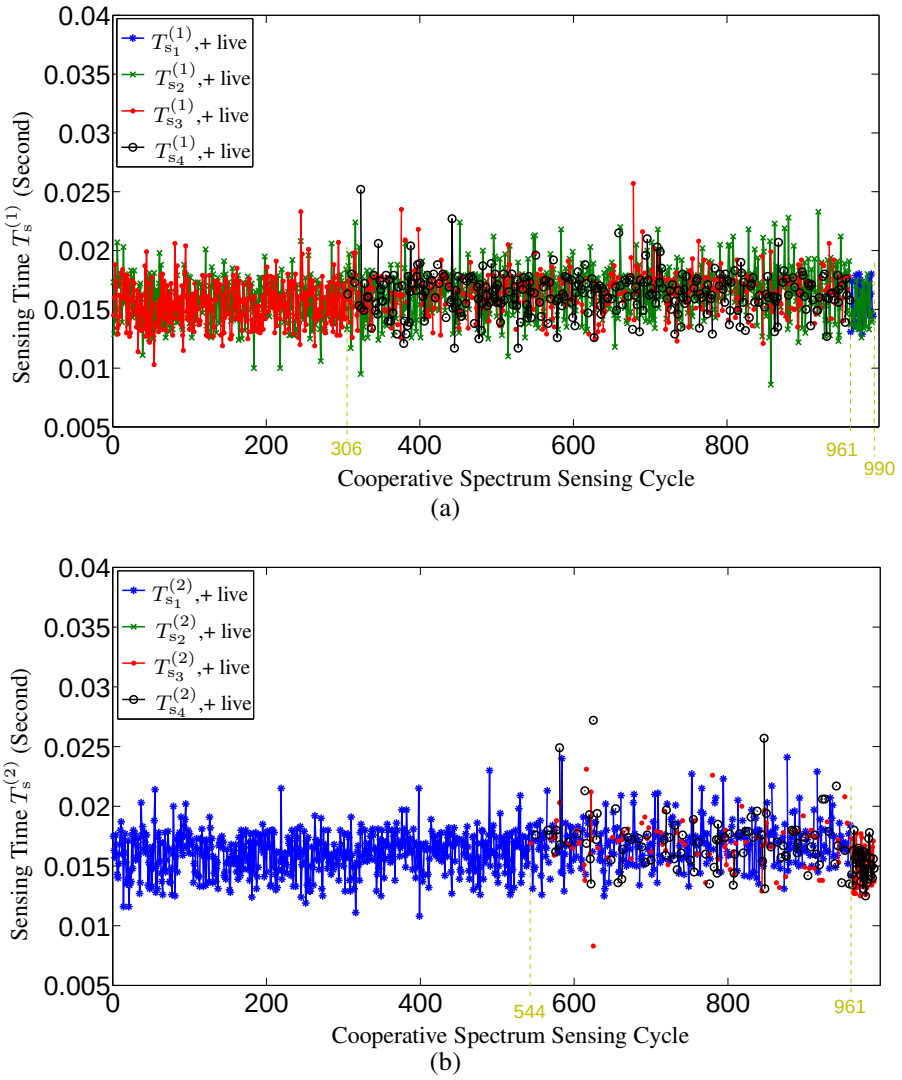

Figure 5.8: The corresponding optimal spectrum sensing time of each device from the proposed sensing device grouping and scheduling scheme, for (a) channel 1, and (b) channel 2, throughout the lifetime of the cluster's network.

5.6 Conclusion

We have shown that it is very important to consider the energy condition of each HAN device in cooperative spectrum sensing sensing-device grouping and scheduling. This is to ensure a fair distribution of spectrum sensing loads among the HAN devices and maximize the lifetime of each device to their expected lifetime. We have proposed an efficient sensing-device grouping and scheduling scheme for cooperative spectrum sensing, that minimizes the cooperative spectrum sensing energy, maximizes the lifetime of each sensing device to its expected lifetime, and at the same time, satisfies the throughput demand of the network. The proposed scheme optimally determines the channel set for the network, selects and groups the available devices together to sense the selected channels in the channel set, schedules the formed group to these the selected channels with the corresponding optimal sensing time and detection probability of each selected sensing device, in which this sensing time and detection probability can be different from one device to another. We have shown that the proposed scheme extends the lifetime of the network (and all devices), as compared to the conventional scheme, to the expected lifetime. By this, we have indicated that the proposed scheme works accordingly. However, the solution can still be improved such as by jointly determining the optimal channel set and sensing device group using the MCMC method or possibly the convex optimization method.

In the next chapter, we will provide the overall conclusion of this thesis and then we suggest some future work and direction based on the works that we have done.

Chapter 6

Conclusion and Future Work

In this chapter, we provide the conclusions to the presented works in this thesis. We then suggest some future research directions.

6.1 Conclusion and Discussion

Section 1.2 formulated the main research questions. We repeat these questions here and summarize our main contributions.

The ever-rising communication demand, particularly from the continually increasing number of home devices and new wireless technologies, will impose a critical interference issue to the home communications. In addition, due to the well-discussed spectrum scarcity issue, we have concluded that there is an urgent need to rethink and redesign the current home communication system to ensure the continuity of HAN operation in the future. Hence, the following research question was investigated.

1) **How to optimally meet the throughput demand**.

To answer this first question, we have proposed a new home area network system, designed based on cognitive radio technology and clustered network topology, called TD-CRHAN. We have shown that the TD-CRHAN can sustainably and efficiently support the throughput demand from the home devices. In TD-CRHAN, the spectrum sensing time, the number of cooperating sensing devices, and the number of active in-band channels needed, that can tightly satisfy the throughput demand have been optimally determined. Moreover, we have shown by extensive numeri-

cal analysis and through simulations that the values for spectrum sensing time and number of cooperative sensing devices, for the TD-CRHAN scheme, are significantly lower as compared to the values for the conventional scheme, and this can be further reduced by using a higher number of active in-band channels.

Spectrum sensing has been recognized as one of the key components in cognitive radio technology. As spectrum sensing also imposes an additional energy consumption that does not exist in the conventional radio, the following research question was addressed.

2) **How to minimize the spectrum sensing energy overhead**.

In order to answer this second research question, we have proposed an energy efficient cooperative spectrum sensing scheme. In doing this, the scheme was also designed such that the throughput demand is kept satisfied efficiently. In this work, the difference in incumbent user signal-to-noise ratio at each home device, which is a more realistic scenario in the HAN, was taken into account. In fact, we show that by considering this difference, the optimal sensing devices can be selected, and the corresponding spectrum sensing time and probability of detection, which can be different from one another, can jointly be determined. Consequently, we have shown that a high energy efficiency can be obtained in CSS, and further, a higher achievable throughput can be reached.

The proposed clustered- and CR-based HAN will operate using multiple channels. Multiple spectrum sensing groups thus have to be optimally formed and scheduled to sense the channels. Hence the following research question was addressed.

3) **How to efficiently and fairly group and schedule sensing devices for spectrum sensing in a multi-channel network**.

We answer this third research question by designing a sensing device grouping and scheduling strategy for the CSS, in which in addition to the energy and throughout efficiency, the proposed scheme has also addressed the fairness in sensing load distribution such that the lifetime of each device is maximized to its expected lifetime. We have shown that without considering fairness such as this, the same devices (e.g., have high incumbent user SNR) will always be selected to perform spectrum sensing, hence will go dead faster. Furthermore, we also have shown that the proposed scheme can provide a balance between energy and lifetime efficiency.

Together, we consider the main contribution of this thesis is the concept of the TD-CRHAN which can sustainably and efficiently support the communication throughput demand in the home environment. In general, we have presented the basic elements of the proposed home communication system in this thesis. We have listed the different types of network components as well as the corresponding functionalities. We have also described the proposed operations of the TD-CRHAN including spectrum management and cooperative spectrum sensing schemes (with several issues were addressed).

In the TD-CRHAN, devices with different properties from one another, such as the communication technology, the expected energy efficiency, and the communication patterns, can be supported and will be treated accordingly. For example, in spectrum sensing, a device that is low in remaining energy but yet has to live for quite some time will not be selected (or only allocated with a very minimum sensing load). In terms of data communication, simple devices such as a smoke detector can be allocated with a simple resource allocation e.g., single channel and a dedicated time slot (TDMA-based), while more sophisticated devices, e.g., have the capability of NC-OFDM, can be allocated with multiple channels and more advanced resource allocations.

Furthermore, by design, any non-CR type of devices are also possible to operate together in a TD-CRHAN network. However, the device should be able to follow the communication procedure of TD-CRHAN e.g., needs to be connected to one of the clusters through the corresponding cluster head (CH). This can be done for example with an update on the device's firmware.

In TD-CRHAN, CH should be able to support multi-standard wireless communication technologies e.g., ZigBee, WiFi and so on. This is possible with several options. The simplest way is by having multiple radio components in each CH, such as in the mobile phone (GSM, 3G, WiFi, Bluetooth and etc. in a single phone). Alternatively, a combination of radio-over-fiber (ROF) and software-radio (SR) technology can be considered. In this option, CH only consists of antenna, RF front-end, and RF-to-light converter. The converted light signal is sent through an optical fiber to a central processing device. In this device, the light signal is sampled by an analog-to-digital converter and then processed by software (including filtering, modulation and etc.).

Subsequently, there are several works that still can be considered in order to realized the proposed communication system. We list some of them in the next section.

6.2 Suggestions for Future Work

In this thesis, we have proposed a cognitive radio-based home area network. There are many interesting research works henceforth that can be further carried out. Based on our experience, we present some of them in the following enumerations.

1. **The optimal candidate and in-band channel**. The allocation of the candidate channel by the cognitive HAN controller to each cluster head, including during the network start-up and whenever there is a decrease in throughput demand, can be optimized. This is the same with the in-band channel i.e., which is the optimal channel that should be returned to the HAN controller from a cluster head whenever there is a decrease in throughput demand, for example. Currently in this thesis, the transition from the candidate channel to in-band channel is by selecting the best channel available at the controller; while from in-band channel to candidate channel is returning the worst channel that the cluster head has. Alternatively, the optimal channels to be allocated or to be returned can be determined based on the communication needs of the cluster, i.e., for example based on the required additional throughput or channel quality needed. The properties of the channel that could be taken into consideration in decision making may include the channel's noise level, the signal-to-noise-ratio of the incumbent user and the incumbent user present probability.

2. **Construction of a spectrum map database**. The concept and the function of this database was initially mentioned in Chapter 3. By design, this database will be constructed by the cognitive HAN controller. It should consist of channel information including the list of possible channels to be exploited by the HAN that can be acquired from the regulator-certified databases, or from a long-time coarse sensing by the controller. The database could also consist of the statistical information on the incumbent user occupancy and the quality of the channels. The statistical information can be built by the controller based on the information reported by the cluster heads.

3. **Channel reuse**. As the HAN controller has a global view of the channels used at each cluster in the house, it could use this information, with the help of the spectrum map database, to further coordinate the reuse of the channels for the HAN. For example, clusters that are more than two hops from each other can utilize the same channels without causing any harmful interference

to one another. Through channel reuse, the number of possible channels that can be allocated to each cluster can be significantly increased. In addition, channels that are good in quality (e.g., higher SNR or lower incumbent user occupancy probability), can be allocated to multiple clusters. When a channel is utilized by multiple clusters in a house, this can further increase the average channel utilization of the particular channel which is already made efficient by the use of the cognitive radio technology. In doing this, a power control mechanism can also be applied to manipulate the coverage size of each cluster and assists for a more flexible channel reused in the house.

4. **Load balancing between clusters**. A certain area in a house such as the living room, where the multimedia entertainment system is located, might have a higher communication load compared to other areas. With the clustered topology proposed in this work, it is possible to off-load some of the communication burden in a cluster to another cluster which has a lower load. This load balancing mechanism and procedure can be designed to further improve the proposed CR-based HAN. Further, some clusters that are adjacent to the neighbor's HAN or with a wider coverage that extends to outside the house, can also accommodate the load from the guest HAN devices (e.g., neighbor's devices or some people that are passing by the house i.e., as the same concept recently proposed in [66]).

Bibliography

[1] U.S. Department of Energy, "The smart grid: an introduction," Prepared by Litos Strategic Communication, 2008, pp. 8.

[2] L. Atzori, A. Iera, and G. Morabito, "The Internet of Things: A survey," *Computer Networks*, vol. 54, no. 15, pp. 2787 – 2805, 2010. [Online]. Available: http://www.sciencedirect.com/science/article/pii/S1389128610001568

[3] M. Nekovee, "A survey of cognitive radio access to TV white spaces," *International Journal of Digital Multimedia Broadcasting*, vol. 2010, no. 236568, 2010.

[4] Bill Kovarik, "Radio and the Titanic," http://www.environmentalhistory.org/revcomm/features/radio-andthe-titanic/, Accessed: 2015-11-24.

[5] M. A. McHenry, P. A. Tenhula, D. McCloskey, D. A. Roberson, and C. S. Hood, "Chicago spectrum occupancy measurements & analysis and a long-term studies proposal," in *Proceedings of the First International Workshop on Technology and Policy for Accessing Spectrum*, ser. TAPAS '06. New York, NY, USA: ACM, 2006. [Online]. Available: http://doi.acm.org/10.1145/1234388.1234389

[6] I. F. Akyildiz, W.-Y. Lee, M. C. Vuran, and S. Mohanty, "Next generation/dynamic spectrum access/cognitive radio wireless networks: A survey," *Computer Networks*, vol. 50, no. 13, pp. 2127 – 2159, 2006. [Online]. Available: http://www.sciencedirect.com/science/article/pii/S1389128606001009

[7] D. Cabric, S. Mishra, and R. Brodersen, "Implementation issues in spectrum sensing for cognitive radios," in *Signals, Systems and Computers, 2004. Conference Record of the Thirty- Eighth Asilomar Conference on*, vol. 1, Nov 2004, pp. 772–776 Vol.1.

[8] P. Kumar, N. Rakheja, A. Sarswat, H. Varshney, P. Bhatia, S. Goli, V. Ribeiro, and M. Sharma, "White space detection and spectrum characterization in urban and rural india," in *International Symposium and Workshops on a World of Wireless, Mobile and Multimedia Networks (WoWMoM), 2013 IEEE 14th*, June 2013, pp. 1–6.

[9] S. Haykin, "Cognitive radio: brain-empowered wireless communications," *Selected Areas in Communications, IEEE Journal on*, vol. 23, no. 2, pp. 201–220, Feb 2005.

[10] *Wireless LAN at 60 GHz - IEEE 802.11ad Explained*, Agilent Technologies, May 2013, Application note. [Online]. Available: http://cp.literature.agilent.com/litweb/pdf/5990-9697EN.pdf

[11] Y. Niu, Y. Li, D. Jin, L. Su, and A. Vasilakos, "A survey of millimeter wave communications (mmWave) for 5G: opportunities and challenges," *Wireless Networks*, vol. 21, no. 8, pp. 2657–2676, 2015. [Online]. Available: http://dx.doi.org/10.1007/s11276-015-0942-z

[12] R. Daniels and R. Heath, "60 GHz wireless communications: emerging requirements and design recommendations," *Vehicular Technology Magazine, IEEE*, vol. 2, no. 3, pp. 41–50, Sept 2007.

[13] "IEEE Standard for Information technology– Local and metropolitan area networks– Specific requirements– Part 11: Wireless LAN Medium Access Control (MAC) and Physical Layer (PHY) Specifications Amendment 5: Enhancements for Higher Throughput," *IEEE Std 802.11n-2009 (Amendment to IEEE Std 802.11-2007 as amended by IEEE Std 802.11k-2008, IEEE Std 802.11r-2008, IEEE Std 802.11y-2008, and IEEE Std 802.11w-2009)*, pp. 1–565, Oct 2009.

[14] "IEEE Standard for Local and Metropolitan Area Networks Part 16: Air Interface for Fixed Broadband Wireless Access Systems," *IEEE Std 802.16-2004 (Revision of IEEE Std 802.16-2001)*, pp. 1–857, 2004.

[15] "LTE physical layer - general discription (Release 8)," *3GPP TSG RAN*, 2007.

[16] E. Larsson, O. Edfors, F. Tufvesson, and T. Marzetta, "Massive MIMO for next generation wireless systems," *Communications Magazine, IEEE*, vol. 52, no. 2, pp. 186–195, February 2014.

[17] B. Z. Maha and R. Kosai, "Multi user MIMO communication: Basic aspects, benefits and challenges," *InTech*, 2013. [Online]. Available: http://www.intechopen.com/books/recent-trends-in-multi-user-mimo-communications/multi-user-mimo-communication-basic-aspects-benefits-and-challenges

[18] Y.-C. Liang, Y. Zeng, E. Peh, and A. T. Hoang, "Sensing-throughput tradeoff for cognitive radio networks," *IEEE Transactions on Wireless Communications*, vol. 7, no. 4, pp. 1326–1337, April 2008.

[19] E. Peh, Y.-C. Liang, Y. L. Guan, and Y. Zeng, "Optimization of cooperative sensing in cognitive radio networks: A sensing - throughput tradeoff view," *IEEE Transactions on Vehicular Technology*, vol. 58, no. 9, pp. 5294–5299, Nov 2009.

[20] L. Tan and L. Le, "Joint cooperative spectrum sensing and MAC protocol design for multi-channel cognitive radio networks," *EURASIP Journal on Wireless Communications and Networking*, vol. 2014, no. 1, p. 101, 2014. [Online]. Available: http://jwcn.eurasipjournals.com/content/2014/1/101

[21] R. Rashid, A. Hamid, N. Fisal, M. Sarijari, R. Rahim, and A. Mohd, "Optimal user selection for decision making in cooperative sensing," in *2012 IEEE Symposium on Wireless Technology and Applications (ISWTA)*, Sept 2012, pp. 165–170.

[22] S. Maleki, S. P. Chepuri, and G. Leus, "Optimization of hard fusion based spectrum sensing for energy-constrained cognitive radio networks," *Physical Communication*, vol. 9, no. 0, pp. 193 – 198, 2013. [Online]. Available: http://www.sciencedirect.com/science/article/pii/S1874490712000663

[23] S. Maleki, S. Chepuri, and G. Leus, "Energy and throughput efficient strategies for cooperative spectrum sensing in cognitive radios," in *IEEE 12th International Workshop onSignal Processing Advances in Wireless Communications (SPAWC)*, June 2011, pp. 71–75.

[24] W. Ejaz, G. A. Shah, N. u. Hasan, and H. S. Kim, "Energy and throughput efficient cooperative spectrum sensing in cognitive radio sensor

networks," *Transactions on Emerging Telecommunications Technologies*, 2014. [Online]. Available: http://dx.doi.org/10.1002/ett.2803

[25] T. Cui and K. Kwak, "Cooperative spectrum sensing with adaptive node selection for cognitive radio networks," in *2013 Fifth International Conference on Ubiquitous and Future Networks (ICUFN)*, July 2013, pp. 506–510.

[26] H. Kim and K. Shin, "Efficient discovery of spectrum opportunities with MAC-layer sensing in cognitive radio networks," *IEEE Transactions on Mobile Computing*, vol. 7, no. 5, pp. 533–545, May 2008.

[27] G. Umashankar and A. Kannu, "Throughput optimal multi-slot sensing procedure for a cognitive radio," *IEEE Communications Letters*, vol. 17, no. 12, pp. 2292–2295, December 2013.

[28] M. Timmers, S. Pollin, A. Dejonghe, L. Van der Perre, and F. Catthoor, "A distributed multichannel MAC protocol for multihop cognitive radio networks," *IEEE Transactions on Vehicular Technology*, vol. 59, no. 1, pp. 446–459, Jan 2010.

[29] D. Cabric, A. Tkachenko, and R. W. Brodersen, "Experimental study of spectrum sensing based on energy detection and network cooperation," in *Proceedings of the First International Workshop on Technology and Policy for Accessing Spectrum*, ser. TAPAS '06. New York, NY, USA: ACM, 2006. [Online]. Available: http://doi.acm.org/10.1145/1234388.1234400

[30] *CC2420 Datasheet – 2.4 GHz IEEE 802.15.4/ZigBee-Ready RF Transceiver*, Texas Instruments, 2013, Rev. C. [Online]. Available: http://www.ti.com/product/CC2420/technicaldocuments

[31] W. Guo, W. Healy, and M. Zhou, "Impacts of 2.4-GHz ISM band interference on IEEE 802.15.4 wireless sensor network reliability in buildings," *IEEE Transactions on Instrumentation and Measurement*, vol. 61, no. 9, pp. 2533–2544, Sept 2012.

[32] A. Sikora and V. Groza, "Coexistence of IEEE802.15.4 with other systems in the 2.4 GHz-ISM-Band," in *Instrumentation and Measurement Technology Conference, 2005. IMTC 2005. Proceedings of the IEEE*, vol. 3, May 2005, pp. 1786–1791.

[33] S. Y. Shin, H. S. Park, S. Choi, and W. H. Kwon, "Packet error rate analysis of zigbee under WLAN and bluetooth interferences," *IEEE Transactions on Wireless Communications*, vol. 6, no. 8, pp. 2825–2830, August 2007.

[34] J. Mitola and J. Maguire, G.Q., "Cognitive radio: making software radios more personal," *Personal Communications, IEEE*, vol. 6, no. 4, pp. 13–18, Aug 1999.

[35] I. F. Akyildiz, B. F. Lo, and R. Balakrishnan, "Cooperative spectrum sensing in cognitive radio networks: A survey," *Phys. Commun.*, vol. 4, no. 1, pp. 40–62, Mar. 2011. [Online]. Available: http://dx.doi.org/10.1016/j.phycom.2010.12.003

[36] N. D. Duong, A. Madhukumar, A. Premkumar, and N. B. Chong, "A novel architecture for distributed spectrum sensing for cognitive radio applications," in *IEEE Region 10 Conference (TENCON)*, Jan 2009, pp. 1–5.

[37] K. Cichoń, L. De Nardis, H. Bogucka, and M. G. Di Benedetto, "Mobility-aware, correlation-based node grouping and selection for cooperative spectrum sensing," *Journal of Telecommunications and Information Technology*, vol. 2014, no. 2, pp. 90–102, January 2014.

[38] X. Zhou and Q. Zhang, "Key nodes based spectrum sensing for cognitive radio," in *2010 Global Mobile Congress (GMC)*, Oct 2010, pp. 1–6.

[39] N. Hasan, W. Ejaz, S. Lee, and H. Kim, "Knapsack-based energy-efficient node selection scheme for cooperative spectrum sensing in cognitive radio sensor networks," *IET Communications*, vol. 6, no. 17, pp. 2998–3005, November 2012.

[40] *ZigBee Specification Document 053474r17*, ZigBee Alliance, 2008.

[41] "IEEE standard for information technology - telecommunications and information exchange between systems - local and metropolitan area networks specific requirements part 15.4: Wireless medium access control (MAC) and physical layer (PHY) specifications for low-rate wireless personal area networks (LR-WPANs)," *IEEE Std 802.15.4-2003*, pp. 1–670, 2003.

[42] *TMote Sky Datasheet*, Moteiv Corporation, 2006. [Online]. Available: http://www.eecs.harvard.edu/~konrad/projects/shimmer/references/tmote-skydatasheet.pdf

[43] "Tinyos," http://www.tinyos.net/, Accessed: 2013-09-24.

[44] T. Taher, M. Misurac, J. LoCicero, and D. Ucci, "Microwave oven signal modelling," in *IEEE Wireless Communications and Networking Conference (WCNC)*, March 2008, pp. 1235–1238.

[45] "Xirrus Wi-Fi inspector," http://www.xirrus.com/products/wi-fi-inspector.aspx, Accessed: 2013-09-28.

[46] O. Holland, "Novel licensing schemes supporting cognitive radio and spectrum coexistance," in *Summer School 2013 on Cognitive Wireless Communicaitons*, 2013, pp. 57–76.

[47] V. Banjade and N. Rajatheva, "Primary user capacity maximization in cooperative detection network using m out of n fusion rule," in *8th International Symposium on Wireless Communication Systems (ISWCS)*, Nov 2011, pp. 482–486.

[48] Y. H. Wang, "On the number of successes in independent trials," *Statistica Sinica*, vol. 3, no. 2, pp. 295–312, 1993.

[49] "IEEE Standard for information technology– local and metropolitan area networks– specific requirements– part 22: Cognitive wireless RAN medium access control (MAC) and physical layer (PHY) specifications: Policies and procedures for operation in the TV bands," *IEEE Std 802.22-2011*, pp. 1–680, July 2011.

[50] W. Zhang, R. Mallik, and K. Letaief, "Optimization of cooperative spectrum sensing with energy detection in cognitive radio networks," *IEEE Transactions on Wireless Communications*, vol. 8, no. 12, pp. 5761–5766, December 2009.

[51] M. Najimi, A. Ebrahimzadeh, S. Andargoli, and A. Fallahi, "A novel sensing nodes and decision node selection method for energy efficiency of cooperative spectrum sensing in cognitive sensor networks," *IEEE Sensors Journal*, vol. 13, no. 5, pp. 1610–1621, May 2013.

[52] K.-L. A. Yau, N. Ramli, W. Hashim, and H. Mohamad, "Clustering algorithms for cognitive radio networks: A survey," *Journal of Network and Computer Applications*, vol. 45, no. 0, pp. 79–95, 2014. [Online]. Available: http://www.sciencedirect.com/science/article/pii/S1084804514001611

[53] S. Chaudhari, J. Lunden, V. Koivunen, and H. Poor, "Cooperative sensing with imperfect reporting channels: Hard decisions or soft decisions?" *IEEE Transactions on Signal Processing*, vol. 60, no. 1, pp. 18–28, Jan 2012.

[54] R. Rajbanshi, A. M. Wyglinski, and G. Minden, "An efficient implementation of nc-ofdm transceivers for cognitive radios," in *1st International Conference onCognitive Radio Oriented Wireless Networks and Communications*, June 2006, pp. 1–5.

[55] C. han Lee and W. Wolf, "Energy efficient techniques for cooperative spectrum sensing in cognitive radios," in *Consumer Communications and Networking Conference, 2008. CCNC 2008. 5th IEEE*, Jan 2008, pp. 968–972.

[56] P. J. Green, "Reversible jump markov chain monte carlo computation and bayesian model determination," *Biometrika*, vol. 82, no. 4, pp. 711–732, 1995. [Online]. Available: http://biomet.oxfordjournals.org/content/82/4/711.abstract

[57] C. P. Robert and G. Casella, *Monte Carlo Statistical Methods*, New York, NY, 2004.

[58] W. R. Gilks, *Markov chain Monte Carlo in Practice*. Boca Raton: Chapman and Hall/CRC, 1998.

[59] H. Kim and K. G. Shin, "In-band spectrum sensing in cognitive radio networks: Energy detection or feature detection?" in *Proceedings of the 14th ACM International Conference on Mobile Computing and Networking*, ser. MobiCom '08. New York, NY, USA: ACM, 2008, pp. 14–25. [Online]. Available: http://doi.acm.org/10.1145/1409944.1409948

[60] E. Peh and Y.-C. Liang, "Optimization for cooperative sensing in cognitive radio networks," in *2007 IEEE Wireless Communications and Networking Conference (WCNC 2007)*, March 2007, pp. 27–32.

[61] P. J. Green and J. Heikkinen, "Trans-dimensional markov chain monte carlo," in *Highly Structured Stochastic Systems*. Oxford University Press, 2003, pp. 179–206.

[62] P. J. Green and D. Hastie, "Reversible jump MCMC," *Genetics*, vol. 155, no. 3, pp. 1391–1403, June 2009.

[63] C. J. Geyer, "Introduction to markov chain monte carlo," *Handbook of Markov Chain Monte Carlo*, pp. 3–48, 2011.

[64] M. N. Rahman and M. Matin, "Efficient algorithm for prolonging network lifetime of wireless sensor networks," *Tsinghua Science and Technology*, vol. 16, no. 6, pp. 561 – 568, 2011. [Online]. Available: http://www.sciencedirect.com/science/article/pii/S100702141170075X

[65] Y. Chen and Q. Zhao, "On the lifetime of wireless sensor networks," *Communications Letters, IEEE*, vol. 9, no. 11, pp. 976–978, Nov 2005.

[66] "Ziggo WiFi Spots," https://www.ziggo.nl/internet/wifispots/, Accessed: 2015-11-08.

Samenvatting

Een toekomstig thuisnetwerk (home area network, HAN) wordt verondersteld te bestaan uit een groot aantal apparaten die diverse toepassingen ondersteunen zoals slimme elektriciteitsnetwerken, beveiligingssystemen, telefonie, en televisiesignalen. Veel van deze thuisapparaten communiceren draadloos gebaseerd op netwerkprotocollen zoals WiFi, ZigBee en Bluetooth, die typisch opereren in de overbelaste licentie-vrije ISM frequentiebanden. Omdat deze apparaten dicht bij elkaar staan (bijvoorbeeld binnen een huis) kunnen ze elkaar storen, waardoor de behaalde kwaliteit van de verbindingen afneemt. Deze situatie wordt verergerd in dichtbebouwde steden waar de HAN ook gestoord wordt door de buren. Cognitieve radio (CR) wordt gezien als een van de meest veelbelovende technologieen om deze problemen op te lossen en tegelijkertijd in de communicatiebehoefte van de HAN te voorzien. CR technologie stelt de HAN apparatuur in staat om intelligent de ongebruikte delen van het spectrum waar een vergunning voor nodig is te benutten, interferentie te vermijden en zelf geen interferentie te veroorzaken (in het bijzonder bij de vergunninghouder van het spectrum). We bestuderen deze problemen en de geschiktheid van CR als kandidaat-oplossing.

We beginnen met het ontwerp van een nieuw communicatiesysteem voor HAN gebaseerd op CR technologie en een geclusterde netwerktopologie, en noemen dit TD-CRHAN. TD-CRHAN beoogt toekomstbestendig te zijn en ondersteunt efficient de groeiende behoefte aan bandbreedte, en probeert ook het storingsprobleem in HAN op te lossen. In TD-CRHAN wordt de beschikbare bandbreedte geoptimaliseerd om precies te voldoen aan de gevraagde bandbreedte, in plaats van die te maximaliseren. Vervolgens modeleren we mathematisch het voorgestelde TD-CRHAN en nemen in het model algemene uitdrukkingen voor de kwaliteitsparameters van cooperatief spectrumschatten op. Hiermee kunnen wij de kwaliteit van TD-CRHAN analyseren voor meer realistische scenarios waarin de signaal-ruisverhouding (SNR) van de vergunninghouder niet bij alle apparaten die dit schatten gelijk is. We geven een kwaliteitsanalyse voor het voorgestelde ontwerp zowel

numeriek als door middel van simulaties.

Omdat een netwerk gebaseerd op cognitieve radio ook extra kost in termen van energieverbruik door het spectrumschatten, ontwerpen we een energie-efficiente manier van cooperatief spectrumschatten (CSS). Deze manier sluit aan op het voorgestelde TD-CRHAN. We zorgen ervoor dat aan de vereiste bandbreedte voldaan wordt. Uit het verschil in de eerder genoemde SNR van de vergunninghouder op de diverse apparaten bepalen we de optimale selectie van spectrumsensoren voor CSS en de benodigde sensortijd en detectiekans, die kan verschillen tussen de diverse apparaten. We evalueren vervolgens de voorgestelde CSS techniek en tonen de winst in energieverbruik en efficientie in bandbreedte.

Tot slot presenteren we een methode voor het groeperen en rangschikken van de sensorapparatuur voor meerkanaals CSS. Naast energieverbruik en efficientie in bandbreedte hanteert deze methode de eerlijkheid in werklast over de diverse sensorapparatuur in een HAN. Dit eerlijkheidskriterium beoogt het maximaliseren van de levensduur van ieder sensorapparaat vergeleken met zijn verwachtte levensduur. We bepalen het optimale aantal frequentiekanalen dat het netwerk zou moeten gebruiken, en de geselecteerde kanalen. We bepalen ok het optimale aantal apparaten in iedere sensorgroep, en de geselecteerde apparaten. Vervolgens bepalen we de optimale volgorde van de sensorgroepen om het spectrum van de geselecteerde kanalen te meten. We presenteren de resultaten en de analyse van de voorgestelde methode om zijn kwaliteit te illustreren.

Acknowledgment

All praises to the Almighty God. The Guide, The Strong and The Merciful, for His guidance and strengths in completing this one of the most challenging journeys in my life. I pray for His continues blessings.

This PhD journey is completed not only with great patience, persistence and continuous hard work for the last four years, but also cooperation, encouragement and support from many people and organizations. I would like to take this opportunity to acknowledge them here.

First and foremost, I would like to thank the Malaysia's government, under the Ministry of Higher Education (MOHE) for awarding me the scholarship and the Universiti Teknologi Malaysia for giving me a full-paid study leave. I will try my very best to contribute back to our beloved country and university, with the knowledge and experiences that I have gained throughout this great PhD journey. Prof. Dr. Norsheila, Prof. Dr. Zaidatun, Assoc. Prof. Dr. Sharifah Kamilah and Dr. Rozeha, for being a great mentor in UTM and giving me many highly-useful advices, particularly during the hard times of my PhD journey. Mr. Ariffin and all his staff, thank you so much for the support from UTMLead, as well as the SLAI department of MOHE for their support on the scholarship matters.

My great acknowledgment also goes to my promotor, Prof.dr.ir Alle-Jan van der Veen, for accepting me into this lovely Circuits and Systems group and for being my advisor. Thank you Alle-Jan for always giving me a practical solution, motivate and showing me the clear way to complete my very tight PhD time line. Even with the very busy schedule that you have, you still make time for me and entertained gladly. Once more, thank you for everything.

I also would like to express my utmost gratitude to my co-promotor, Assoc. Prof. Dr.ir Gerard Janssen for the invaluable guidance. Gerard trained me to crit-

ically formulate and analyze a scientific problem. He taught me the art of well-organized technical writing. Your feedback is always valuable despite being very challenging. Working under your supervision was a great experience.

Next, I would like to express my appreciation to all my co-authors and the people who have helped me in the technical part of this journey. Sharil, I highly thank you for the great brainstorms that cleared up all the messy roads. We always come out with a great solution through our discussion. Dr. Georg Kail, thank you for the guidance on the optimization and solutions. Dr. Anthony Lo, Prof.dr.ir Sonia Heemstra, Prof.dr.ir Ignas Niemegeers, Diptanil and Qing, thank you for being part of my PhD journey. Hadi, Rozaini and Hamdan for the far away discussions and knowledge exchange.

From the CAS group, my office mates Sundeep and Jing, our kind secretary Minaksie, Rosario, Antoon, and to all my fellow PhD students and postdocs, thank you so much for being really friendly and helpful.

I also would like to sincerely thank the H.E. Ambassador Dato' Ahmad Nazri, the Embassy Counsellor Mr. Ahmad Zuwairi, the Second Secretary Mr. Mohd Fadzil, the former Agricultural Attache Mr. Ahmadul, the Assistance Agricultural Attache Mr. Wafi, and all other Malaysian Embassy staff in Den Haag, for the enormous support and assistance particularly during my time as the Chairman of the Malaysian Student Association in the Netherlands (MAS-NL).

My warmest thanks to all my Malaysian friends in the Netherlands, including Allahyarham abg Zaidi and kak Yan, Dila, Yon and Syu, Zihan and Fai, Apai dan Kyra, Faiz and Nani, Asrul and Nora, kak Latifah and Mr. Idris, abg Anuar and kak Ina, Hafiz and Ayu, abg Fauzi and kak Linda, Farabi and Muni, Kimi and Syud, Hilmi and Yan, Zairi and Ekin, Yati and Hafiz, Rozaini, and Zulkhairi. I might not be able to write all your names here, but I am very thankful to each and every one of you for making my stay here feels like home.

Last but not least, the most important acknowledgment goes to my beloved mother Norkhayati and father Sarijari, my dearly loved wife Nur Hija, our cherished son Umar and daughter Fatimah, my sisters kak In, kak Ejun, Aan and Ila, and not forgetting my in-laws Allahyarhamah emak Merzanah, abah Mahalin, kak long Syalwa, Allahyarham adik Syarul, abg Yem, abg Usop, Zaris and Nizam. Thank you for all the the prayes, and for being eternally supportive and encouraging. This thesis is dedicated to you, and may the Almighty God bless you all.

Adib
Delft, March 2015.

Biography

M.A.B (Mohd Adib bin) Sarijari was born in Johor, Malaysia in 1984. He received his Bachelors in Engineering degree (first class, and with honors) in 2007, and the Master of science in Electrical Engineering degree in 2011, both from Universiti Teknologi Malaysia (UTM), Johor, Malaysia. His M.Sc study was supported by the government of Malaysia under the Ministry of Higher Education and UTM. He is currently with the Department of Communication Engineering at the Faculty of Electrical Engineering, UTM. In 2012, he received a sponsorship from the government of Malaysia under the Ministry of Higher Education and UTM, to pursue a PhD degree with the Circuits and Systems group at the Faculty of Electrical Engineering, Mathematics and Computer Science of the Delft University of Technology, the Netherlands. His general research interest lies in the field of communications, optimization, and system design. In particular, he is interested in cognitive radio, home area networks, wireless sensor networks, software defined radio, smart home and smart city.

Publications during Ph.D

Journals

- **Mohd Adib Sarijari**, Georg Kail, Gerard J.M. Janssen, Alle-Jan van der Veen, "Energy and Throughput Efficient Cooperative Spectrum Sensing for Cognitive Radio-based Home Area Network", Submitted to the *IEEE Transactions on Cognitive Communications and Networking*.
- **Mohd Adib Sarijari**, Mohd Sharil Abdullah, Gerard J.M. Janssen, Alle-Jan van der Veen, "On Achieving Network Throughput Demand in Cognitive Radio-based Home Area Networks", *EURASIP Journal on Wireless Communications and Networking*, Vol. 2015, No. 1, pp. 221, 2015.
- Hamdan Sayuti, Rozeha A. Rashid, M.A. Latiff, A. H.F.A. Hamid, N. Fisal, **Mohd Adib Sarijari**, A. Mohd, K.M. Yusof, R.A. Rahim, Lightweight Priority Scheduling Scheme for Smart Home and Ambient Assisted Living System. *International Journal of Digital Information and Wireless Communications (IJDIWC)*, 2014.
- **Mohd Adib Sarijari**, A. Lo, R.A.Rashid and N. Fisal, "Interference Issues in Smart Grid Home Area Network to Enable Demand Response And Advanced Metering Infrastructure: Survey And Solutions", *Open International Journal of Informatics (OIJI)*, 2013.
- Rozeha A. Rashid, A. Hadi Fikri A. Hamid, N. Fisal, **Mohd Adib Sarijari**, "Low Complexity Optimal Sensing Strategy for Maximized Throughput in Cognitive Radio Networks", *IEEE COMSOC MMTC E-Letter*, vol.7 No.6, July 2012.

Conferences

- R.A. Rashid, M.R.B. Resat, **Mohd Adib Sarijari**, N.H. Mahalin, Mohd Shahril Abdullah, A.H.F.A. Hamid, "Performance Investigations of Frequency Agile Enabled TelosB Testbed in Home Area Network", *IEEE International Symposium on Telecommunication Technologies (ISTT)*, Langkawi, pp. 335–340, Nov. 2014.

- **Mohd Adib Sarijari**, M.S. Abdullah, A. Lo and R.A. Rashid, "Experimental Studies of the ZigBee Frequency Agility Mechanism in Home Area Networks", *39th IEEE Conference on Local Computer Networks Workshops (LCN Workshops)*, Edmonton, Canada, pp. 711–717, Sept. 2014;

- **Mohd Adib Sarijari**, A. Lo, M.S. Abdullah, S.H. de Groot, I.G.M.M. Niemegeers and R.A. Rashid, "Coexistence of Heterogeneous and Homogeneous Wireless Technologies in Smart Grid-Home Area Network", *2013 International Conference on Parallel and Distributed Systems (ICPADS)*, Seoul, South Korea, pp. 576–581, Dec. 2013;

- Rozeha A. Rashid, H. Sayuti, N.M.A Latiff, N. Fisal, **Mohd Adib Sarijari**, A.H.F.A Hamid, R.A Rahim, "Simple Scheduling Scheme for Smart Home and Ambient Assisted Living", *International Conference on Informatics Engineering & Information Science (ICIEIS)*, Kuala Lumpur, pp. 295–301, Nov. 2013.

- S.K.S Yusof, K.M.K. Rashid, N.M.A. Latiff, N. Fisal, **Mohd Adib Sarijari**, R.A. Rashid, N. Ramli," TDMA-based Cooperative Sensing using SDR Platform for Cognitive Radio", *Asia-Pacific Conference on Communications (APCC)*, Jeju Island, pp.278–283, October 2012.

- Rozeha A.Rashid, A.Fikri A.Hamid, N.Fisal, **Mohd Adib Sarijari**, Rozaini A.Rahim, Alias Mohd, "Optimal user selection for decision making in cooperative sensing", *IEEE Symposium on Wireless Technology and Applications (ISWTA)*, Bandung, pp. 165–170, Sept 2012.

Glossary

Acronyms

3GPP	3rd generation partnership project
BPSK	Binary phase shift keying
C	Cognitive home area network controller
CH	Cluster head
CR	Cognitive radio
CSS	Cooperative spectrum sensing
FC	Fusion center
FCC	Federal communications commission
G	Home area network gateway
GSM	Global system for mobile communications
HAN	Home area network
HD	High definition
IoT	Internet-of-things
ISM	Industrial, scientific and medical
ISP	Internet service provider

ITU	International telecommunication union
ITU-R	International telecommunication union radiocommunication Sector
DOA	Direction of Arrival
LTE	Long term evolution
MAC	Medium access control
MCMC	Markov-Chain-Monte-Carlo
MIMO	Multiple input multiple output
MU-MIMO	Multi user multiple input multiple output
NC-OFDM	Non-contigous Orthogonal frequency-division multiplexing
OFDM	Orthogonal frequency-division multiplexing
PER	Packet error rate
QoS	Quality-of-service
QPSK	Quadrature phase shift keying
RF	Radio frequency
RSSI	Received signal strength indicator
SDMA	Space division multiple access
SNR	Signal-to-noise-ratio
TD-CRHAN	Throughput demand based cognitive radio home area network
TETRA	Terrestrial trunked radio
WiMAX	Worldwide interoperability for microwave access
WLAN	Wireless local area network
WPAN	Wireless local area network

Notations

x	Scalar x
$\hat{x}$	Estimate of scalar x
$\mathbf{x}$	Vector $\mathbf{x}$
$\mathcal{X}$	Set $\mathcal{X}$
$[\mathbf{x}]_i$	i-th entry of the vector $\mathbf{x}$
$\lceil x \rceil$	Smallest integer larger or equal to x
$\triangleq$	Defines an entity
$\emptyset$	Empty set
$p(x)$	Probability of x
$Q(x)$	Gaussian tail probability, i.e., $1/\sqrt{2\pi}\int_x^\infty e^{-u^2/2}du$

Symbols

D	Demanded throughput
$\mathcal{H}_0$	Hypothesis of the channel is idle
$\mathcal{H}_1$	Hypothesis of the channel is occupied
i	Channels number
I	Total active in-band channel in the cluster
j	CR-based HAN devices number
J	Total number of CR-based HAN devices in the HAN
K	Total number of devices that decides the sensed channel is occupied
N	Total number of cooperating nodes for cooperative spectrum sensing
P_{f}	Local probability of false alarm
P_{d}	Local probability of detection
Q_{f}	Cooperative probability of false alarm
Q_{d}	Cooperative probability of detection
R	Achievable throughput
$u[l]$	Received incumbent signal during the l-th sample
$\mathrm{SNR}_{\mathrm{p}}$	SNR of the incumbent signal measured at the CR-device
T_{sf}	Superframe duration
T_{css}	Cooperative spectrum sensing time
T_{s}	Local spectrum sensing time
T_{sr}	Time duration for sending a single local sensing report
T_{com}	Data communication time
$w[l]$	Noise signal during the l-th sample
α	Fraction of data communication time from the frame time

ε	Difference between the achievable and the demanded throughput
τ	Sampling time
γ	Local spectrum sensing threshold